STUDIES ON THE BIOSYNTHESIS OF CYSTEINE IN MYCOBACTERIUM TUBERCULOSIS AND STUDIES ON THE BIOSYNTHESIS OF VITAMIN B6 IN BACILLUS SUBTILIS

A Dissertation

Presented to the Faculty of the Graduate School

of Cornell University

In Partial Fulfillment of the Requirements for the Degree of

Doctor of Philosophy

by

Kristin Elaine Burns

August 2006

STUDIES ON THE BIOSYNTHESIS OF CYSTEINE IN MYCOBACTERIUM TUBERCULOSIS AND STUDIES ON THE BIOSYNTHESIS OF VITAMIN B6 IN BACILLUS SUBTILIS

Kristin Elaine Burns, Ph. D.

Cornell University 2006

Cysteine is one of the 22 natural amino acids used to make proteins. Three pathways are currently known for the biosynthesis of cysteine and all include sulfide as the sulfur source. A new pathway for cysteine biosynthesis was elucidated and reconstituted from *Mycobacterium tuberculosis*. This pathway involves a protein bound thiocarboxylate (CysO-SH) as the sulfide donor, similar to thiamin and molybdopterin biosynthesis. MoeZ, a paralog of ThiF (thiamin) and MoeB (molybdopterin), transfers sulfide onto CysO from an unidentified source. Cysteine synthase M (CysM) catalyzes the addition of O-acetylserine to the carboxy terminus of the protein bound thiocarboxylate to generate a CysO-cysteine adduct. A protease, Mec^{+}, hydrolyzes the CysO-cysteine adduct to release cysteine and regenerate CysO. Mec^{+} contains the JAMM motif and this work provides the first functional characterization of the JAMM motif in prokaryotes. This pathway could be important for *M. tuberculosis* under conditions of oxidative stress, as it would provide a more stable source of sulfide than the traditional pathways for cysteine formation.

Vitamin B6, an essential cellular cofactor, is biosynthesized by bacteria and lower eukaryotes and is required in the human diet. Two *de novo* pathways for PLP biosynthesis were known, however, the most common pathway involving the YaaD

and YaaE family of genes had not been reconstituted. The substrates for *Bacillus subtilis* PLP synthase (YaaD and YaaE) were identified as ribose-5-phosphate, glyceraldehyde-3-phosphate and glutamine; the product is pyridoxal-5'-phosphate. In addition to PLP formation, we identified three activities catalyzed by the YaaD subunit of PLP synthase, including ribosephosphate isomerase activity, triose phosphate isomerase activity, and adduct formation with ribulose-5-phosphate. We also investigated the early steps of the mechanism of pyridoxal-5'-phosphate formation. In the absence of triose, PLP synthase forms a stable intermediate which absorbs at 320nm. This intermediate then reacts with glyceraldehyde-3-phosphate to form PLP.

BIOGRAPHICAL SKETCH

Kristin Burns was born on September 9, 1979, in Philadelphia, a city dear to her heart. Growing up in Roxborough, Kristin spent her time eating water ice, playing dodgeball with neighborhood friends, watching her brother's baseball games, and getting her sugar fix (along with her sister) from the corner store. Reverend Russell Burns and Betty Burns bused Kristin and her siblings, Brian and Karen, to Fitler Academics Plus School in Germantown. Kristin loved Fitler: a school rich in diversity and double-dutch games! After a quick stay in Quakertown, PA, the Burnses moved to Alburtis, PA, and Kristin attended Perkiomen School where her mom worked. With the encouragement of her 9th grade Biology teacher, Mr. Gallagher, Kristin got very interested in science, even asking for more homework in Chemistry class (something her friends will never let her forget). At Perkiomen, Kristin also delved into sports – field hockey and softball. Franklin and Marshall College allowed Kristin to continue her love of field hockey and science, as she became a member of the hockey team for 4 years, and a Chemistry major. Under the guidance of Dr. VanArman, Kristin worked in a synthetic lab for two summers and an academic year prior to attending Cornell University to obtain a PhD in Biochemistry, Molecular and Cell Biology. This field enabled Kristin to explore biology while keeping up with the chemistry she learned in college. She found the perfect mix of biology and chemistry in Tadhg Begley's lab, where she rotated in her first year. At Cornell, Kristin has continued playing field hockey on the club team, has become and avid runner and enjoys taking walks through beautiful Ithaca. After receiving her PhD, Kristin plans to attend Clif Barry's lab at the National Institutes of Health in Bethesda, Maryland, where she will be studying the pathogenesis of *Mycobacterium tuberculosis*.

ACKNOWLEDGMENTS

Many thanks to Tadhg Begley, whose guidance, patience and encouragement made all the difference for me. I would also like to thank my committee members Steve Ealick and Patrick Stover for supporting me at seminars, writing letters of recommendation, and talking football every now and then. Thanks also to Volker Vogt and David Russell for the constant support at seminars and for the encouragement.

My family has supported me in every decision I made. They kept me humble for the good ones and let me learn from the mistakes of the bad ones. I admire the love my parents have for one another and for their family. Thank you mom, dad, Brian and Karen.

Every now and then I'm reminded of the awesome feeling true friendships bring. I am very blessed and honored to call these people friends. It makes me smile knowing the few best friends I have all have different qualities I admire, and to which I aspire. In doing so, I've become a better person. Thank you Amanda for your inspiration, Beth for your support, Bucky for your courage, Cia for your enthusiasm and Smita for your wisdom. Thank you all for the love.

Thank you Mark for walking me through my first few years here; Collynn for teaching me biochemistry and providing an ear; AKPome for the treats, the laughs, the support and the love; and Asma for the chats.

Thank you Denise and Dick for the morning smiles from the stockroom, June for the quick and friendly orders, Ralph and Jim for fixing everything, Ivan for making my NMRs look bigger and better, and Diane for all your help with everything and

anything BMCB. Thanks to Mr. Gallagher and Dr. VanArman: the teachers who have shaped me scientifically, who have led me down this path, and who allowed me to ask any question.

In graduate school, we often find ourselves spending more time in lab than at home. Sometimes this is because we actually have experiments to do; other times this is because lab is where we find the comfort of a family. Thank you big brother Joo-Heon, Cynthia, Erick, Brian, Pieter, Vasiliy and Keri: older students who showed me the ropes. Amy G. for the friendship we've developed, Amy H. for the laughs, and Jennie for the marathon and running addiction! Abhishekda, Toads, Barack, Tim, Katie, Jackie, Amrita, Seán, Jeremiah and Dave, keep the Begley lab strong!

TABLE OF CONTENTS

LIST OF FIGURES

LIST OF TABLES

LIST OF ABBREVIATIONS

Amp	Ampicillin
ATP	Adenosine triphosphate
BLAST	Basic Local Alignment Search Tool
BSA	Bovine serum albumin
DHAP	Dihydroxyacetone phosphate
DMSO	Dimethylsulfoxide
dNTPs	Deoxyribonucleotide triphosphates
DNA	Deoxyribonucleic acid
DTT	Dithiothreitol
EDTA	Ethylenediaminetetraacetic acid
ESI-FTMS	Electrospray ionization – Fourier transform mass spectrometry
G3P	glyceraldehyde-3-phosphate
HPLC	High perfomance liquid chromatography
IPTG	Isopropyl β-D-1-thiogalactopyranoside
Kan	Kanamycin
kDa	Kilodalton
LB	Luria-Bertani broth
MS	Mass spectrometry
MS/MS	Tandem mass spectrometry
MWCO	molecular weight cut off
NAD	β-nicotinamide adenine dinucleotide
NADH	β-nicotinamide adenine dinucleotide, reduced form
Ni-NTA	Nickel-nitrolotriacetic acid
NMR	Nuclear magnetic resonance
OD_{xxx}	Optical density at xxx nm
PCR	Polymerase chain reaction
PDTC	Pyridine-2,6-(bis)monothiocarboxylic acid
PLP	Pyridoxal-5'-phosphate
PMP	Pyridoxamine-5'-phosphate
Ro5P	ribose-5-phosphate
Ru5P	ribulose-5-phosphate
SDS-PAGE	Sodium dodecyl sulfate-polyacrylamide gel electrophoresis
TLC	Thin-layer chromatography

Chapter 1

Identifying a New Cysteine Biosynthetic Pathway

1.1 Introduction

As one of the twenty-two naturally occurring amino acids, cysteine plays an important role in many cellular functions. Cysteine residues are often critical for enzyme catalysis and structure and serves as a source of sulfur for many cellular metabolites. The pKa of the cysteine thiol is approximately pH8, which enables it to serve as a general acid or as a general base in enzyme catalysis, depending on the active site environment. The thiol group is also very reactive as a nucleophile, broadening the scope of reactions that enzymes are able to catalyze. Glyceraldehyde-3-phosphate dehydrogenase, an enzyme involved in glycolysis, is one of many enzymes that utilize cysteine as a nucleophile during catalysis.[1] Due to its nucleophilicity, cysteine is the site of many post-translational modifications, and also serves as a target for site-directed labeling studies which allows researchers to study protein dynamics.

In addition to its role in enzyme catalysis, cysteine also plays a structural role in many proteins. Under oxidizing conditions, cysteine oxidizes to cystine, forming a disulfide bond between the two thiols. Such disulfide bond formation at the protein level has several consequences. Most disulfides form in secretory, lysosomal or membrane proteins, where the environment is non-reducing. Both inter- and intramolecular disulfide bonds modify protein structure and stability, and can be essential for proper protein function. Insulin is modified with disulfide bonds that are necessary for function and disulfide bonds in the protein keratin provide rigidity and strengthen our hair.

Disulfide formation in certain proteins in the cytosol is a sign of oxidative stress, and it triggers the cell to respond appropriately.[2]

Apart from its role in protein catalysis, structure and stability, cysteine provides a sulfur source for several cellular metabolites. Cysteine serves as the sulfur donor, directly or indirectly, for the synthesis of all sulfur containing molecules in the cell.[3] It is the final step in the sulfur assimilation pathway and the first step in the biosynthesis of several essential compounds in the cell, including the cofactors thiamin, biotin, S-adenosyl methionione, molybdopterin and lipoic acid, the important cellular redox factor glutathione, as well as several siderophores and antibiotics. Some of this structural diversity is shown in figure 1.1.

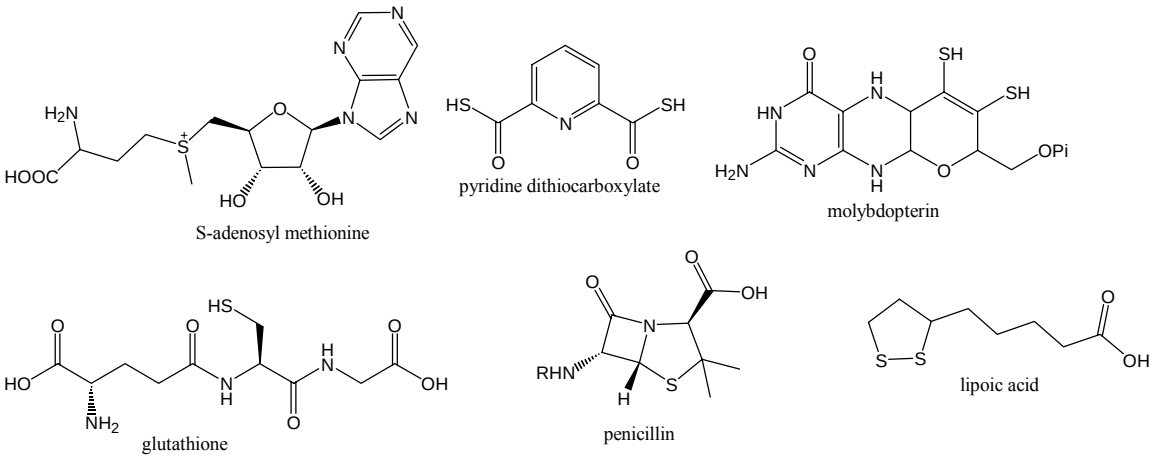

Figure 1.1 Structures of various sulfur containing metabolites.

1.2 The biosynthesis of cysteine

Cysteine is not an essential amino acid, and humans are able to synthesize their own by the reverse transsulfuration pathway. This pathway uses methionine, an essential amino acid that is required in the diet, to make cysteine. Only a few organisms have the reverse transsulfuration pathway, and most either use the direct sulfuration pathway or the

cystathionine pathway to synthesize cysteine. All of these pathways first require sulfate assimilation to reduce sulfate to sulfide.

Sulfate, the ultimate sulfur source of cysteine biosynthesis, is assimilated in bacteria, plants, and yeast by the route summarized in figure 1.2. Sulfate is first transported into the cell by a sulfate permease. Intracellular sulfate is adenylated by ATP sulfurylase, forming adenosine phosphosulfate **1**. This reaction consumes a lot of energy (K_{eq} = 1.1 x 10^{-8}; $\Delta G^{o'}_{hydrolysis}$ ~ -19 kcal/mol) and is highly disfavored, therefore it is coupled to the favorable hydrolysis of the β, γ bond of GTP, which shifts the reaction equilibrium towards sulfate assimilation.[4] In bacteria, yeast, and fungi, adenosine phosphosulfate kinase phosphorylates adenosine phosphosulfate **1**, resulting in 3'-phosphoadenosine phosphosulfate **2** (plants and algae do not have adenosine phosphosulfate kinase). Phosphoadenosine phosphosulfate **2** (or adenosine phosphosulfate in plants and algae) is subsequently reduced to sulfite **3** by the thioredoxin-dependent phosphoadenosine phosphosulfate reductase, yielding adenosine-3'-5'-diphosphate as the by-product. Sulfite **3** is reduced to sulfide **4** by NADPH-sulfite reductase, an enzyme that utilizes FAD as well as an iron-sulfur center and a siroheme prosthetic group.[5]

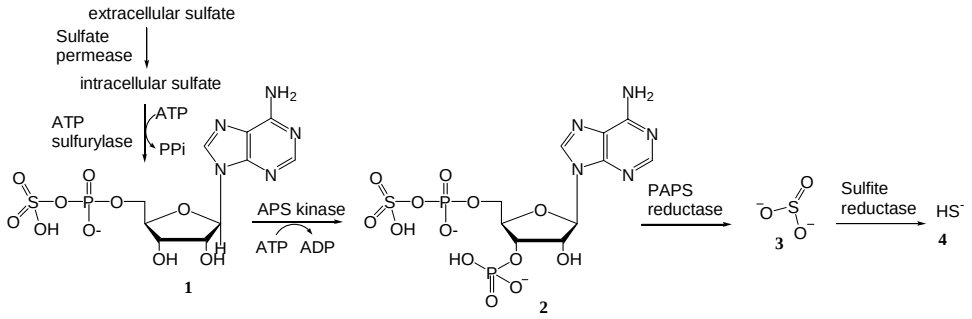

Figure 1.2 Summary of the sulfate assimilation pathway found in bacteria, yeast, and fungi.

Although most organisms use the same pathway to assimilate sulfate, there are three known pathways to biosynthesize cysteine. In most bacteria including *E. coli*, plants such as spinach,[6] and a few archaea,[7,8] cysteine is biosynthesized using the direct sulfuration pathway. In this pathway, shown in figure 1.3, serine **5** is acetylated by serine acetyltransferase to form O-acetylserine **6**. Cysteine synthase K (CysK), which forms a complex with serine acetyltransferase, is a pyridoxal-5'-phosphate (PLP)-dependent enzyme that catalyzes the addition of sulfide **4** onto O-acetylserine **6** to form cysteine **7**. Cysteine synthase M (CysM), an isozyme of CysK, does not complex with serine acetyltransferase and *in vitro* evidence suggests that it can use sulfide or thiosulfate to transfer sulfur onto O-acetylserine **6**. Evidence also suggests that CysM may be required for anaerobic growth because CysM mutants grow poorly under anaerobic conditions.[9,10]

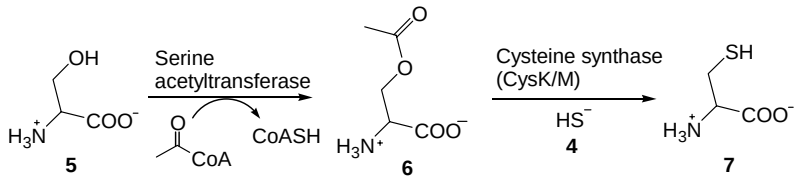

Figure 1.3 Reactions catalyzed by serine acetyltransferase and cysteine synthase in the direct sulfurylation pathway.

In contrast to the direct sulfuration pathway, yeast and some bacteria use the cystathionine pathway to make cysteine (figure 1.4).[6] In the cystathionine pathway, homoserine **8** is acetylated by homoserine O-acetyltransferase. O-acetylhomoserine sulfhydrylase transfers sulfide **4** to O-acetylhomoserine **9**, forming homocysteine **10**, which is also an intermediate in methionine biosynthesis. Serine **5** and homocysteine **10** are condensed by the PLP-dependent enzyme cystathionine β-synthase. Cystathionine γ-lyase cleaves cystathionine **11**, releasing cysteine **7**, ammonia and α-ketobutyrate **12**.

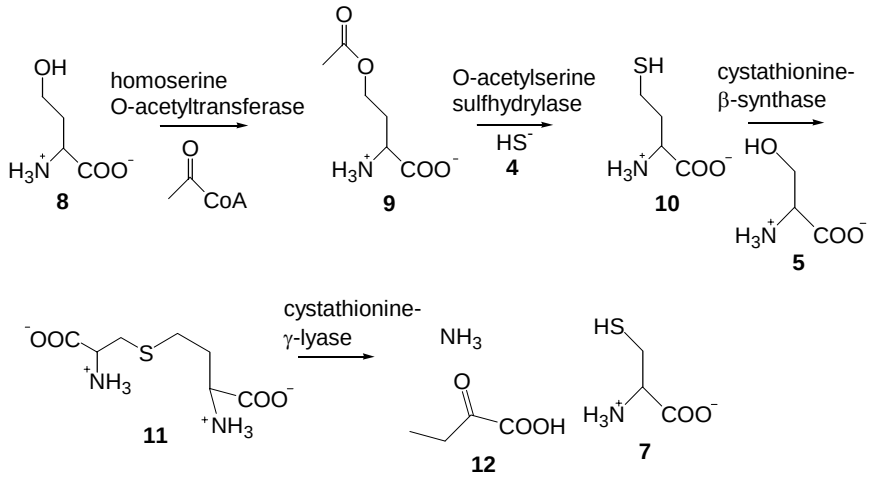

Figure 1.4 The cystathionine pathway for cysteine biosynthesis, as found in yeast.

The third pathway to cysteine is through reverse transsulfuration. Reverse transsulfuration begins with methionine. Methionine forms the cofactor S-adenosylmethionine, which is demethylated to form S-adenosylhomocysteine. This is cleaved to form homocysteine **10**, which shuttles back into the cystathionine pathway shown in figure 1.4.

1.3 Identification of a new cysteine biosynthetic gene cluster

The biosynthesis of cysteine in *Mycobacterium tuberculosis* (TB) has not been studied extensively. The sulfate assimilation pathway has just recently been characterized in TB[11] and genomic sequence analysis suggests TB could biosynthesize cysteine using several routes. Recent analysis of a sulfate uptake mutant ($cysA^-$) that leads to methionine auxotropy and not cysteine auxotrophy in TB provides evidence for the reverse transsulfuration pathway in this organism;[12] however, the genome contains a cysteine synthase *cysK* gene (Rv2334) upstream of a putative serine acetyltrasferase, suggesting direct sulfuration may be responsible for cysteine biosynthesis (figure 1.3). In addition to CysK, another putative cysteine synthase gene, *cysM* (Rv1336), exists in TB. This gene is clustered with two other genes in TB and several other organisms. The

cluster, shown in figure 1.5, includes the genes *mec*$^{+}$ (Rv1334), *cysO* (Rv1335), and *cysM*, and is also present in *Mycobacterium smegmatis*, *Nocardia farcinica*, *Streptomyces avermitilis, Streptomyces coelicolor*, *Streptomyces scabiei*, and *Thermomonospora fusca*, all of which are gram-positive actinomycetes. This gene organization suggests that they may work in a common pathway and since the gene cluster includes CysM, the organisms may employ a modified version of cysteine biosynthesis. There are three lines of reasoning which suggest that this cluster may be responsible for a novel pathway for cysteine biosynthesis in these organisms, and these are listed below.

1.3.1 Upregulation and coregulation of the cluster

Bacterial cytoplasms are reducing environments and under conditions of oxidative stress such as the addition of heavy metals or reactive oxygen intermediates, cells have to respond appropriately to survive. A result of oxidative stress is the formation of disulfide bonds in both proteins and small molecules and these disulfide bonds can become deleterious if they are not reduced. One response to disulfide stress is the induction of a specific transcription factor, sigma (σ), which can bind to and upregulate a number of genes involved in the disulfide response as well as genes responsible for the biosyntheses of important sulfur-containing molecules. Examples of genes upregulated under oxidative stress in bacteria include those for thioredoxin, sulfate uptake, and cysteine biosynthesis. Both *M. tuberculosis* and *S. coelicolor* have a homologous sigma factor (σ^{H} and σ^{R}, respectively) that is induced upon oxidative stress. Manganelli and co-workers used microarray analysis to identify genes upregulated by σ^{H} in response to oxidative stress in *M. tuberculosis*.[13] In addition to thioredoxin and sulfate uptake genes, *cysM*, *cysO*, and *mec*$^{+}$ were all up-regulated in response to oxidative stress, and showed no upregulation in the σ^{H} mutant. Likewise, Paget and coworkers mapped a consensus sequence for σ^{R} to a variety of genes in *S. coelicolor*[14]. Among the genes that have the consensus sequence were *cysO* and *cysM*, which they believe may compose one

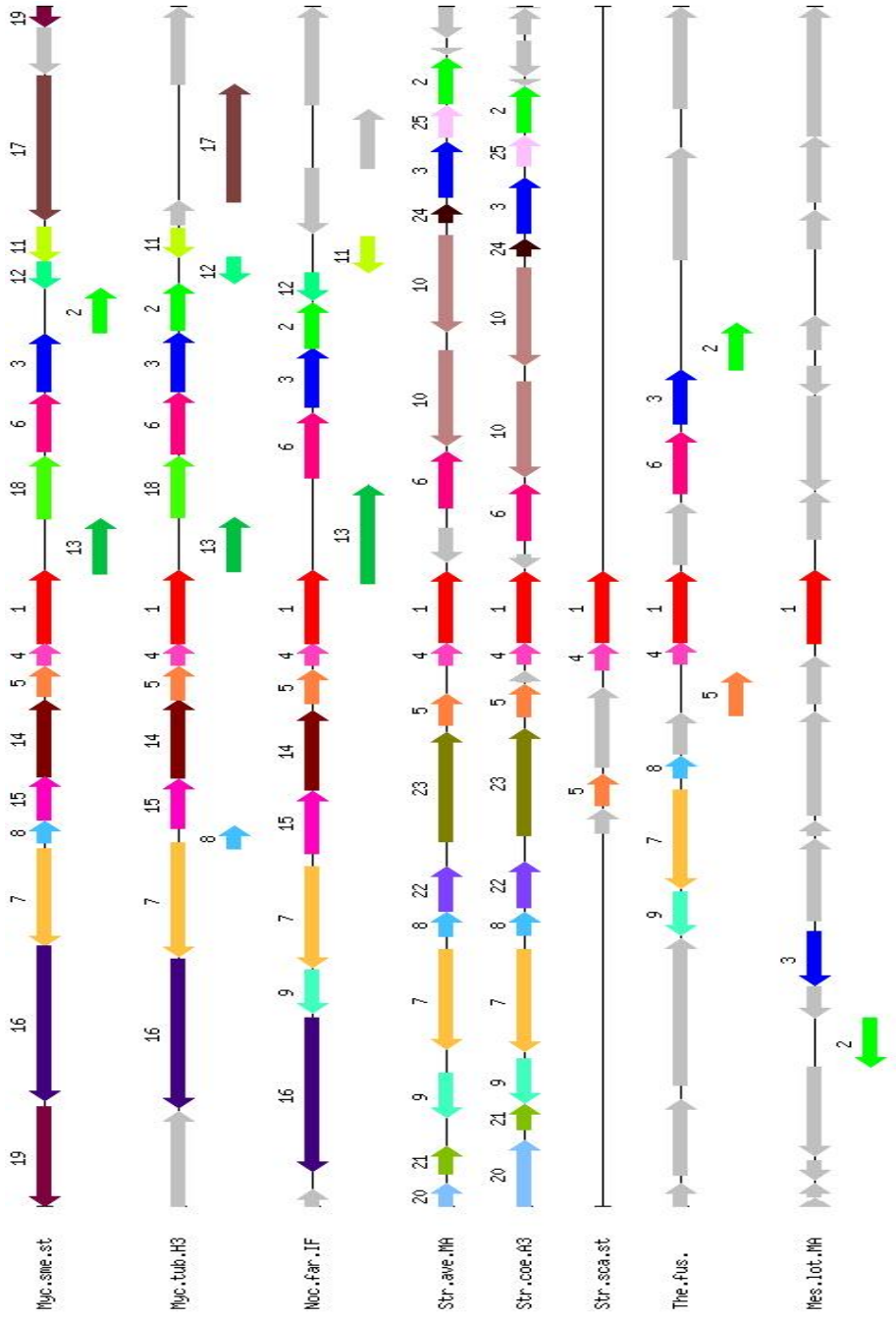

Figure 1.5 Gene organization in several actinomycetes suggesting a new pathway for cysteine biosynthesis. 1: cysM (Rv1336); 2: cysO (Rv1335); 5: mec+ (Rv1334).

transcriptional unit.[14] No other genes involved in cysteine biosynthesis were shown to be upregulated in these experiments. The results suggest that this cluster may be involved in synthesizing cysteine to overcome the potential deleterious effects of oxidative stress.

1.3.2 Mec$^+$ is involved in cysteine biosynthesis

In 1985, Hirasawa identified a gene, *mec*$^+$, which restored the nutritional requirement of *me*thionine and *c*ysteine in a mutant strain of *Streoptomyces kasugaensis*.[15] Although the *S. kasugaensis* genome has not been sequenced, related organisms' genomes, such as *S. coelicolor* and *M. tuberculosis*, have been sequenced. In these organisms, the *mec*$^+$ gene is clustered with *cysM* and *cysO*, as noted above. This suggested that *mec*$^+$ plays a role in the cysteine biosynthesis in these organisms, although this activity has yet to be demonstrated. This finding also suggests that for at least some of the actinomycetes, this cluster could be responsible for all of the cellular cysteine.

1.3.3 Sulfide carrier protein

Recently, the mechanism of sulfur transfer into the thiazole ring in thiamin biosynthesis in *Bacillus subtilis* was elucidated.[16,17] As figure 1.6 shows, a small protein, ThiS (7.6 kDa) **13**, is adenylated at the carboxy terminus to **14**. ThiS has two characteristic glycine residues at its carboxy terminus and the adenylation activates the C-terminal carbonyl for addition of sulfide, which is donated by cysteine via a cysteine desulfurase. The sulfide on the thiocarboxylate **15** is eventually incorporated into the thiazole ring **16** of thiamin. Thus, ThiS acts as a sulfide carrier protein.

A similar protein to ThiS has been found in molybdopterin biosynthesis. *E. coli's* MoaD (8.7 kDa) **17** also has two glycine residues at the carboxy terminus and has been shown to be activated by adenylation **18** for sulfide transfer, forming **19**.[18] The sulfide at the carboxy terminus of MoaD is subsequently transferred into the cofactor molybdopterin

20, as shown in figure 1.6. Proteins in the pyridine-2,6-dithiocarboxylate and quinolobactin (both sulfur containing siderophores) biosynthetic clusters have two glycine residues at the carboxy terminus and have been proposed to be sulfide carrier proteins for these secondary metabolites as well.[19,20] Interestingly, these clusters also contain a gene homologous to the *mec*$^{+}$ gene.

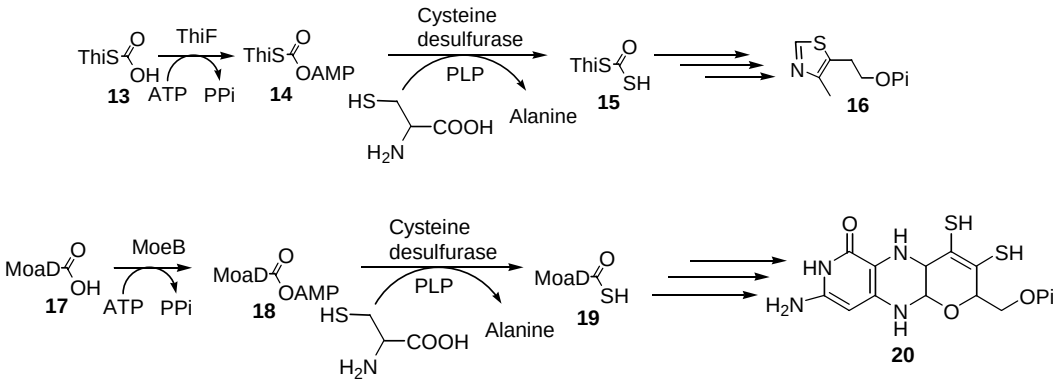

Figure 1.6 Sulfur transfer to the sulfur carrier protein ThiS in thiamin biosynthesis and MoaD in molybdopterin biosynthesis.

Both ThiS and MoaD, the sulfide carrier proteins in thiamin and molybdopterin biosynthesis, share structural similarity to ubiquitin **21**, the small protein that tags cellular proteins for degradation by the proteasome.[21,22] The activation of ubiquitin prior to tagging doomed proteins is similar to the activation of ThiS and MoaD for sulfide transfer. Ubiquitin, which has two glycine residues at its carboxy terminus, is first activated through adenylation to **22**. The adenylation activates ubiquitin for conjugation to cysteine residues of E1 and E2 proteins. E3 conjugates the doomed protein onto ubiquitin, which is then transferred to the proteasome. At the proteasome, the Rpn11 subunit releases ubiquitin and delivers the doomed protein into the proteasome for degradation (figure 1.7).

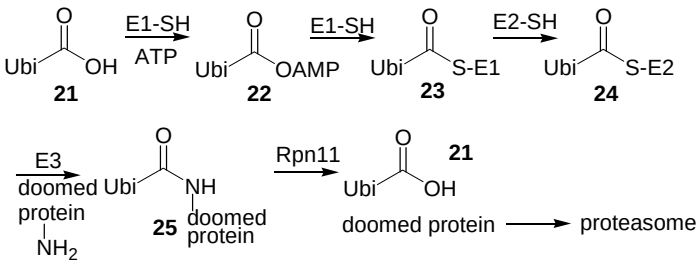

Figure 1.7 Ubiquitin is activated through adenylation followed by conjugation onto the E1 and E2 proteins. E3 catalyzes the conjugation of doomed proteins onto ubiquitin, which is transferred to the proteasome.

In the putative cysteine biosynthetic cluster in the actinomycetes mentioned above, the *cysO* gene (Rv1335) encodes a protein which shares 13% sequence similarity with *B. subtilis* ThiS. This protein, which is 10 kDa, also has two glycine residues at the carboxy terminus. Amino acid alignment of CysO and sulfide carrier proteins ThiS and MoaD as well as ubiquitin is shown in figure 1.8. The similarity between these proteins suggests that CysO may be a sulfide carrier protein for cysteine biosynthesis.

```
           1       10        20        30        40        50        60        70        80        90  94
           |--------+---------+---------+---------+---------+---------+---------+---------+---------+---|
ThiS                                    MLQLNGKDVKWKKDTGTIQDLLASYQLENKIVIVERNKEIIGKERYHEVELCDRDVIEIVHFVGGG
MoaD                 MIKILLFAGLAEQAGTQAIEIDMEQATTDEIKASLKEQYGLESIDTAM-IAV-NESYVKEN----TSVSSGDTVAIIPPVSGG
CysO      MNVTVSIPTILRPHTGGQKSVSASGDTLGAVISDLEANYSGISERLMDPSSPGKLHRFVNIYV-NDEDVRFSGGLATAIADGDSVTILPAVAGG
Ubiquitin                MQIFVKTLTGKTITLEVEPSD-TIENVKAKIQDKEGIPPDQQRL-IFA-GKQLEDGRTLSDYNIQKESTLHLVLRLRGG
Consensus  ..........................t..l.....#.........iq#......l.....I...nke.............d.d...iv..v.GG
```

Figure 1.8 Amino acid alignment of sulfide carrier proteins ThiS, MoaD, ubiquitin and CysO using MultAlin.

1.4 Biosynthetic proposal

The *M. tuberculosis* cluster, which is upregulated upon oxidative stress, encodes a putative cysteine synthase (CysM), a gene necessary for cysteine and methionine biosynthesis (*mec*$^+$), and a putative sulfide carrier protein (CysO). We propose this cluster of genes is required to catalyze a novel route to cysteine, in which a sulfide carrier

protein is used instead of sulfide as the immediate sulfur donor. Based on annotation and sequence homology, we propose the mechanism for cysteine biosynthesis shown in figure 1.9.

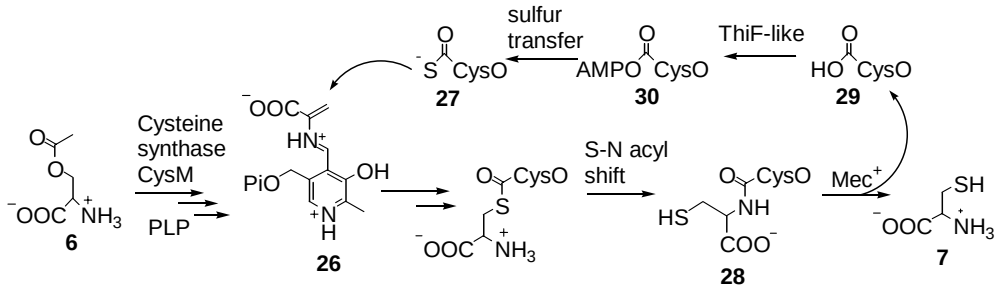

Figure 1.9 Proposed mechanism of cysteine formation by the new cluster in *M. tuberculosis*.

We propose the PLP-dependent deacetylation of O-acetylserine **6** by CysM, forming the α-aminoacrylate **26**. In the direct sulfuration pathway, sulfide would add to the α-aminoacrylate **26** to form cysteine **7**. In our proposed pathway, the thiocarboxylate **27** at the carboxy terminus of CysO would add to the α-aminoacrylate **26**, forming a covalent adduct between the small protein CysO and cysteine. CysO would act as a sulfide carrier protein. Following an S-N acyl shift, we propose that the *mec*$^+$ gene product, which is a putative protease, hydrolyzes the covalent adduct **28** to release cysteine **7** and regenerate CysO-carboxylate **29**. Mec$^+$ has a JAMM (Jab1/MPN domain metalloenzyme) motif, which consists of $EX_nHXHX_{10}D$ and is found in a proteasomal subunit. The two histidines and aspartate are proposed to chelate a metal ion, facilitating hydrolysis of the substrate. The proteasomal subunit Rpn11 in budding yeast, for example, is proposed to hydrolyze the amide bond between the carboxy terminus of ubiquitin and the doomed protein sent to the proteasome (figure 1.7).[23] A similar reaction is proposed for Mec$^+$.

As in thiamin and molybdopterin biosyntheses, we propose that CysO **29** would be activated through adenylation to **30** by a ThiF or MoeB-like protein. There are no

proteins in or near the *M. tuberculosis* cluster that resemble ThiF or MoeB, however, the sequence of *Pseudomonas aeruginosa* PAO1 could provide some insights. *P. aeruginosa* PAO1 contains the cluster of putative cysteine biosynthetic genes which was described above. This cluster contains *mec*$^{+}$, *cysM*, an acetyltransferase gene, as well as a gene annotated as *moeB*. The cluster is depicted in figure 1.10. Interestingly, there is no *cysO* gene present in the cluster and there is no evidence of a *cysO* reading frame (no glycine-glycine motif followed by a stop codon and no evidence of gene fusion with *moeB*). The MoeB in *P. aeruginosa* PAO1 aligns well with a MoeZ protein (Rv3206) in *M. tuberculosis* (44% identity, 28% similarity) and this gene was upregulated by σ^{H} upon oxidative stress in *M. tuberculosis*, along with the putative cysteine biosynthetic genes.[13] *M. tuberculosis* MoeZ contains a dinucleotide binding domain and a rhodanese domain, which could potentially serve as the adenylation and sulfide transfer protein needed for thiocarboxylate formation on CysO. We propose that the gene product of Rv3206 (MoeZ) will adenylate and transfer sulfide (from an unknown source) to CysO.

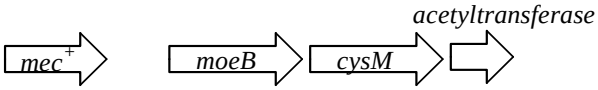

Figure 1.10 Gene organization of a putative cysteine biosynthetic gene cluster in *P. aeruginosa*.

In summary, we have described a unique set of genes that we believe is involved in a novel route to cysteine biosynthesis in several organisms. We have outlined the proposed biosynthetic route and the first few chapters of this thesis will provide biochemical evidence for this new biosynthetic pathway for cysteine.

1.5 References

1. Segal, H. L.; Boyer, P. D. (1953) *J. Biol. Chem.* **204,** 265-281.

2. Cumming, R.; Andon, N.; Haynes, P.; Park, M.; Fischer, W.; Schubert, D. (2004) *J. Biol. Chem.* **279,** 21749-21758.

3. Seiflein, T.; Lawrence, J. (2001) *J. Bacteriol.* **183,** 336-346.

4. Wei, J.; Tang, Q.; Varlamova, O.; Roche, C.; Lee, R.; Leyh, T. (2002) *Biochemistry* **41,** 8493-8498.

5. Schnell, R.; Sandalova, T.; Hellman, U.; Lindqvist, Y.; Schneider, G. (2005) *J. Biol. Chem.*

6. Ono, B.; Hazu, T.; Yoshida, S.; Kawato, T.; Shinoda, S.; Brzvwczy, J.; Paszewski, A. (1999) *Yeast* **15,** 1365-1375.

7. Kitabatake, M.; So, M.; Tumbula, D.; Soll, D. (2000) *J. Bacteriol.* **182,** 143-145.

8. White, R. (2003) *Biochim. Biophys. Acta* 25595.

9. Kredich, N. (1971) *J. Biol. Chem.* **246,** 3474-3484.

10. Filutowicz, M.; Waiter, A.; Hulanicka, D. (1982) *J. Gen. Microbiol.* **128,** 1791-1794.

11. Sun, M.; Andreassi, J.; Liu, S.; Pinto, R.; Triccas, J.; Leyh, T. (2005) *J. Biol. Chem.* **2280,** 7861-7866.

12. Wooff, E.; Michell, S.; Gordon, S.; Chambers, M.; Bardarov, S.; Jacobs, W.; R., H.; Wheeler, P. (2002) *Mol. Microbiol.* **43,** 653-663.

13. Manganelli, R.; Voskuil, M.; Schoolnik, G.; Dubnau, E.; Gomez, M.; Smith, I. (2002) *Mol. Microbiol.* **45,** 365-374.

14. Paget, M.; Molle, V.; Cohen, G.; Aharonowitz, Y.; Buttner, M. (2001) *Mol. Microbiol.* **42,** 1007-1020.

15. Hirasawa, K.; Ichihara, M.; Okanishi, M. (1985) *J. Antibiotics* **38,** 1795-1798.

16. Park, J.-H.; Dorrestein, P.; Zhai, H.; Kinsland, C.; McLafferty, F.; Begley, T. (2003) *Biochemistry* **42,** 12430-12438.

17. Dorrestein, P.; Zhai, H.; McLafferty, F.; Begley, T. (2004) *Chem. Biol.* **11,** 1373-1381.

18. Leimkuhler, S.; Wuebbens, M.; Rajagopalan, K. (2001) *J. Biol. Chem.* **276,** 34695-34701.

19. Sepulveda-Torres, L.; Huang, A.; Kim, H.; Criddle, C. (2002) *J. Mol. Microbiol. Biotechnol.* **4,** 151-161.

20. Matthijs, S.; Baysse, C.; Koedam, N.; Tehrani, K.; Verheyden, L.; Budzikiewicz, H.; Schaefer, M.; Hoorelbeke, B.; Meyer, J.; De Greve, H.; Cornelis, P. (2004) *Mol. Microbiol.* **52,** 371-384.

21. Wang, C.; Xi, J.; Begley, T.; Nicholson, L. (2001) *Nat. Struct. Biol.* **8,** 47-51.

22. Rudolph, M.; Wuebbens, M.; Rajagopalan, K.; Schindelin, H. (2001) *Nat. Struct. Biol.* **8,** 42-46.

23. Maytal-Kivity, V.; Reis, N.; Hofmann, K.; Glickman, M. (2002) *BMC Biochemistry* **3,**

Chapter 2

Cloning, Expression and Gene Characterization[i]

2.1 Reconstituting the pathway

To determine whether the proposed biosynthetic pathway is correct, each gene had to be cloned, overexpressed and purified as a soluble protein. The quickest way to determine whether this pathway was operable was to directly form the thiocarboxylate **27** on the carboxy terminus of CysO and check for adduct formation **28** with CysM and O-acetylserine **6**, as this was the most critical part of the proposal outlined in figure 1.9. Once the adduct formation was confirmed, we could test MoeZ for sulfide transfer to CysO. This chapter describes the cloning, expression and activity assays for CysM, CysO and MoeZ.

2.2. Results and discussion

2.2.1 CysM expression and activity assays

M. tuberculosis cysM was cloned into a pET vector, overexpressed in *E. coli* BL21(DE3) cells and purified by Ni-Nta affinity chromatography. The enzyme was stable in 50mM tris, pH8 and stored in 10% glycerol at -80^{o}C until use. Typical yield for 1L of culture was 10 mg. An SDS-PAGE gel of CysM is shown in figure 2.1a. CysM purified with an absorption at 410 nm (figure 2.1b), indicative of a bound PLP cofactor.

[i] Reproduced in part with permission from Burns, K.; Baumgart, S.; Dorrestein, P.; Zhai, H.; McLafferty, F.; Begley, T. (2005) *J. Am. Chem. Soc.* **127**, 11602-11603.

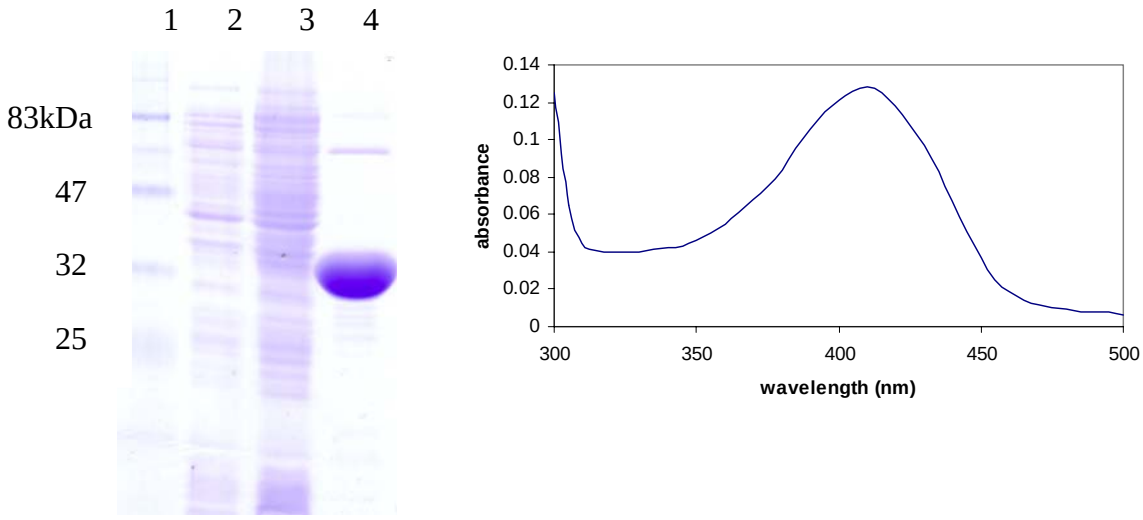

Figure 2.1 a. 12% SDS-PAGE of purified CysM protein. Lane 1, MW markers; lane 2, pre-induction; lane 3, post-induction; lane 4, purified CysM b. UV-Visible absorption scan of pure CysM.

CysM is annotated as a cysteine synthase, so we first tested sulfide **4** and O-acetylserine **6** as substrates using the ninhydrin assay to monitor cysteine **7** formation. Ninhydrin **30** reacts with cysteine **7** under acidic conditions to produce a pink color (λmax 560nm) as shown in figure 2.2.[1] For *M. tuberculosis* CysM, cysteine **7** release is time dependent, enzyme concentration dependent, and substrate concentration dependent. Kinetics were performed on CysM using this assay, and the K_m for O-acetylserine is 4.4mM and the K_m for sulfide is 40μM. These compare well with data reported for other cysteine synthases.[2]

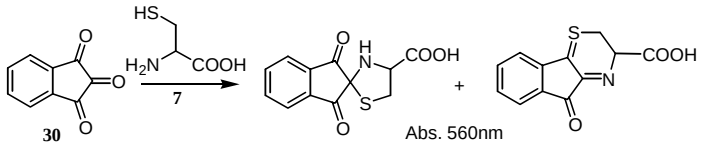

Figure 2.2 Ninhydrin assay for cysteine formation.

2.2.2 CysO-SH as a substrate for CysM

To determine whether CysM catalyzes the formation of a cysteine adduct at the carboxy terminus of CysO, we used intein chemistry to generate the thiocarboxylate on CysO.[3] Forming the thiocarboxylate *in vitro* by-passes the activation of CysO as well as the sulfide transfer steps so that we can rapidly test our hypothesis. The IMPACT (Intein Mediated Purification with an Affinity Chitin-binding Tag) system was used to produce CysO-thiocarboxylate **27**. Briefly, *cysO* was cloned into the amino terminus of an intein construct that is engineered to self-cleave under specific conditions, and has a chitin binding domain (CBD) at the carboxy terminus for purification. When added to chitin affinity resin, washed, and eluted with ammonium sulfide, the eluted protein contains a carboxy terminal thiocarboxylate, as depicted in figure 2.3. CysO was eluted with 30mM ammonium sulfide and desalted into 50mM tris, pH8. Purification of the CysO-thiocarboxylate **27** is shown in the 15% SDS-PAGE gel in figure 2.4.

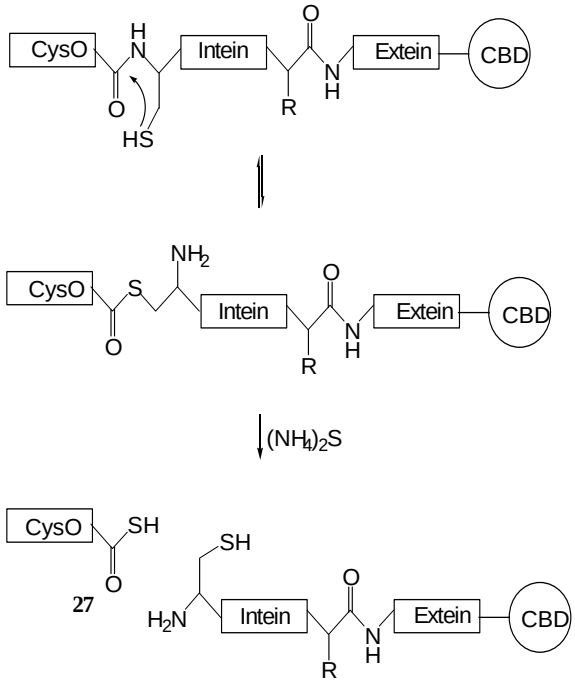

Figure 2.3 Summary of the intein processing used to produce CysO-thiocarboxylate **27**.

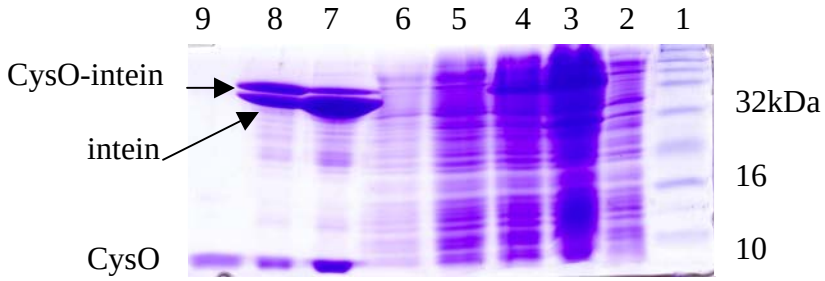

Figure 2.4 15% SDS-PAGE of CysO-thiocarboxylate overexpression and purification. From the right: lane 1, MW markers; lane 2, pre-induction; lane 3, post-induction; lane 4, cleared lysate; lane 5, column flow through; lane 6, wash; lane 7, resin after 30hrs. of cleavage at room temperature; lane 8, resin after 30hrs. of cleavage at 4^{o}C; lane 9, elute from room temperature cleavage.

Analysis of the CysO-thiocarboxylate **27** by ESI-FTMS (ElectroSpray Ionization Fourier Transform Mass Spectrometry) confirmed the formation of a thiocarboxylate with a peak at 9572Da. CysO-thiocarboxylate **27** was incubated with CysM and O-acetylserine **6** in tris buffer at 37^{o}C for various times. When analyzed by ESI-FTMS, a covalent adduct with mass of 9559Da appears with time, as shown in figure 2.5 (in collaboration with Huili Zhai and Fred McLafferty). After 60 minutes, nearly all of the CysO-thiocarboxylate **27** is converted to the 9559Da adduct, and without CysM in the reaction, no adduct forms after 30 minutes. By MS/MS, the covalent adduct was localized to the carboxy terminus of CysO, as expected. By MALDI (Matrix Assisted Laser Desorption/Ionization) mass spectrometry, when CysO-thiocarboxylate **27** and cysteine are incubated, no adduct is formed after one hour, suggesting that adduct formation is dependent on CysM. TB's other cysteine synthase, CysK (Rv2334), was cloned, expressed, purified and tested for adduct formation on CysO-thiocarboxylate **27**. CysK was unable to catalyze adduct formation on CysO, also suggesting the reaction was dependent on CysM (CysK was active as a cysteine synthase with sulfide **4** and O-acetylserine **6** as substrates). Likewise, when serine **5** was substituted for O-acetylserine

6, no adduct was formed, suggesting that the reaction is specific for O-acetylserine **6**. To determine whether the reaction is specific for CysO-thiocarboxylate **27**, ThiS-thiocarboxylate **15** (the sulfide carrier protein for thiamin biosynthesis shown in figure 1.6) was added to the reaction mixture in place of CysO-thiocarboxylate **27** and no shift was observed by MALDI mass spectrometry.

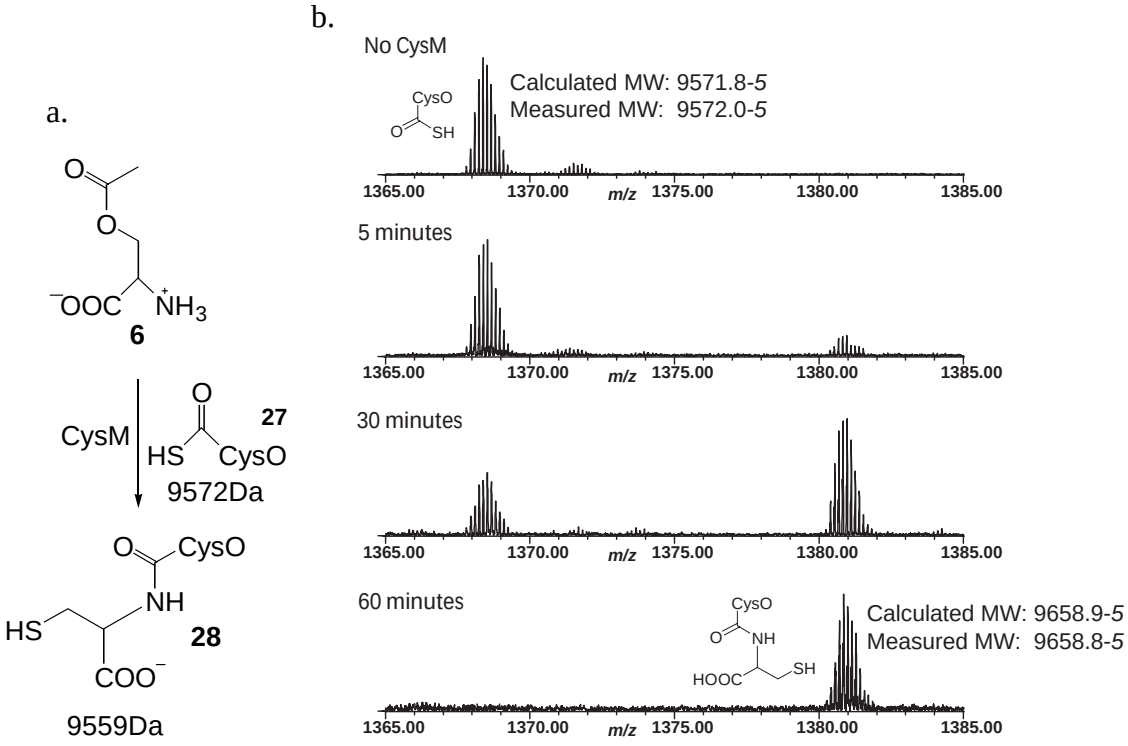

Figure 2.5 ESI-FTMS analysis of the reaction between CysM and CysO-thiocarboxylate **27** in the presence of O-acetylserine **6** a. Reaction monitored by ESI-FTMS b. 70μM CysO-SH, 33μM CysM, 13mM O-acetylserine, and DTT incubated for various times at 37^{o}C.

2.2.3 Expression and activity of MoeZ

In the formation of ThiS-thiocarboxylate **13** in thiamin biosynthesis, ThiS is activated as an acyl adenylate **14** in a reaction catalyzed by ThiF (figure 1.6). The resulting ThiS-adenylate then reacts with sulfide from cysteine desulfurase, which donates the sulfur for

ThiS-thiocarboxylate **15** formation.[4,5] Cysteine is the sulfide donor for ThiS, however, it is unlikely that it is the sulfide donor for CysO-thiocarboxylate **27** as well. Although we have not yet identified the sulfide donor for CysO, we have identified a protein, MoeZ (Rv3206), which has a nucleotide binding domain and may activate CysO **29** through adenylation similar to how ThiF activates ThiS in thiamin biosynthesis. BLAST searches reveal that MoeZ also has a rhodanese homology domain. Proteins with this domain catalyze sulfide transfer, usually from thiosulfate or from mercaptopyruvate, to an acceptor molecule (*in vitro* the acceptor is $^{-}$CN).[6,7] It is likely that MoeZ adenylates and transfers sulfide to CysO **29**.

To test whether MoeZ could catalyze adenylation and sulfide transfer to CysO, both MoeZ and CysO-carboxylate **29** were cloned, expressed and purified by Ni-Nta affinity chromatography. When pure MoeZ was combined with pure CysO, we were unable to observe thiocarboxylate formation on CysO using ATP and sulfide **4** or thiosulfate as the sulfur source. When MoeZ and CysO were co-lysed and co-purified from *E. coli* crude cell lysate, however, we were able to observe CysO-thiocarboxylate **27** formation as shown in figure 2.6 (in collaboration with Sabine Baumgart and Fred McLafferty). We observe conversion to the CysO-thiocarboxylate **27** without the addition of exogenous substrates, which suggests that MoeZ is able to catalyze adenylation and sulfide transfer to CysO from an unidentified sulfur source that is present in *E. coli*.

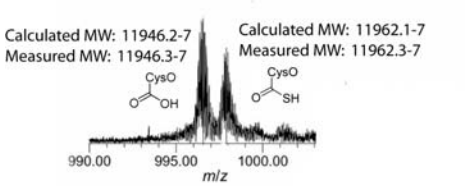

Figure 2.6 ESI-FTMS analysis of the MoeZ catalyzed sulfide transfer onto CysO.

2.3 Conclusion

We've shown that a sulfide carrier protein from *M. tuberculosis*, CysO (Rv1335), in its thiocarboxylate **27** form, is modified to a cysteine adduct **28** by CysM (Rv1336) in the presence of O-acetylserine **6**. The reaction was specific for CysO, CysM and O-acetylserine: no reaction was detected when CysO was replaced with ThiS **15**, the sulfur carrier protein from thiamin biosynthesis; no reaction was detected when CysM was replaced by CysK, another cysteine synthase from TB; and no reaction was detected when O-acetylserine **6** was replaced with serine **5**. Preliminary results suggest that MoeZ (Rv3206) is responsible for activating CysO to the C-terminal thiocarboxylate **27**, however, the details of this reaction, including the sulfur source, have yet to be established. The results are summarized in figure 2.7.

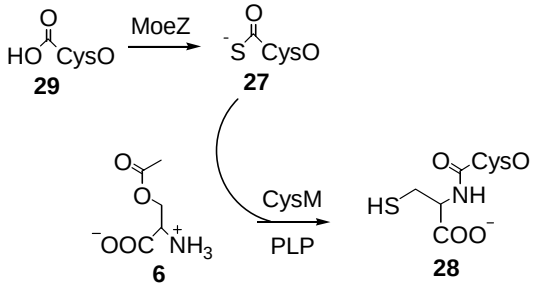

Figure 2.7 In this pathway, MoeZ catalyzes sulfide transfer to CysO. The CysO-thiocarboxylate **27** combines with O-acetylserine **6** to form CysO-cysteine **28**.

2.4 Experimental procedures

2.4.1 Materials and methods

2.4.1.1 Materials: pET16b vector was from Novagen, restriction enzymes from New England Biolabs, primers were ordered from Integrated DNA technologies. *M. tuberculosis* H37Rv DNA was a gift from Clifton Barry, NIH. Pfx Platinum polymerase was from Invitrogen. A Perkin Elmer GeneAmp PCR System 2400 was used for PCR. QIAquick gel extraction kit and PCR purification kit were purchased from Qiagen, and

miniprep kit was from Promega. T4 DNA ligase was purchased from New England Biolabs, One Shot TOP10 cells were from invitrogen. Clones were sequenced at the Bioresource Center at Cornell University. DH5α was used for propagation and storage; BL21(DE3) for overexpression; both were purchased from Novagen. Ni-Nta resin was from Qiagen, chitin resin was from New England Biolabs and all chemicals were purchased from Sigma. DG10 desalting columns were purchased from BioRad, and Centricon ultra concentrators were from Amicon. Coommassie was purchased from Pierce.

2.4.1.2 Cloning, Expression and Purification of CysM (CysM.16): *M. tuberculosis* Rv1336 was amplified using the following primers: 5'for-GGG TGA GCG GAG CAT ATG ACA CGA TAC GAC-3'; 5'rev-TTC GGA TCC GGC GGA TCC TCA TGC CCA TAG-3'. *Nde*I and *Bam*HI restriction sites were added to the forward and reverse primer, respectively. The gene was amplified using Pfx Platinum polymerase with a 1.5min extension time with *M. tuberculosis* H37Rv DNA as the template. Upon purification of the PCR fragment from the agarose gel, the product and the pET16b vector were cut with *Nde*I and *Bam*HI. Enzymes were removed using the PCR purification kit and by agarose gel electrophoresis. The cut pET16b vector and cut PCR product were ligated with T4 ligase at room temperature for 2 hours. One Shot TOP10 cells were transformed with 2.5μL of the ligation mixture and plated on LB-Amp plates. Colonies were checked for insert by prepping out the plasmid and cutting with Nde1/BamH1. Colonies with insert were sequenced.

E. coli BL21(DE3) cells were used for protein expression. Cells were grown to an OD_{600} of 0.5 and induced with 1mM IPTG at 25^{o}C. After 8 hours of induction, the cells were harvested at 8,000 rpm for 10 minutes and stored at -20^{o}C until purification.

Cells containing overexpressed protein were resuspended in lysis buffer (20mM tris pH7.9, 500mM NaCl, 5mM imidazole) with lysozyme. The cells were lysed by sonication (30-2 second pulses, 3 cycles), and the cell debris was removed by centrifugation for 30minutes at 17,000 rpm. The cleared lysate was passed through pre-equilibrated (with lysis buffer) Ni-Nta resin. Following a quick wash with lysis buffer, the resin was washed with wash buffer (20mM tris pH7.9, 500mM NaCl, 60mM imidazole) until little protein eluted by Coommassie. CysM was eluted with elution buffer (10mM tris pH7.9, 250mM NaCl, 500mM imidazole), desalted into 50mM tris pH8 using DG10 desalting columns, and concentrated. CysM was stored in 10% glycerol at -80^{o}C until use. Typical yield for 1L of culture was 10 mg.

2.4.1.3 Cloning, Expression and Purification of CysO-thiocarboxylate (CysO.TYB1): *M. tuberculosis* Rv1335 was amplified using the following primers: 5' for-CCG AGA AAG GCC CAT ATG AAC GTC ACC GTA-3'; 5' rev-CGT GTC ATG GCT CTT CCG CAC CCA CCG GCC ACG-3'. *Nde*I and *Sap*I restriction sites were added to the forward and reverse primer, respectively. The gene was amplified using Pfx Platinum DNA polymerase with a 30sec extension time using *M. tuberculosis* H37Rv as the template DNA. Upon purification of the PCR fragment from the agarose gel, the product and the pTYB1 vector were cut with *Nde*I and *Sap*I. Enzymes were removed using the PCR purification kit and by agarose gel electrophoresis. The cut pTYB1 vector and cut PCR product were ligated with T4 ligase at room temperature for 2 hours. One Shot TOP10 cells were transformed with 2.5μL of the ligation mixture and plated on LB-Amp plates. Colonies were checked for insert by prepping out the plasmid and cutting with *Pvu*I (the *Sap*I site is lost during cloning). Colonies with insert were sequenced.

E. coli BL21(DE3) cells were used for protein expression. Cells were grown to an OD_{600} of 0.5 and induced with 1mM IPTG at 15^{o}C. After 16 hours of induction, the cells were harvested at 8,000 rpm for 10 minutes and stored at -20^{o}C until purification.

Cells containing overexpressed protein were resuspended in lysis buffer (20mM tris pH8, 500mM NaCl, 1mM EDTA and 0.1% triton X-100). The cells were lysed by sonication (30-2 second pulses, 3 cycles), and the cell debris was removed by centrifugation for 30 minutes at 17,000 rpm. The cleared lysate was passed through pre-equilibrated (column buffer: 20mM tris pH8, 500mM NaCl, 1mM EDTA) chitin resin. The column was washed with column buffer until little protein eluted by Coommassie. When little protein washed off, the column was quickly rinsed with cleavage buffer (20mM tris pH8, 500mM NaCl, 1mM EDTA, 30mM $(NH_4)_2S$), capped and let sit at 4^{o}C for 40 hours. After 40 hours, the protein was eluted and immediately desalted into 50mM tris pH8 using DG10 desalting columns, and concentrated. CysO-SH was stored in 10% glycerol at -80^{o}C until use. Typical yield for 1L of culture was 2 mg.

2.4.1.4 Cloning, Expression and Purification of CysK (CysK.16): *M. tuberculosis* Rv2334 was amplified using the following primers: 5'for-TGT TGG GCG TAG CAT ATG AGC ATC GCC GAG-3'; 5'rev-CAT GGC CGT CAG CTC GAG TTA GTC AGC CAC-3'. *Nde*I and *Xho*I restriction sites were added to the forward and reverse primer, respectively. The gene was amplified using Pfx Platinum DNA polymerase with a 1.5min extension time using *M. tuberculosis* H37Rv as the template DNA. Cloning, expression and purification proceeded as for CysM. CysK was stored in 10% glycerol at -80^{o}C until use. Typical yield for 1L of culture was 8 mg.

2.4.1.5 Cloning, Expression and Purification of MoeZ (MoeZ.16): *M. tuberculosis* Rv3206 was amplified using the following primers: 5'for-TAA CCG AGG

AGA CAT ATG GTG TCG ACA TCC-3'; 5'rev-GGG CCT GTA CTC GAG CTA GTA CAT CAC CAT-3'. *Nde*I and *Xho*I restriction sites were added to the forward and reverse primer, respectively. The gene was amplified using Pfx Platinum DNA polymerase with a 1.5min extension time using *M. tuberculosis* H37Rv as the template DNA. Cloning, expression and purification proceeded as for CysM, except expression was only 4 hours. MoeZ often precipitated upon purification if expressed longer than 4 hours. Typical yield for 1L of culture was 50 mg.

2.4.1.6 Cloning, Expression and Purification of CysO (CysO.16): *M. tuberculosis* Rv1335 was amplified using the following primers: 5'for-CCG AGA AAG GCC CAT ATG AAC GTC ACC GTA-3'; 5'rev-TCG TGT CAT GTC CTC GAG TCA CCC ACC GGC-3'. *Nde*I and *Xho*I restriction sites were added to the forward and reverse primer, respectively. The gene was amplified using Pfx Platinum DNA polymerase with a 30 second extension time using *M. tuberculosis* H37Rv as the template DNA. Cloning, expression and purification proceeded as for CysM. Typical yield for 1L of culture was 7 mg.

2.4.2 Assays

2.4.2.1 Materials: All chemicals were purchased from Sigma. Biospin-6 desalting columns are from Bio-Rad. ESI-FTMS was performed by the McLafferty group at Cornell University. MALDI data was collected at the Bioresource Center at Cornell University.

2.4.2.2 Ninhydrin assay with CysM, O-acetylserine and sulfide: In 1.2mL total, 39μg CysM was added to 10mM O-acetylserine, 10mM DTT in 100mM phosphate pH8 with various concentrations of Na_2S (10μM – 200μM). The reactions were kept at

37°C. At 1, 2, 4, 6 and 10 minutes, 200μL samples were withdrawn and added to 350μL of ninhydrin solution (1.3% ninhydrin in 1 HCl: 4 acetic acid). After 10 minutes at 100°C, the samples were cooled, 700μL ethanol was added, and absorbance at 560nm was recorded. Samples were done in triplicate and the blank had no enzyme.

In 1.2mL total, 39μg CysM was added to 3mM Na_2S, 10mM DTT in 100mM phosphate pH8 with various concentrations of O-acetylserine (0.4mM – 7.5mM). Samples were analyzed as for sulfide.

2.4.2.3 CysO-cysteine formation by ESI-FTMS: 13mM O-acetylserine, 300μg CysO-thiocarboxylate, and 6.7mM DTT were incubated with 480μg CysM in 50mM tris pH8. After incubation at 37°C for various time points, the samples were frozen at -80°C. The samples were analyzed by ESI-FTMS.

ThiS control: ThiS-SH was formed in vitro using recombinant ThiSGF obtained from Pieter Dorrestein. Briefly, 7.5mg ThiSGF was added to 126μg NifZ (provided by Colleen McGrath), 1mM cysteine, 4.3mM ATP and 4.3mM $MgCl_2$. After 2 hours at room temperature, 100μL of reaction was desalted into tris biospin-6 columns. To 50μL of the desalted reaction, 26μg CysM and 6.7mM O-acetylserine were added in 67mM tris pH8 to a final volume of 150μL. After 1 hour at room temperature (the sample at 37°C precipitated, presumably due to ThiF, which is unstable), the samples were desalted into water and analyzed by MALDI mass spectrometry.

CysO and cysteine control: CysO-SH (unknown amount) was added to 1mM O-acetylserine, 1mM DTT and 1mM cysteine in 100mM phosphate pH8 in 50μL total volume. The sample was desalted into water after 1 hour at 37°C and analyzed by MALDI mass spectrometry.

CysK control: Purified CysK was active by the ninhydrin assay using O-acetylserine and Na_2S as substrates. 10μg CysK was added to 75μg CysO-SH, 20mM O-acetylserine and 5mM DTT in 50mM tris pH8 in a total volume of 50μL for 1 hour at 37°C. The sample was desalted into water and analyzed by MALDI mass spectrometry.

Serine control: CysO-SH (unknown amount) was added to 100μg CysM, 1mM DTT and 1mM serine in 100mM phosphate pH8 in 50μL total volume. The sample was desalted into water after 1 hour at 37°C and analyzed by MALDI mass spectrometry.

2.4.2.4 Copurification of CysO and MoeZ: CysO and MoeZ were expressed separately in *E. coli* at reduced temperature. After the cell pellets were resuspended in lysis buffer and incubated with lysozyme, the pellets were combined and sonicated, as usual. Purification proceeded according to normal protocol. The sample was desalted into 50mM tris pH8 and concentrated prior to analysis by ESI-FTMS.

2.5 References

1. Chinard, F. (1952) *J. Biol. Chem.* **199,** 91-95.

2. Mino, K.; Ishikawa, K. (2003) *J. Bacteriol.* **185,** 2277-2284.

3. Kinsland, C.; Taylor, S.; Kelleher, N.; McLafferty, F.; Begley, T. (1998) *Protein Sci.* **7,** 1839-1842.

4. Park, J.-H.; Dorrestein, P.; Zhai, H.; Kinsland, C.; McLafferty, F.; Begley, T. (2003) *Biochemistry* **42,** 12430-12438.

5. Dorrestein, P.; Zhai, H.; McLafferty, F.; Begley, T. (2004) *Chem. Biol.* **11,** 1373-1381.

6. Bordo, D.; Bork, P. (2002) *EMBO Rep.* **3,** 741-746.

7. Matthies, A.; Nimtz, M.; Leimkuhler, S. (2005) *Biochemistry* **44,** 7912-7920.

Chapter 3

Studies on Mec^{+i}

3.1 The JAMM motif

The *mec*$^+$ gene (Rv1334), which encodes for a protein with a JAMM motif (Jab1/MPN domain metalloenzyme motif; $EX_nHS/THX_{10}D$), is clustered with the *cysO* and *cysM* genes in several actinomycetes (figure 1.5). *mec*$^+$ was originally identified by its ability to restore the nutritional requirement for *me*thionine and *c*ysteine in a mutant strain of *S. kasugaensis*, however, no function was attributed to this gene at the time.[1] BLAST searches annotate it as a metal-dependent hydrolase.

The JAMM motif is found in archaea, bacteria and eukaryotes and until recently, no function was associated with it. In 2002, Verma found that the eukaryotic JAMM motif found in the Rpn11 subunit of the proteasome is responsible for cleaving doomed proteins from the C-terminus of ubiquitin prior to delivery into the proteasome (figure 1.7).[2] This process regenerates ubiquitin. The amino acid sequence alignment of Rpn11 and Mec$^+$ is shown in figure 3.1, with the JAMM motif highlighted with arrows. Based on the JAMM motif homology, we propose that Mec$^+$ would cleave the cysteine from the C-terminus of CysO-cysteine adduct. This process would generate CysO-carboxylate and cysteine, as shown in figure 3.2. This chapter will describe the reconstitution of Mec$^+$ activity with regard to the proposed cysteine biosynthetic pathway, discuss the importance of the JAMM motif, and define the substrate specificity of Mec$^+$.

[i] Reproduced in part with permission from Burns, K.; Baumgart, S.; Dorrestein, P.; Zhai, H.; McLafferty, F.; Begley, T. (2005) *J. Am. Chem. Soc.* **127**, 11602-11603.

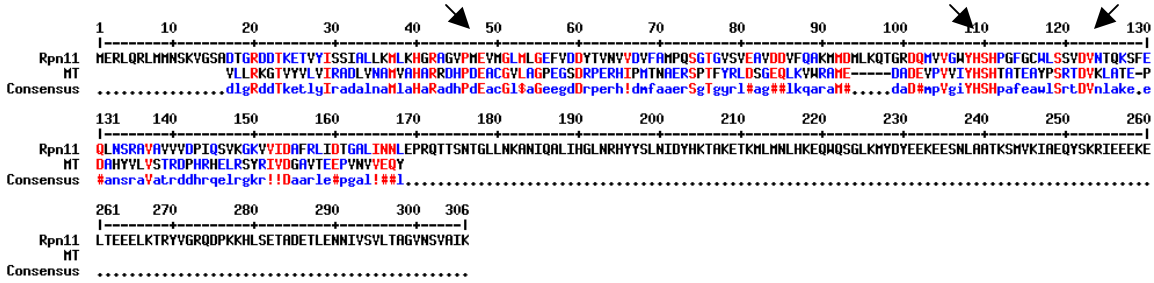

Figure 3.1 Amino acid sequence alignment of Mec$^+$ and Rpn11 using MultAlin. MT, *M. tuberculosis* Mec$^+$. Arrows indicate the amino acids in the JAMM motif EX$_n$HS/THX$_{10}$D.

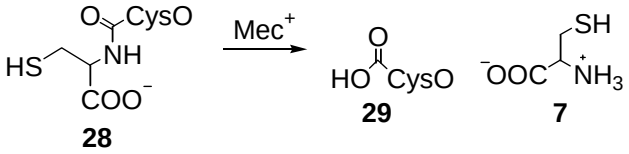

28 **29** **7**

Figure 3.2 Proposed reaction catalyzed by Mec$^+$.

3.2 Results and discussion

3.2.1 Expression and activity of Mec$^+$

M. tuberculosis mec$^+$ was cloned into the plasmid pET-MAL-HT (6 histidine residues at the carboxy terminus of maltose binding protein), which is a home-made vector made by Joanne Widom at Cornell University. The maltose binding protein helped to solubilize Mec$^+$ (which was not very soluble as a his-tag construct) and the 6x histidine tag allowed for purification by Ni-Nta affinity chromatography. The protein was cloned, overexpressed, purified and desalted into 50mM tris buffered to pH8. An SDS-PAGE gel of pure Mec$^+$ is shown in figure 3.3. Typical yield for 1L of culture was 7 mg.

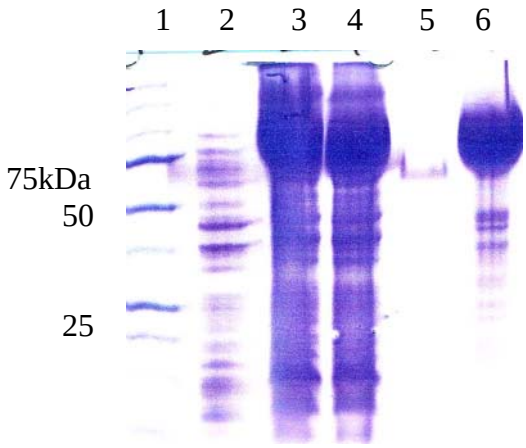

Figure 3.3 12% SDS-PAGE of purified Mec^+ protein. Lane 1, MW markers; lane 2, pre-induction; lane 3, soluble protein; lane 4, flow through; lane 5, wash; lane 6, eluted Mec^+.

Upon addition of Mec^+ to reaction mixtures containing the CysM-derived cysteine adduct on CysO, we observe the formation of CysO-carboxylate **29** (9556Da) by ESI-FTMS (figure 3.4) (in collaboration with Sabine Baumgart and Fred McLafferty). In addition to the hydrolysis of the adduct, we also observe the formation of cysteine **7** with ninhydrin, confirming that Mec^+ hydrolyzes cysteine from the carboxy terminus of CysO. When 2.6 nmoles of CysO-thiocarboxylate **27** was added to CysM and Mec^+ in the presence of O-acetylserine **6**, 2.7±0.16 nmoles of cysteine **7** were produced, indicating full conversion to cysteine.

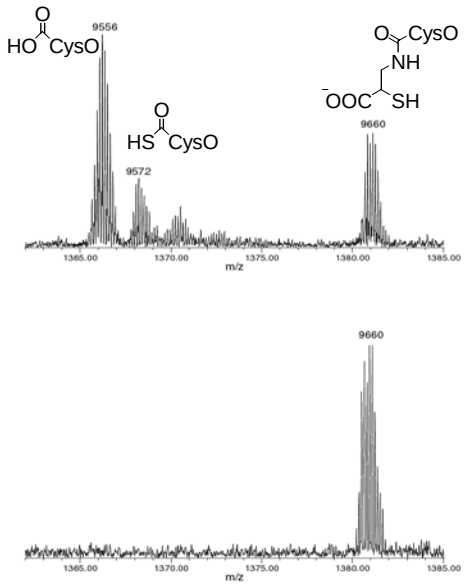

Figure 3.4 ESI-FTMS analysis of the Mec$^+$ reaction a. Reaction containing CysO-SH **27**, CysM, O-acetylserine **6**, and Mec$^+$ b. Reaction containing CysO-SH **27** and O-acetylserine **6**.

3.2.2 Mec$^+$ cleaves the amide bond

Prior to cleavage by Mec$^+$, we propose the CysO-cysteine adduct **28** that is initially formed by CysM will undergo an S-N acyl shift to yield the more stable amide, as shown in figure 3.5.[3] To provide additional support for Mec$^+$ hydrolysis of the amide and not the thioester, we created a CysO construct containing an additional cysteine at the carboxy terminus and cloned it into a pET vector for overexpression (hisCysO-cysteine). Upon incubation of hisCysO-cysteine with Mec$^+$, we observe the production of cysteine **7** by the ninhydrin assay and hydrolysis of the hisCysO-cysteine construct by ESI-FTMS. The mass spectrum is shown in figure 3.6a (in collaboration with Sabine Baumgart and Fred McLafferty). To rule out the possibility that the hisCysO-cysteine construct was forming the thioester through an N-S acyl shift and that is what Mec$^+$ hydrolyzes, we created a CysO construct with an alanine residue at the C-terminus (CysO-ala). This construct would be unable to form the thioester. Mec$^+$ hydrolyzes the CysO-alanine

construct, which suggests that it recognizes and cleaves the amide and not the thioester at the C-terminus of CysO.

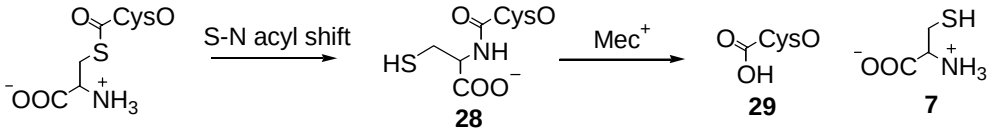

Scheme 3.5 Proposed non-enzymatic S-N acyl shift.

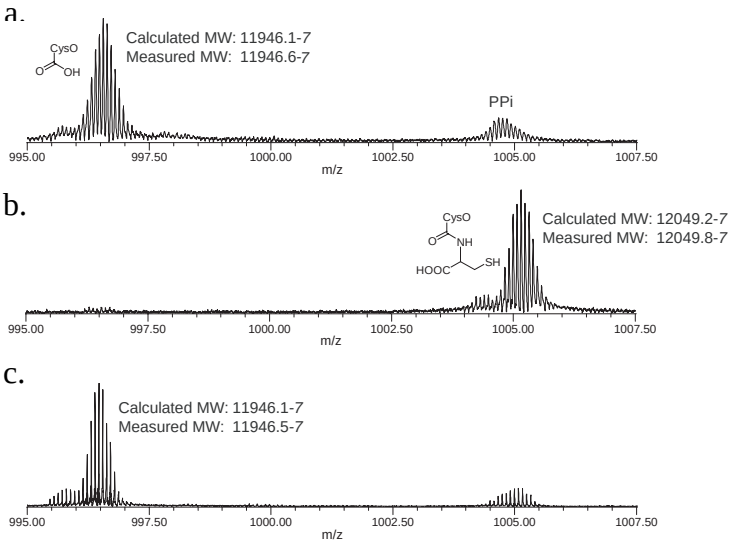

Figure 3.6 The reaction between the hisCysO-cysteine construct and Mec^+ a. hisCysO-cysteine with Mec^+ b. hisCysO-cysteine, where Mec^+ was pre-incubated with EDTA c. hisCysO-cysteine, Mec^+ pre-incubated with EDTA, and recovered with Zn^{2+}.

3.2.3 Mec^+ is a metal dependent hydrolase

Mec^+ is annotated as a metal-dependent hydrolase. The protein is active upon purification, without addition of exogenous metal. To confirm the dependence on a metal ion, Mec^+ was pre-incubated with EDTA and desalted to remove any chelated metal ion. No cysteine was evident by the ninhydrin assay when hisCysO-cysteine was used as the substrate for EDTA-treated Mec^+. When Mec^+ was pre-incubated with EDTA, no hydrolysis is observed by ESI-FTMS as well (figure 3.6b). Addition of Zn^{2+} to this

reaction restored the hydrolytic activity (figure 3.6c), and Mg^{2+} had no affect. This result confirms that Mec^{+} is a Zn^{2+} dependent hydrolase, and it purifies with a bound metal ion.

3.2.4 JAMM motif analysis

To confirm the importance of the JAMM motif ($EX_nHS/THX_{10}D$) for Mec^{+} activity, we used site-directed mutagenesis to mutate two of the conserved residues in the motif. Serine 89 and Aspartate 101 were mutated to alanine and the mutants were analyzed for cysteine production by the ninhydrin assay as well as hisCysO-cysteine hydrolysis by ESI-FTMS. The ninhydrin assay indicated that no cysteine was produced and ESI-FTMS analysis of the hisCysO-cysteine construct also indicated that the mutants were inactive. This suggests that these two residues, and the JAMM motif in general, are essential for Mec^{+} activity.

3.2.5 Substrate specificity of Mec^{+}

The proteasomal subunit Rpn11 is able to recognize and cleave the amide bond between ubiquitin and a lysine residue of the doomed protein. Similarly, Mec^{+} hydrolyzes the amide between CysO and a C-terminal cysteine residue. Both ubiquitin and CysO are small proteins with two glycine residues at the C-terminus. We wanted to understand the substrate specificity of Mec^{+} to identify a possible recognition motif on CysO. To determine the substrate specificity of Mec^{+}, a variety of CysO analogs were constructed and analyzed for hydrolysis by Mec^{+}. The C-terminal cysteine residue was replaced by a serine (CysO-ser), an alanine (CysO-ala), an alanine-cysteine (CysO-ala-cys), and a cysteine-alanine (CysO-cys-ala). These are displayed in figure 3.7. All of these constructs were substrates for Mec^{+}, however, they were not as efficient as hisCysO-cysteine. In all cases, Mec^{+} recognized and cleaved after the conserved C-terminal glycine residues on CysO, even in the CysO-ala-cys construct. When one of the C-terminal glycine residues was removed, cleavage by Mec^{+} was greatly reduced,

indicating that the glycine residues at the C-terminus are important for recognition and cleavage and the residues following the glycines are not as important.

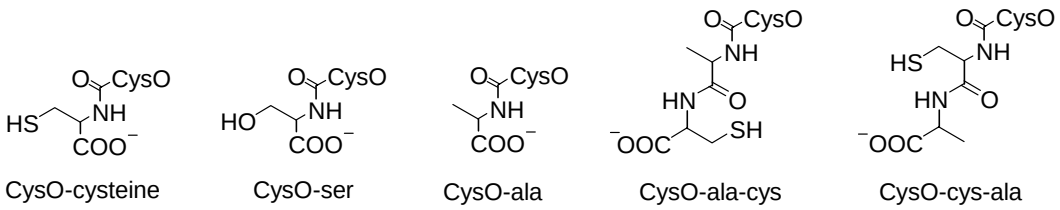

Figure 3.7 Structures of the CysO constructs made and tested as substrates for Mec^{+}.

3.3 Conclusion

The Mec^{+} protein, a Zn^{2+} dependent hydrolase, is able to recognize and cleave the amide bond at the C-terminus of CysO-cysteine **28**. This reaction releases cysteine **7** and regenerates CysO-carboxylate **29**. The JAMM motif requires a metal ion for activity, and this metal most likely activates water for hydrolysis of the amide bond. The JAMM motif is important for catalysis; mutagenesis of two of the conserved residues abolishes activity, presumably due to the loss of the metal ion. Although it appears that Mec^{+} is promiscuous in its substrates, it has some specificity for cleaving after the C-terminal glycine residues of CysO.

3.4 Experimental procedures

3.4.1 Materials and methods

3.4.1.1 Materials: pET16b vector was from Novagen, restriction enzymes from New England Biolabs, primers were ordered from Integrated DNA technologies. A Perkin Elmer GeneAmp PCR System 2400 was used for PCR and mutagenesis. Pfx Platinum polymerase was from Invitrogen. Site directed mutagenesis kit was from Stratagene. QIAquick gel extraction kit and PCR purification kit were purchased from Qiagen, and

miniprep kit was from Promega. T4 DNA ligase was purchased from New England Biolabs and One Shot TOP10 cells were from Invitrogen. Clones were sequenced at the Bioresource Center at Cornell University. DH5α was used for propagation and storage; BL21(DE3) for overexpression; both were purchased from Novagen. Ni-Nta resin was from Qiagen and all chemicals were purchased from Sigma. DG10 desalting columns were purchased from BioRad, and Centricon ultra concentrators were from Amicon.

3.4.1.2 Cloning, Expression and Purification of Mec$^+$ (Mec$^+$.MBPHT): *M. tuberculosis* Rv1334 was amplified using the following primers: 5'for-TCG GGT CCT GAA GGA TCC GTG TTG CTT AGG-3'; 5'rev-GGC CTT TCT CGG CTC GAG TCA GTA CTG CTC-3'. *Bam*HI and *Xho*I restriction sites were added to the forward and reverse primer, respectively. The gene was amplified using Pfx Platinum DNA polymerase with a 1.5min extension time using *M. tuberculosis* H37Rv as the template DNA. Mec$^+$ was cloned into pMal.HT (6 histidine residues at the carboxy terminus of maltose binding protein), which is a homemade vector from Joanne Widom at Cornell University. Cloning, expression and purification proceeded as for CysM. Mec$^+$ was stored in 10% glycerol at -80^{o}C until use. Typical yield for 1L of culture was 8 mg.

3.4.1.3 Cloning, Expression and Purification of hisCysO-cysteine (hisCysO-cys.16): An additional cysteine residue was added to the carboxy terminus of CysO using the following primers: 5'for- CCG AGA AAG GCC CAT ATG AAC GTC ACC GTA-3'; 5'rev-CGG ATC CTC GAG TGA GCA CCC ACC GGC CAC GGC-3'. *Nde*I and *Xho*I restriction sites were added to the forward and reverse primer, respectively. The gene was amplified using Pfx Platinum DNA polymerase with a 30 second extension time using CysO.16 as the template. Cloning, expression and purification proceeded as for CysM. hisCysO-cysteine was stored in 10% glycerol at -80^{o}C until use. Typical yield for 1L of culture was 9 mg.

3.4.1.4 Cloning, Expression and Purification of CysO analogs: CysO-cys.16 was used as the template. Cloning, expression and purification proceeded as for CysO-cys.16. CysO-cys-ala (CysO-CA.16): 5'for-CCG AGA AAG GCC CAT ATG AAC GTC ACC GTA-3'; 5'rev-CGG ATC CTC GAG TCA GGC GCA CCC ACC GGC CAC-3'

CysO-ser (CysO-S.16): 5'for-CCG AGA AAG GCC CAT ATG AAC GTC ACC GTA-3'; 5'rev-CGG ATC CTC GAG TCA GGA CCC ACC GGC CAC GGC-3'

CysO-ala-cys (CysO-AC.16): 5'for-CCG AGA AAG GCC CAT ATG AAC GTC ACC GTA-3'; 5'rev-CGG ATC CTC GAG TCA GCA GGC CCC ACC GGC CAC-3'

CysO-ala (CysO-A.16): 5'for-CCG AGA AAG GCC CAT ATG AAC GTC ACC GTA-3'; 5'rev-CGG ATC CTC GAG TCA GGC CCC ACC GGC CAC GGC-3'

CysO(G->A)+cys: (CysOG->A-cys.16): 5'for-CCG AGA AAG GCC CAT ATG AAC GTC ACC GTA-3'; 5'rev-CGG ATC CTC GAG TCA GCA GGC ACC GGC CAC GGC-3'

3.4.1.5 Mutagenesis of Mec^+ JAMM motif residues: Serine 89 was mutated to alanine from Mec^+.MBPHT using the following primers: 5'for-CGT CAT CTA TCA CGC GCA CAC TGC GAC CGA AGC-3'; 5'rev-GCT TCG GTC GCA GTG TGC GCG TGA TAG ATG ACG-3'. Aspartic acid 101 was mutated to alanine using the following primers: 5'for-GCG TAC GCG AGC CGT ACG GCC GTG AAG CTT GCC-3'; 5'rev-GGC AAG CTT CAC GGC CGT ACG GCT CGC GTA CGC-3'. Stratagene site directed mutagenesis kit was used to amplify the plasmid DNA. Expression and purification proceeded as for WT Mec^+.MBPHT.

3.4.2 Assays

3.4.2.1 Materials: All chemicals were purchased from Sigma. ESI-FTMS was performed by the McLafferty group at Cornell University. MALDI data was collected at the Bioresource Center at Cornell University.

3.4.2.2 Ninhydrin assay for cysteine: Briefly, 6mM O-acetylserine, 10mM DTT, 250μg CysO-thiocarboxylate, 100μg CysM, 0.1mM Zn^{2+}, and 140μg Mec^{+} were incubated in 100mM Phosphate buffer, pH 8.0. Samples were withdrawn at appropriate times, ninhydrin was added, boiled for 10 minutes, cooled, and ethanol added. Absorbance at 560nm was measured.

3.4.2.3 Cleavage of hisCysO-cysteine by Mec^{+}:

255μg of hisCysO-cysteine, 10mM DTT, 10μM $ZnCl_2$, and 45μg Mec^{+} were incubated in 50mM Tris, pH 8 for 1 hour, then frozen. Samples were analyzed by ESI-FTMS.

3.4.2.4 Metal-dependence of Mec^{+}:

Ninhydrin: 100μg Mec^{+} was pre-incubated with and without 0.1mM EDTA for 10 minutes at room temperature. The sample was desalted into tris bio-spin columns. To the samples, 367.5μg hisCysO-cysteine and 8.5mM DTT were added to a final volume of 350μL in 100mM potassium phosphate pH8. To test whether activity could be restored with a metal ion, 0.1mM Zn^{2+} or 0.1mM Mg^{2+} were added to two of the samples. At 15 and 40minutes, 150μL was removed and 262μL of the ninhydrin solution was added. The samples were placed at 100^{o}C for 10 minutes, allowed to cool, and 525μL ethanol was added. The absorbance at 560nm was taken for each sample.

ESI-FTMS: 25μg Mec^+ was pre-incubated with and without 0.24mM EDTA for 10 minutes at room temperature. To the samples, 170μg hisCysO-cysteine and 9.7mM DTT were added to a final volume of 155μL in 50mM tris pH8. The samples were placed at 37°C for 1 hour and frozen until analyzed by ESI-FTMS.

3.4.2.5 Substrate specificity of Mec^+:

CysO-ser: 45μg Mec^+ was added to 198μg CysO-ser, 10μM Zn^{2+} and 10mM DTT in 50mM tris pH8 to a final volume of 150μL. The sample was incubated at 37°C for 1 hour and frozen until analysis by ESI-FTMS.

CysO-cys-ala: 200μg CysO-cys-ala was used in a reaction identical to CysO-ser.

CysO-ala: 39 μg Mec^+ was added to 150μg CysO-ala-cys, 7.5μM Zn^{2+} and 7.5mM DTT in 50mM tris pH8 to a final volume of 200μL. The sample was incubated at 37°C for 1 hour and frozen until analysis by ESI-FTMS.

CysO-ala-cys: 150μg CysO-ala-cys was used in a reaction identical to CysO-ala.

CysO(G->A)-cys: 150μg CysO(G->A)-cys was used in a reaction identical to CysO-ala.

3.4.2.6 Mec^+ mutagenesis:

S89A: 37.5μg S89A Mec^+ was added to 200μg hisCysO-cysteine, 7.5mM DTT and 7.5μM Zn^{2+} in 200μL total volume of 50mM tris pH8. Samples were incubated at 37°C for 1 hour, desalted into bio-spin tris columns, and frozen until analysis by ESI-FTMS.

D101A: 52.5mg D101A was used in a reaction identical to S89A.

3.5 References

1. Hirasawa, K.; Ichihara, M.; Okanishi, M. (1985) *J. Antibiotics* **38,** 1795-1798.

2. Verma, R.; Aravind, L.; Oania, R.; McDonald, W.; Yates, J.; Koonin, E.; Deshaies, R. (2002) *Science* **298,** 611-615.

3. Shao, Y.; Paulus, H. (1997) *J. Peptide Res.* **50,** 193-198.

Chapter 4

Conclusion and Outlook

4.1 An Overview

We've shown that a sulfide carrier protein from *M. tuberculosis*, CysO (Rv1335), in its thiocarboxylate form **27**, is alkylated to a cysteine adduct **28** by CysM (Rv1336) in the presence of O-acetylserine **6**. Following an S-N acyl rearrangement, Mec^+ (Rv1334) hydrolyzes the CysO adduct, releasing cysteine **7** and generating CysO-carboxylate **29**. Preliminary results suggest MoeZ (Rv3206) is responsible for activating CysO through adenylation to **30** and sulfur transfer, however, the details of this reaction, including the sulfur source, have yet to be established. We hypothesize that the sulfur source may be an intermediate in the sulfate assimilation pathway, or an oxidized form of sulfide. The cysteine biosynthetic pathway is summarized in figure 4.1.

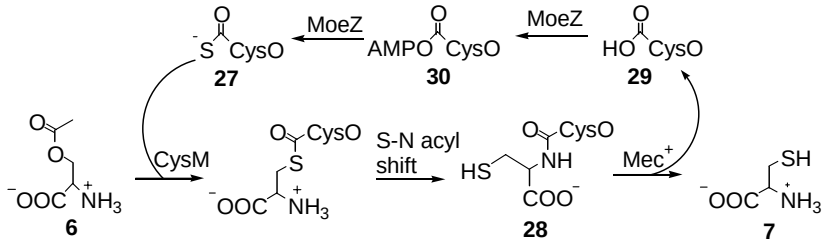

Figure 4.1 Cysteine biosynthesis by the new pathway reconstituted from *M. tuberculosis*.

The new cysteine biosynthetic pathway in *M. tuberculosis* shares many parallels with thiamin and molybdopterin biosyntheses, as well as with ubiquitinylation. Each pathway contains a small protein of less than 100 amino acids that is characterized by two C-terminal glycine residues. The activation for sulfide transfer onto these proteins is believed to be similar in all cases: a protein activates the C-terminus first by adenylation,

followed by sulfide transfer to form the active thiocarboxylate, or thioester in the case of ubiquitin. The protein-bound thiocarboxylate has been shown to deliver sulfide to thiamin, molybdopterin, and now to cysteine.[1,2] In ubiquitin, a sulfur from the activating enzyme E1 displaces the activated adenylate.[3]

The most intriguing aspect of this cysteine pathway goes beyond the homology of the sulfide carrier proteins. The reaction catalyzed by Mec^+ resembles the deubiquitination reaction of the 26S proteasomal subunit Rpn11, which sends doomed proteins into the proteasome for degradation and regenerates ubiquitin (figure 1.7).[4] Both Rpn11 and Mec^+ contain the JAMM motif, which is found in bacteria, archaea, and eukaryotes (figure 3.1). The proteins are both able to recognize a homologous motif in ubiquitin and CysO and catalyze a similar reaction on their substrates, both in completely different pathways and biological systems. These parallels suggest an evolutionary relationship between the cysteine pathway in bacteria and the ubiquitin pathway in eukaryotes.

Mycobacterium tuberculosis is one of the most virulent pathogens on record, causing at least two million deaths a year.[5] TB can evade the normal immune response and survive in the macrophage without being destroyed, remaining dormant in the body for years. When TB is engulfed by the macrophage, it is able to prevent phagosome-lysosome fusion[6] and can lie dormant until the macrophage is activated. The metabolism and environment of latent TB is poorly understood and current research efforts focus on studying latent TB. TB also has a unique cell envelope that enables the pathogen to resist common antibiotics. Mycolic acid forms a waxy wall around TB and aids in its pathogenicity[7,8,9]. Macrophages have developed the method of oxidative stress to defeat harmful bacteria.[10] Bacteria are often unable to counteract these reactive oxygen intermediates and reactive nitrogen intermediates that are associated with oxidative stress and that alter the cellular redox balance. In addition to latency and the impenetrable

envelope, TB expresses proteins which protect the cell from oxidizing conditions in the macrophage.[11] Such proteins include the sigma factor discussed in chapter 1, thioredoxins, and proteins related to thiol metabolism.[12] We are just beginning to understand the unique cellular processes which protect TB from the immune response. Identifying genes responsible for the persistence of TB is critical in developing new and more affordable treatments against the pathogen.

To survive the harsh conditions of the macrophage, TB must be equipped with the appropriate tools, including pathways leading to the upregulation of reductants such as thioredoxin and alternate pathways for the biosynthesis of oxygen-sensitive molecules. Because cysteine is an essential amino acid for bacteria and it is a substrate for many cellular metabolites, it is important that this molecule is still synthesized in the macrophage, but little is known about the operable biosynthetic pathway for cysteine in TB. An alternate pathway involving the four genes characterized here, *mec*$^{+}$, *cysO*, *cysM*, and *moeZ*, could be responsible for cysteine biosynthesis in TB under oxidative stress in the macrophage. These genes were the only putative cysteine biosynthetic genes upregulated under oxidative stress in TB.[12] This cysteine biosynthetic pathway, involving a protein-bound thiocarboxylate and not sulfide, could represent a more stable source of sulfur for TB under oxidizing conditions; the protein-bound thiocarboxylate is less oxygen-sensitive than sulfide and more easily reduced.

4.2 Future directions

Cysteine is an essential cellular metabolite and bacteria need to biosynthesize it when it is not readily available in the environment. To determine whether TB could survive without this cysteine pathway, and to define the environmental conditions that make this pathway necessary for TB, the Russell group attempted to knock out, or knock down, the pathway in *M. tuberculosis*. All attempts to mutate the pathway failed, suggesting its

importance for TB growth under the conditions used by the Russell group. While this data is interesting, it does not agree with other reports regarding gene essentiality in TB.[13,14] For example, Sassetti used transposon site hybridization (TraSH) to identify essential genes for optimal growth in TB and this pathway was not 'a hit'.[14] Unfortunately, there is no widely used model system for studying TB, and none of the current models are able to reproduce the true growth conditions of TB in the lungs. This makes the interpretation of mutants and gene essentiality studies difficult. An alternative method for defining gene essentiality is through the use of inhibitors. Developing inhibitors for this new pathway will shorten the analysis time compared to traditional mutagenesis studies and also enable us to quickly investigate how the pathway functions in a variety of growth conditions because we can modulate inhibitor concentration. Humans synthesize cysteine using a different pathway, so the inhibitors should be specific for the pathway in TB.

Knowledge of protein function provides a solid foundation for which to design inhibitors, however, there are certain limits to enzymology which only crystallography is able to strengthen. Obtaining a high resolution crystal structure of the proteins involved in the new cysteine biosynthetic pathway enables us to understand the system at a deeper level. We can see binding pockets, important loops, and key interactions which we are blind to in solution and which directs our inhibitor targeting. In collaboration with Chris Jurgenson and Steve Ealick, the structure of the CysO/CysM complex was solved to 2.1 Å resolution (unpublished). The crystal structure of the CysO/CysM complex enables us to gain insight into the design and development of molecules that would disrupt this interaction and thus inhibit cysteine biosynthesis. For example, we can infer from the crystal structure that the crucial interaction between CysM and CysO is at the C-terminus of CysO, encompassing the last third of the protein. Development of a peptide mimic of the C-terminus of CysO, encompassing the minimal binding region to CysM, may be a

good starting point for inhibitor design. Similarly, the structure of the complex suggests that the diglycyl C-terminus of CysO is curved, unlike most sulfide carrier proteins. This feature provides extra space in the CysM active site, a feature which should be exploited in inhibitor design. Future work will focus on the design, synthesis and development of inhibitors of the CysO/CysM interaction, all guided by the crystal structure of the complex.

Future studies on this cysteine biosynthetic pathway will also focus on kinetic characterization of the system. How fast does CysO-thiocarboxylate **27** react with the CysM-α-aminoacrylate intermediate **26** and how does this compare to sulfide and other sulfur-containing compounds? TB grows very slowly: does the reaction rate parallel the growth rate of TB? Investigating the kinetics of this pathway will also enable us to design better inhibitors, and enable us to probe the inhibition.

Finally, we'd like to explore the mechanism and substrates for sulfide transfer by MoeZ in more detail. We were able to observe thiocarboxylate formation on CysO when the two proteins were co-purified from *E. coli*, however, not when the proteins were purified separately. It could be that the system requires protein stabilization for activity. This was tested in an additional experiment where the small molecules were removed from the cell lysates of CysO and MoeZ prior to combining them. No thiocarboxylate was formed. Interestingly, addition of ATP and sulfide back to this desalted mixture restored thiocarboxylate formation. In the pure system, this reaction did not work. It is possible that sulfide is modified in *E. coli* crude cell lysates, and MoeZ is able to use the modified sulfide as a substrate. It would be interesting to determine if MoeZ is modified by sulfide in any way, as is observed for similar proteins.[15] To determine the source of sulfur and to reconstitute thiocarboxylate formation in a purified system will require careful and in depth analysis of these experiments as well as others.

4.3 References

1. Dorrestein, P.; Zhai, H.; McLafferty, F.; Begley, T. (2004) *Chem. Biol.* **11,** 1373-1381.

2. Burns, K.; Baumgart, S.; Dorerstein, P.; Zhai, H.; McLafferty, F.; Begley, T. (2005) *J. Am. Chem. Soc.* **127,** 11602-11603.

3. Hershko, A.; Ciechanover, A. (1998) *Annu. Rev. Biochem.* **67,** 425-479.

4. Verma, R.; Aravind, L.; Oania, R.; McDonald, W.; Yates, J.; Koonin, E.; Deshaies, R. (2002) *Science* **298,** 611-615.

5. Dye, C.; Scheele, S.; Dolin, P.; Pathania, V.; Raviglione, M. (1999) *JAMA* **282,** 677-686.

6. Russell, D. (2003) *Nat. Cell. Biol.* **5,** 776-778.

7. Ozeki, Y.; Kaneda, K.; Fujiwara, N.; Morimoto, M.; Oka, S.; Yano, I. (1997) *Infect. Immun.* **65,** 1793-1799.

8. Vachula, M.; Holzer, T.; Andersen, B. (1989) *J. Immunol.* **142,** 1696-1701.

9. Ng, V.; Zanazzi, G.; Timpl, R.; Talts, J.; Salzer, J.; Brennan, P.; Rambukkana, A. (2000) *Cell* **103,** 511-524.

10. Chan, J.; Xing, Y.; Magliozzo, R.; Bloom, B. (1992) *J. Exp. Med.* **175,** 1111-1122.

11. Li, Z.; Kelley, C.; Collins, F.; Rouse, D.; Morris, S. (1998) *J. Infect. Dis.* **177,** 1030-1035.

12. Manganelli, R.; Voskuil, M.; Schoolnik, G.; Dubnau, E.; Gomez, M.; Smith, I. (2002) *Mol. Microbiol.* **45,** 365-374.

13. Lamichhane, G.; Zignol, M.; Blades, N.; Geiman, D.; Dougherty, A.; Grosset, J.; Broman, K.; Bishai, W. (2003) *Proc. Natl. Acad. Sci. USA* **100,** 7213-7218.

14. Sassetti, C.; Boyd, D.; Rubin, E. (2003) *Mol. Microbiol.* **48,** 77-84.

15. Matthies, A.; Nimtz, M.; Leimkuhler, S. (2005) *Biochemistry* **44,** 7912-7920.

Chapter 5

Vitamin B6 Biosynthesis

5.1 Vitamin B6: An introduction

Vitamin B6 is an essential cofactor in all living systems. The cofactor aids in amino acid and carbohydrate metabolism and has recently been implicated in singlet oxygen resistance.[1] Pyridoxine, pyridoxamine, pyridoxal and their phosphates are collectively termed vitamin B6, however, pyridoxal-5'-phosphate (PLP; **1**) is the active form of the cofactor (figure 5.1).

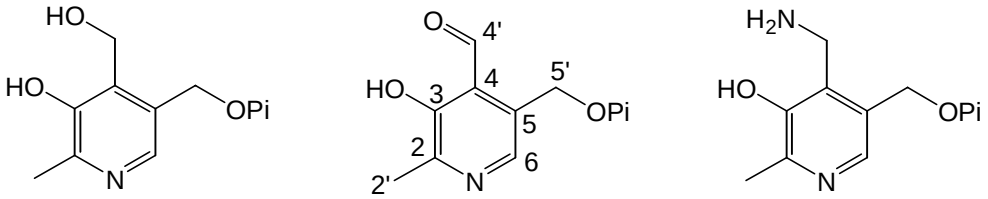

1

Figure 5.1 The three forms of vitamin B6 found in the cell, shown here in their phosphorylated forms.

PLP covalently attaches to enzymes through a Shiff base (imine) with an active site lysine. This attachment positions the cofactor in the active site and activates the PLP aldehyde for a transimination reaction, which is faster than an imination so the reaction with the substrate is fast.[2] In all enzymes for which it is a cofactor, PLP **1** covalently links to the substrate via an imine. The cofactor acts as an electrophilic catalyst that stabilizes carbanions via its electron deficient pyridine ring.[3] From transaminations to dehydrations and eliminations, this coenzyme increases the breadth of reactions available in nature. The enzyme commission has identified more than 140 different activities that

depend on PLP, constituting 4% of classified enzyme activities. In prokaryotes, almost 1.5% of the genes encode for PLP-utilizing enzymes, highlighting its importance in basic metabolism.[4]

Humans obtain vitamin B6 from their diet; we are unable to synthesize our own. Bacteria, fungi, protozoa, archaea and plants provide the B6 found in nature, and we depend on these resources for our supply. Importantly, many pathogens are able to synthesize PLP *de novo*, and vitamin B6 biosynthesis, and vitamin biosynthesis in general, is an attractive target for antibiotics and antifungals. To optimize dietary consumption of vitamin B6 and to identify potential drug leads, it is critical to understand the enzymes involved in its biosynthesis.

5.2 Salvage and *E. coli de novo* Vitamin B6 pathways

Three pathways exist for PLP formation: the salvage pathway and two distinct *de novo* pathways. The salvage pathway involves the uptake of pyridoxine **2** into the cell, followed by phosphorylation by PdxK and oxidation to the aldehyde PLP **1** by PdxH (Figure 5.2). The *de novo* biosynthesis of PLP has been well characterized in *Escherichia coli*.[5-11] It involves six enzymes, four of which are unique to PLP biosynthesis. GapA and PdxB perform sequential NAD-dependent oxidations on D-erythrose-4-phosphate **3**, which is followed by amine transfer from glutamate catalyzed by PdxF. The product 4-phosphohydroxy-L-threonine **4** is then decarboxylated by PdxA to form 3-hydroxy-1-aminoacetone-3-phosphate **5**, which combines with 1-deoxyxylulose-5-phosphate **6** (from 1-deoxyxylulose-5-phosphate synthase) in a reaction catalyzed by PdxJ. The product of the PdxJ reaction, pyridoxine-5'-phosphate **7**, is oxidized to PLP **1** by PdxH.

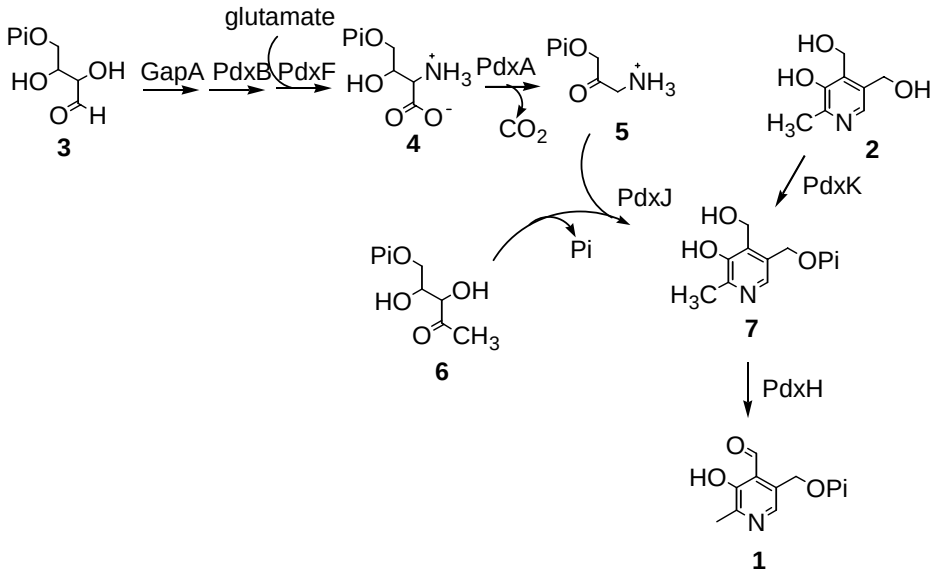

Figure 5.2 The *E. coli de novo* PLP biosynthetic pathway and the salvage pathway for PLP biosynthesis. The *de novo* pathway involves enzymes GapA, PdxB, PdxF, PdxA, PdxJ, and PdxH. The salvage pathway involves PdxK and PdxH.

5.3 Alternate *de novo* Vitamin B6 biosynthetic pathway: PLP synthase

It had been observed that many organisms, including yeast and bacteria such as *Bacillus subtilis*, do not contain homologs of the Pdx genes found in *E. coli*.[12,13] Labeling studies in yeast suggested an alternate pathway exists for B6 biosynthesis; this pathway incorporates an intact five carbon sugar, an intact three carbon sugar, as well as the amide nitrogen of glutamine into vitamin B6 (figure 5.3).[14-16] Neither the oxidation state nor the phosphorylation state of the substrates and B6 product was known. Mutagenesis implicated a highly conserved gene, SNZ (YaaD in *B. subtilis*), as well as a glutaminase SNO (YaaE in *B. subtilis*), in the biosynthesis of vitamin B6 in these organisms.[12, 13, 17] It was suggested that YaaD served as the PLP synthase subunit and YaaE provided the ammonia needed for the pyridine ring.

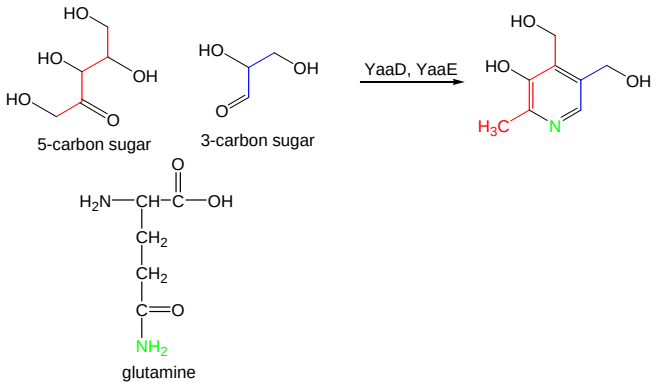

Figure 5.3 Labeling studies suggest a five carbon sugar, a three carbon sugar and the amide nitrogen of glutamine form the backbone of vitamin B6 in yeast.

YaaD and YaaE are found clustered in many organisms, and in contrast to the *E. coli* pathway, which has only been identified in bacteria, the YaaD and YaaE genes are present in bacteria as well as fungi, yeast, plants, some metazoa and archaea. The two pathways are also mutually exclusive: they do not coexist in any organism that has been sequenced to date. A few of these organisms are shown in Table 5.1.[18,19]

The sequence of YaaE suggests it belongs to the class I triad amidotransferase family, where highly conserved active site histidine, glutamine and cysteine residues hydrolyze ammonia from the amide of glutamine to form glutamate.[20] Addition of acivicin irreversibly inhibits these glutaminases through labeling of the active site cysteine, suggesting a covalent intermediate is part of the mechanism, which is shown in figure 5.4 [20]. The structure of the amidotransferase YaaE from *B. subtilis* was solved in 2004 at 2.5 Å,[21] and shortly thereafter amidotransferase activity had been reconstituted in both *B. subtilis*[17] and *S. cerevisiae*.[22] These studies confirm the glutaminase activity of YaaE both structurally and biochemically.

Table 5.1 Mutual exclusiveness of the PLP biosynthetic pathways.

Organism (selected subset)		YaaD/E (*B. subtilis*)	PdxA/J (*E. coli*)
Plants	*A. thaliana*	+	-
	O. sativa	+	-
Fungi	*S. cerevisiae*	+	-
	A. nidulans	+	-
	C. albicans	+	-
Archaebacteria	*M. jannaschii*	+	-
	P. abyssi	+	-
	A. fulgidus	+	-
Eubacteria	*B. subtilis*	+	-
	M. tuberculosis	+	-
	T. maratima	+	-
	E. coli	-	+
	H. pylori	-	+
	B. cepacia	-	+
	P. aeruginosa	-	+
	V. chlorea	-	+

+ indicates the presence of the genes; - indicates the absence.

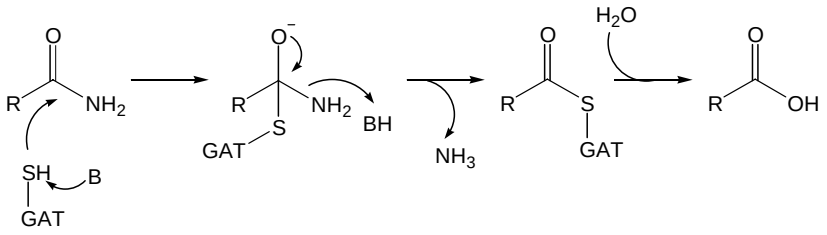

Figure 5.4 General mechanism for class I glutamine amidotransferases (GAT). A catalytic cysteine residue forms a covalent adduct with the substrate, which releases ammonia. The covalent adduct is eventually hydrolyzed.

Most amidotransferases have two domains, a GAT domain (glutamine amidotransferase domain) and a synthase domain. The GAT domain forms ammonia which travels through a tunnel connecting the active sites of the two domains. The synthase domain catalyzes the ammonia-dependent reaction. Where GAT domains are often very similar, the synthase domains differ greatly depending on the system.[20] Amidotransferases are found in histidine, tryptophan, arginine and purine biosyntheses,[20] all of which produce very different molecules. YaaD is the synthase subunit of PLP synthase. When 91 sequences of YaaD were aligned, all pairs of sequences (including sequences from archaea, prokaryotes and eukaryotes) shared at least 60% identity.[23] Due to its high sequence conservation, shown in figure 5.5, very little reaction information can be gained from a Psi-BLAST search. The one protein that shows up besides YaaD is thiazole synthase ThiG, a protein that forms an imine with the substrate 1-deoxyxylulose-5-phosphate prior to thiazole formation. The imine is cleaved by an intramolecular transimination later in the reaction sequence.[24] Analogous imine formation with a 5-carbon sugar substrate was a reasonable possibility for the YaaD catalyzed PLP reaction.

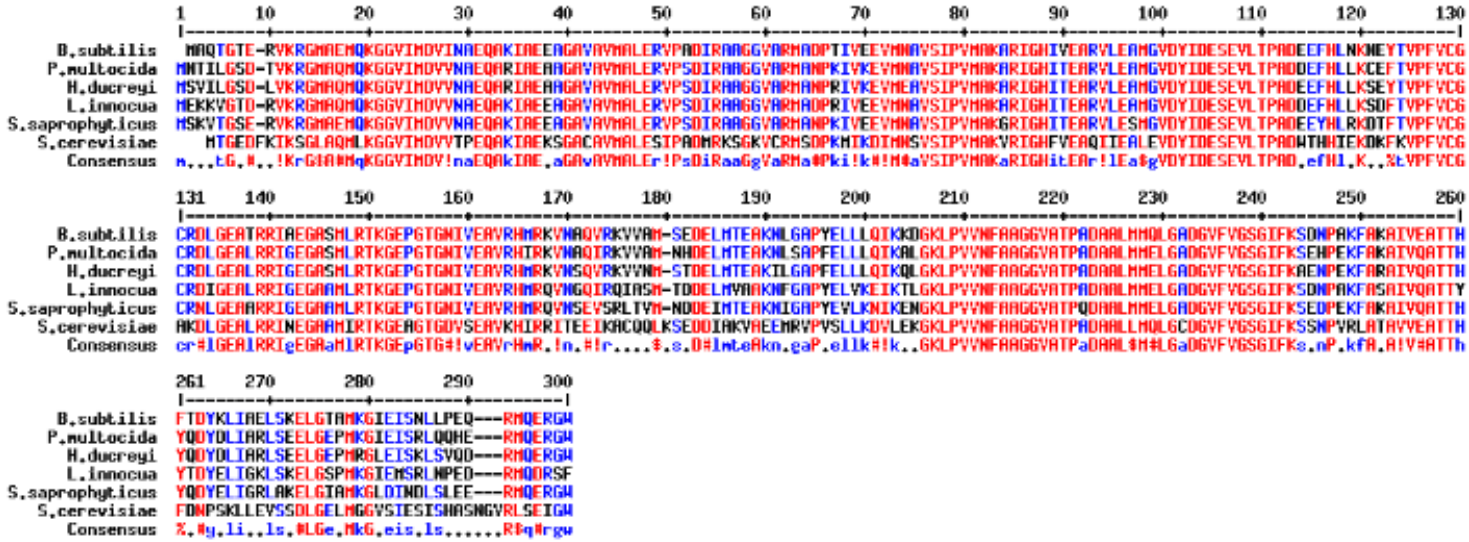

Figure 5.5 Amino acid sequence alignment of several YaaD orthologs using MultAlin.

The structural model of YaaD shows a high level of similarity to imidazole glycerolphosphate synthase (HisF),[21] the enzyme that catalyzes the formation of the imidazole ring of histidine. One of the steps catalyzed by this enzyme involves an amine addition (from HisH GAT domain) to the C2 carbonyl of a 1-amino-ribulose-5-phosphate analog (figure 5.6).[25] This similarity suggested that YaaD might also catalyze an amine addition (from YaaE) to the carbonyl group of a 5-carbon sugar.

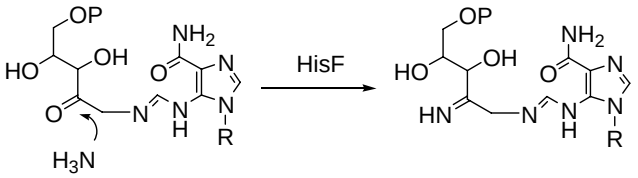

Figure 5.6 Reaction catalyzed by HisF in histidine biosynthesis.

Chapters 6-9 will describe the identification of the substrates for PLP synthase, describe the reconstitution of the pathway in a defined system, outline a mechanism for the transformation, and discuss efforts at developing inhibitors and mutants of the PLP synthase complex.

5.4 References

1. Daub, M.; Ehrenshaft, M. (2000) *Annu. Rev. Phytopathol.* **38,** 461-490.

2. Silverman, R. (2000) *Academic Press*

3. John, R. (1995) *Biochim. Biophys. Acta* **1248,** 81-96.

4. Percudani, R.; Peracchi, A. (2003) *EMBO Rep.* **4,** 850-855.

5. Cane, D.; Du, S.; Robinson, J.; Hsiung, Y.; Spenser, I. (1999) *J. Am. Chem. Soc.* **121,** 7722-7723.

6. Garrido-Franco, M.; Laber, B.; Huber, R.; Clausen, T. (2002) *J. Mol. Biol.* **321,** 601-612.

7. Yeh, J.; Du, S.; Pohl, E.; Cane, D. (2002) *Biochemistry* **41,** 11649-11657.

8. Sivaraman, J.; Li, Y.; Banks, J.; Cane, D.; Matte, A.; Cygler, M. (2003) *J. Biol. Chem.* **278,** 43682-43690.

9. Zhao, G.; Winkler, M. (1995) *J. Bacteriol.* **177,** 883-891.

10. Cane, D.; Du, S.; Spenser, I. (2000) *J. Am. Chem. Soc.* **122,** 4213-4214.

11. Banks, J.; Cane, D. (2004) *Bioorg. Med. Chem. Lett.* **14,** 1633-1636.

12. Ehrenshaft, M.; Bilski, P.; Li, M.; Chignell, C.; Daub, M. (1999) *Proc. Natl. Acad. Sci. USA* **96,** 9374-9378.

13. Mittenhuber, G. (2001) *J. Mol. Microbiol. Biotechnol.* **3,** 1-20.

14. Gupta, R.; Hemscheidt, T.; Sayer, B.; Spenser, I. (2001) *J. Am. Chem. Soc.* **123,** 11353-11359.

15. Zeidler, J.; Gupta, R.; Sayer, B.; Spenser, I. (2003) *J. Org. Chem.* **68,** 3486-3493.

16. Tazuya, K.; Adachi, Y.; Masuda, K.; Yamada, K.; Kumaoka, H. (1995) *Biochim. Biophys. Acta* **1244,** 113-116.

17. Belitsky, B. (2004) *J. Bacteriol.* **186,** 1191-1196.

18. Ehrenshaft, M.; Daub, M. (2001) *J. Bacteriol.* **183,** 3383-3390.

19. Osmani, A.; May, G.; Osmani, S. (1999) *J. Biol. Chem.* **274,** 23565-23569.

20. Massiere, F.; Badet-Denisot, M.-A. (1998) *Cell. Molec. Life Sci.* **54,** 205-222.

21. Bauer, J.; Bennet, E.; Begley, T.; Ealick, S. (2004) *J. Biol. Chem.* **279,** 2704-2711.

22. Dong, Y.; Sueda, S.; Nikawa, J.; Kondo, H. (2004) *Eur. J. Biochem.* **271,** 745-752.

23. Zhu, J.; Burgner, J.; Harms, E.; Belitsky, B.; Smith, J. (2005) *J. Biol. Chem.* **280,** 27914-27923.

24. Dorrestein, P.; Zhai, H.; Taylor, S.; McLafferty, F.; Begley, T. (2004) *J. Am. Chem. Soc.* **126,** 3091-3096.

25. Chaudhuri, B.; Lange, S.; Myers, R.; Davisson, V.; Smith, J. (2003) *Biochemistry* **42,** 7003-7012.

Chapter 6

Reconstitution and identification of three partial reactions of PLP synthase[i]

6.1 Introduction

Although labeling studies in yeast suggested that the backbone of vitamin B6 was formed with an unidentified five carbon sugar,[1] an unidentified three carbon sugar[2] and the amide nitrogen of glutamine,[3] the reaction of YaaE and YaaD had not been reconstituted. This chapter confirms the identity of the substrates as ribose-5-phosphate, glyceraldehyde-3-phosphate and glutamine, and the product as pyridoxal-5'-phosphate (PLP; **1**). Three surprising partial reactions for the synthase subunit of PLP synthase will also be described.

6.2 Results and discussion

6.2.1 Expression of YaaD and YaaE

B. subtilis YaaD and YaaE express as insoluble protein in LB media. The best way to express them is in Tuner(DE3) cells in M9 minimal media with addition of glucose, $MgSO_4$ and $CaCl_2$. Expression can be done at 37^{o}C for 5 hours or at reduced temperature for extended times. YaaD and YaaE need to be purified in buffer above pH7.5. Purification into more acidic buffers causes the proteins to precipitate. A gel of purified YaaD and YaaE is shown in figure 6.1.

[i] Reproduced in part with permission from Burns, K.; Xiang, Y.; Kinsland, C.; McLafferty, F.; Begley, T. (2005) *J. Am. Chem. Soc.* **127**, 3682-3683.

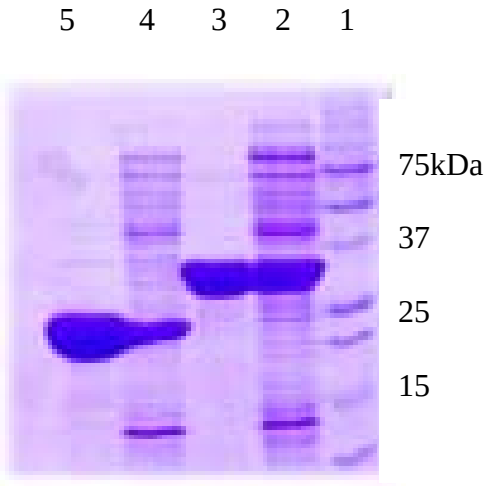

Figure 6.1 15% SDS-PAGE of soluble and pure samples of YaaD and YaaE from *B. subtilis*. From the right: lane 1, MW markers; lane 2, YaaD soluble protein; lane 3, pure YaaD; lane 4, YaaE soluble protein; lane 5, pure YaaE.

6.2.2 YaaE glutaminase activity

To determine if the amidotransferase subunit of PLP synthase from *B. subtilis*, YaaE, is able to hydrolyze glutamine to glutamate, thin layer chromatography (TLC) was used with dansyl chloride as the visualization agent. When YaaE was incubated with glutamine in buffer, no glutamate was observed by TLC. When YaaD was added to the reaction, however, glutamine was converted to glutamate. This suggested that YaaD is needed to activate YaaE for hydrolysis of glutamine. This dependence on a binding partner is not unusual for glutaminases; it would be harmful to have ammonia released randomly in the cell.[4] These results are consistent with previous studies with YaaE[5,6] and confirm that our YaaE was active and most likely forming a complex with YaaD.

6.2.3 Covalent modification of YaaD

As mentioned above, YaaD activates the amidotransferase activity of YaaE: when YaaD, YaaE and glutamine are combined, glutamate formation is observed using dansyl chloride. In addition, we also observe an increase in absorbance at 320nm. Because the

absorbance was not dependent on the addition of either the 5-carbon sugar or the 3-carbon sugar, we proposed there may be some substrate pre-bound to YaaD and that a reaction between YaaE, glutamine and YaaD with pre-bound substrate causes this absorbance increase. ESI-FTMS (in collaboration with Yun Xiang and Fred McLafferty) analysis of freshly isolated YaaD demonstrated the presence of unmodified YaaD (34209 Da) as well as an adduct (34421 Da) that was 212 Da heavier than native YaaD. The mass spectrum is shown in figure 6.2a. The mass of this adduct is consistent with that expected for a YaaD-pentulose phosphate imine. To confirm this, ribulose-5-phosphate **8**

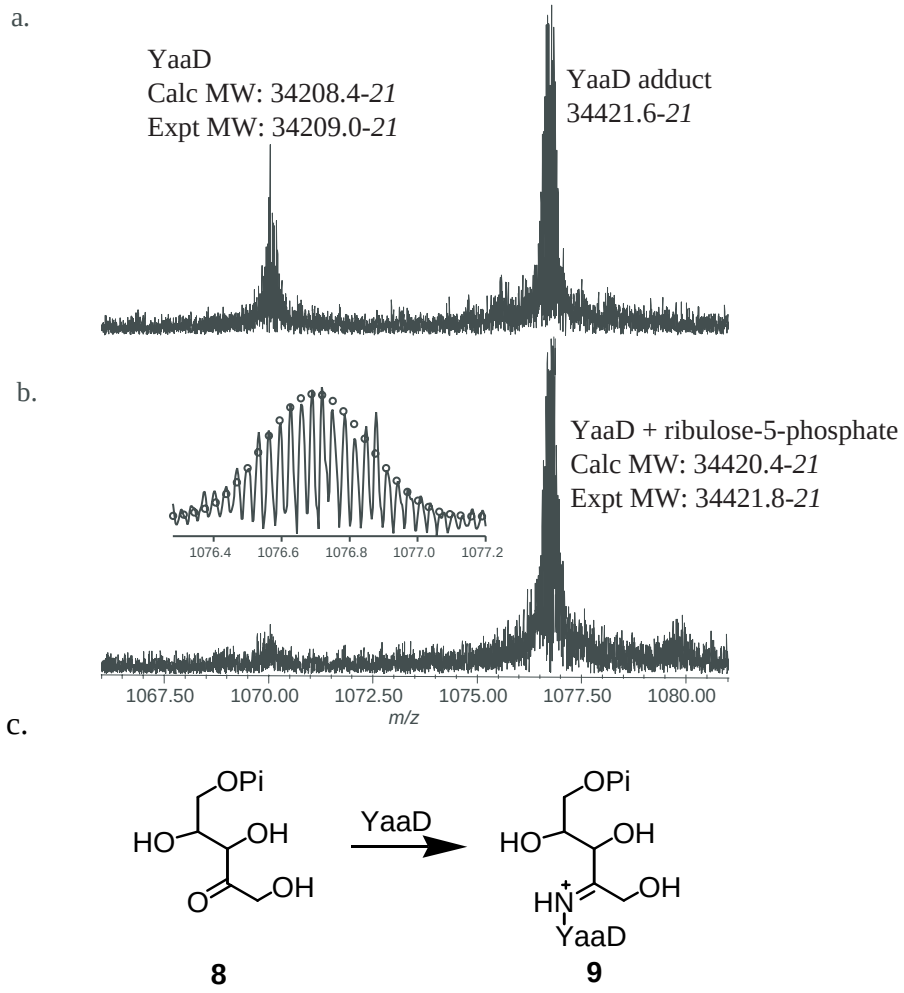

Figure 6.2 ESI-FTMS of freshly purified YaaD a. YaaD as isolated b. Ribulose-5-phosphate treated YaaD c. Reaction catalyzed by YaaD.

was added to YaaD and most of the unmodified YaaD was converted to the adduct, as shown in figure 6.2b. This suggests that ribulose-5-phosphate **8** is the bound carbohydrate and it is either a substrate or an intermediate in the PLP synthase reaction, as proposed in figure 6.2c. This reaction is similar to that catalyzed by thiazole synthase ThiG in thiamin biosynthesis (substrate is 1-deoxyxylulose phosphate).[7]

MS-MS analysis of the YaaD adduct localized the imine to lysine 149, which is absolutely conserved in the YaaD family of proteins. The results were confirmed by demonstrating that the K149A mutant did not form an adduct with ribulose-5-phosphate, suggesting that the YaaD-ribulose-5-phosphate imine adduct **9** is an intermediate in the PLP synthase reaction. A recent structure of YaaD from *Geobacillus stearothermophilus* at 2.2Å shows that lysine 149 is pointing away from the active site of YaaD and rotation about the peptide bond positions it nicely for imine formation with ribulose-5-phosphate.[8]

6.2.4 YaaD isomerization of ribose-5-phosphate

Treatment of YaaD with ribulose-5-phosphate **8** yielded a 212 Da adduct on YaaD. Interestingly, ribose-5-phosphate **10**, an isomer of ribulose-5-phosphate **8**, could also form this adduct. The observation that the YaaD adduct could be reconstituted with equal ease from both ribulose-5-phosphate **8** and ribose-5-phosphate **10** suggested that YaaD catalyzed the interconversion of these two compounds. This was confirmed by NMR analysis of a reaction mixture containing ribose-5-phosphate **10** and YaaD, which is shown in figure 6.3a. Signals with chemical shifts at 3.75 (m, 2H, H5), 3.88 (m, 1H, H4) and 4.29 (d, J=5.8Hz, 1H, H3) confirm the formation of ribulose-5-phosphate. This suggests that YaaD has ribose-5-phosphate isomerase activity (figure 6.3b).

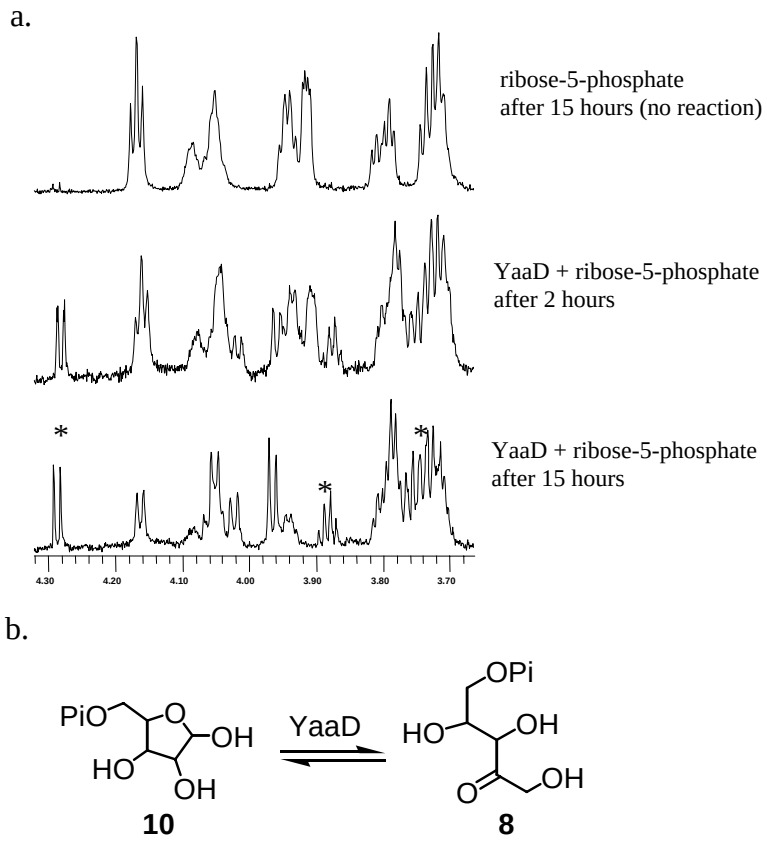

Figure 6.3 Ribose-5-phosphate **10** isomerization by YaaD a. ^{1}H NMR of the YaaD-catalyzed isomerization of ribose-5-phosphate **10** to ribulose-5-phosphate **8**. * indicate signals from ribulose-5-phosphate **8**. The triplet at 4.16 (H2 of ribulose-5-phosphate **8**) collapses to a doublet due to deuterium exchange at C1 b. Isomerization reaction catalyzed by YaaD.

6.2.5 Reconstitution of PLP biosynthesis

While previous labeling studies did not identify the triose precursor to carbons 5, 5' and 6 of PLP,[2] dihydroxyacetone phosphate or glyceraldehyde-3-phosphate were the most likely precursors and the stage was now set for attempting the *in vitro* reconstitution of the biosynthesis. In the event, when ribulose-5-phosphate **8**, dihydroxyacetone phosphate **11** and glutamine were incubated with PLP synthase, the reaction mixture turned yellow after 30 minutes at 37^{o}C and showed a UV-visible spectrum with an absorbance

maximum at 390 nm, similar to that in figure 6.4a. HPLC analysis demonstrated the formation of two reaction products that comigrated with PLP and pyridoxal (PL) standards (figure 6.4b) (note that tris buffer catalyzes the dephosphorylation of PLP after extended periods). A sample for NMR analysis was generated by treating the reaction mixture with alkaline phosphatase, followed by HPLC purification. Signals with chemical shifts of 2.35 (s, 3H, H2'), 4.86 (d, J=14.2Hz, 1H, H5'), 5.10 (d, J=14.2Hz, 1H, H5'), 6.41 (s, 1H, H6) and 7.45 (s, 1H, H4') unambiguously identified the isolated product as pyridoxal hemiacetal. The NMR is displayed in figure 6.4c.

The rate of formation of PLP, under various conditions, was monitored by measuring the absorbance increase at 390 nm (figure 6.5). Both ribulose-5-phosphate **8** and ribose-5-phosphate **10**, as well as glyceraldehyde-3-phosphate **12** and dihydroxyacetone phosphate **11**, are substrates for PLP synthase. The absorption at 390 nm is dependent on the YaaD concentration. Although purification of YaaD and YaaE requires higher pHs for stability, the optimal pH for the PLP synthase reaction is 6-6.5. The initial lag of about 3 minutes is observed with all substrates so substrate isomerization does not play a role in the lag.

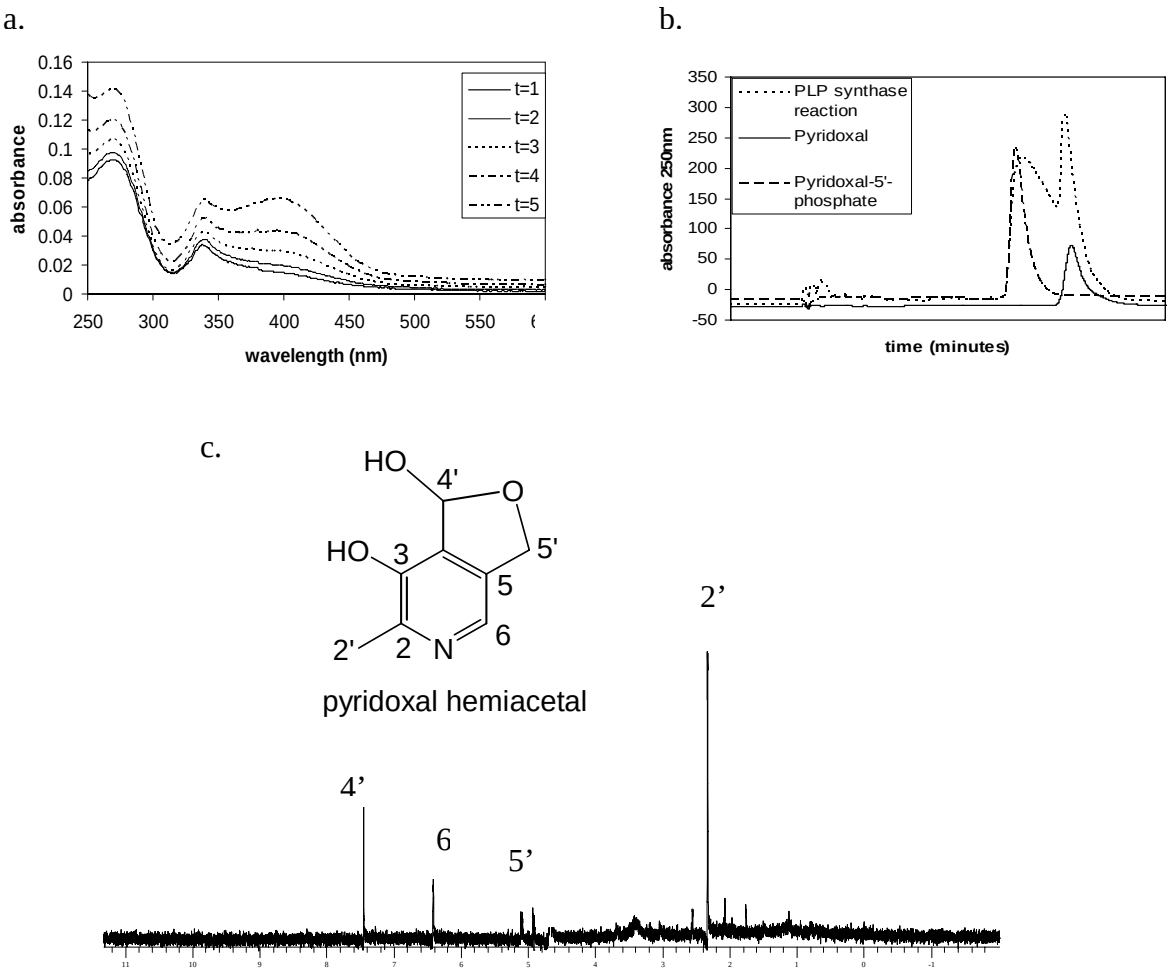

Figure 6.4 Reconstitution of PLP biosynthesis a. UV-Vis absorbance spectrum of the PLP synthase reaction with YaaD, YaaE, glutamine, ribulose-5-phosphate **8** and dihydroxyacetone phosphate **11** b. HPLC of the PLP synthase reaction containing the same components c. ^{1}H-NMR of phosphatase treated and HPLC-purified reaction product.

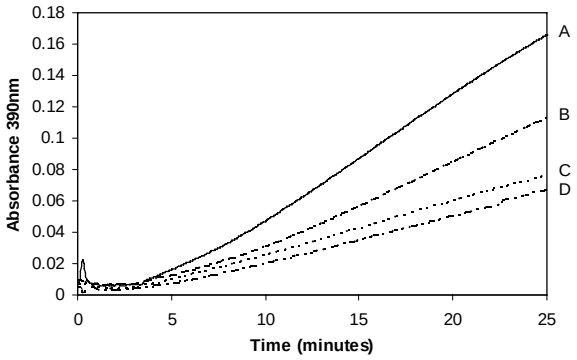

Figure 6.5. Rate of formation of PLP under various conditions. Ribose-5-phosphate **10** and glyceraldehyde-3-phosphate **12** (A); ribulose-5-phosphate **8** and glyceraldehyde-3-phosphate **12** (B); ribose-5-phosphate **10** dihydroxyacetone phosphate **11** (C); ribulose-5-phosphate **8** and dihydroxyacetone phosphate **11** (D).

6.2.6 YaaD catalyzed isomerization of dihydroxyacetone phosphate

The observation that dihydroxyacetone phosphate **11** and glyceraldehyde-3-phosphate **12** were both substrates suggested that PLP synthase also has triose phosphate isomerase activity. To test this, we incubated dihydroxyacetone phosphate **11** with YaaD in deuterated buffer. NMR analysis of this sample indicated that YaaD catalyzed partial H-D exchange at C-1 of dihydroxyacetone phosphate **11**, and no glyceraldehyde-3-phosphate **12** was detected. The NMR is shown in figure 6.6a. The triplet partially overlapping the C-3 doublet corresponds to the single proton at C-1 of dihydroxyacetone phosphate **11** after the stereospecific isomerization reaction.[9] The absence of glyceraldehyde-3-phosphate **12** from the reaction mixture is not unexpected as the equilibrium constant lies in favor of dihydroxyacetone phosphate **11.**[10] In addition, triose phosphate isomerase activity was confirmed when we detected the formation of dihydroxyacetone phosphate **11** from YaaD and glyceraldehyde-3-phosphate **12** by NMR. This suggests that YaaD has triose phosphate isomerase activity, which is shown in figure 6.6b.

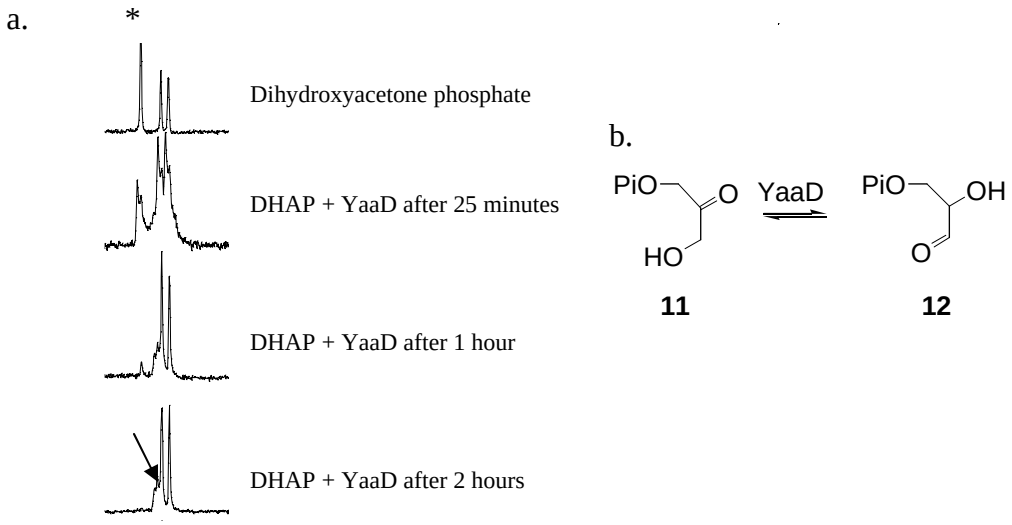

Figure 6.6 Dihydroxyacetone phosphate (DHAP; **11**) isomerization by YaaD a. ^{1}H NMR of the YaaD-catalyzed isomerization of dihydroxyacetonephosphate **11**. * indicates the H-D exchange of the C1 proton and the arrow shows the triplet that results from the proton left after the stereospecific isomerization b. Isomerization reaction catalyzed by YaaD.

6.2.7 Kinetics of PLP synthase

Because cofactors aren't needed in huge quantities in the cell, their biosyntheses are relatively slow.[11] It is clear that this is the case for PLP synthase as well. As indicated in figure 7.5, PLP synthase has a lag in the formation of PLP. We wanted to get a better idea of the overall kinetics of the PLP synthase reaction. In addition, kinetics would allow us to ascertain the true substrates among the isomers. The kinetics were obtained by monitoring the formation of PLP at 390nm with time. The K_m for glutamine in the PLP synthase reaction is 115±17μM (with ribose-5-phosphate **10** and glyceraldehyde-3-phosphate **12**); dihydroxyacetone phosphate **11** is 119±17μM (with ribose-5-phosphate **10**); glyceraldehyde-3-phosphate **12** is 56±5μM (with ribose-5-phosphate **10**); ribose-5-phosphate **10** is 30±5μM (with glyceraldehyde-3-phosphate **12**). The turnover number

(k_{cat}) averaged 0.05min^{-1}. These numbers compare well with those recently published for *B. subtilis* PLP synthase [12].

Older literature suggests that YaaD is guanylylated *in vivo*.[13,14] Confirmation of guanylylation and its purpose have yet to be established. It is possible that this or other cellular modifications could modulate PLP synthase activity, making it more or less active at certain stages of cell growth. To determine whether a modification or other proteins are needed to increase or alter PLP synthase activity, PLP synthase was incubated in both *B. subtilis* and *E. coli* crude cell lysates and analyzed for activity. Neither *B. subtilis* nor *E. coli* cell lysates were able to increase PLP synthase activity beyond that in the purified system, and the lag was still present.

6.3 Conclusion

We have demonstrated the first successful reconstitution of PLP synthase from the YaaE and YaaD family of genes in *B. subtilis*. Glutamine, ribose-5-phosphate **10** or ribulose-5-phosphate **8**, and glyceraldehyde-3-phosphate **12** or dihydroxyacetone phosphate **11** are the substrates, and the product was identified as pyridoxal-5'-phosphate **1**. YaaE hydrolyzes glutamine to glutamate and ammonia, and ammonia travels to the active site of YaaD. Glutaminase activity depends on the presence of YaaD. In addition to catalyzing PLP formation, we have identified three partial reactions catalyzed by YaaD in the transformation to PLP: isomerization of ribose-5-phosphate **10** and ribulose-5-phosphate **8**; isomerization of dihydroxyacetone phosphate **11** and glyceraldehyde-3-phosphate **12**; and imine formation with ribulose-5-phosphate **8** and lysine 149. The kinetics of the PLP synthase reaction suggest the enzymes are slow, and the best substrates are ribose-5-phosphate **10**, glyceraldehyde-3-phosphate **12**, and glutamine.

6.4 Experimental procedures

6.4.1 Materials and methods

6.4.1.1 Materials: pET28a vector was from Novagen, restriction enzymes from New England Biolabs, primers were ordered from BioResource Center at Cornell University. A Perkin Elmer GeneAmp PCR System 2400 was used for PCR and mutagenesis. Pfx Platinum polymerase was from Invitrogen. QiaExII gel extraction kit and PCR purification kit were purchased from Qiagen, and miniprep kit was from Promega. T4 DNA ligase was purchased from New England Biolabs. Clones were sequenced at the Bioresource Center at Cornell University. DH5α was used for propagation and storage; BL21(DE3) for overexpression; both were purchased from Novagen. Ni-Nta resin was from Qiagen and all chemicals were purchased from Sigma. DG10 desalting columns were purchased from BioRad, Centricon ultra concentrators were from Amicon, as were the microcon concentrators.

6.4.1.2 Cloning, overexpression and purification of YaaD and YaaE (YaaD.28; YaaE.28): (Done by Cynthia Kinsland) *B. subtilis* CU1065 genomic DNA was amplified using the following primers: YaaD 5'for-TAG GGG GAC CAA CAT ATG GCT CAA ACA GGT ACT GAA CG-3'; 5'rev-TTG TTA ACA TGT CTC GAG CGC TCC TAT GTT CTT ACC AGC-3'; YaaE 5'for-AGG AGC GCT GCT CAT ATG TTA ACA ATA GGT GTA CTA GG-3'; YaaE 5'for-CTA TCA ACG CTT CTC GAG CTT TAT TTG TGC TTA TAA TG-3'. *Nde*I and *Xho*I restriction sites were added to the forward and reverse primer, respectively. The gene was amplified using Pfx Platinum DNA polymerase with a 1.5min extension time. Upon purification of the PCR fragment from the agarose gel, the product and the pET28a vector were cut with *Nde*I and *Xho*I. Digested pET28a was treated with CIP. The cut pET28a vector and cut PCR product

were purified by gel and ligated with T4 ligase at room temperature for 2 hours. Competent DH5α cells were transformed with 2.5μL of the ligation mixture and plated on LB-Kan plates. Colonies were checked for insert by colonly PCR. Colonies with insert were sequenced.

E. coli Tuner(DE3) cells were used for protein expression. Cells were grown to an $OD6_{00}$ of 0.5 and induced with 1mM IPTG at 37^{o}C. After 5 hours of induction, the cells were harvested at 8,000 rpm for 10 minutes and stored at -20^{o}C until purification.

Cells containing overexpressed protein were resuspended in lysis buffer (50mM phosphate pH9, 300mM NaCl, 10mM imidazole) with lysozyme. The cells were lysed by sonication (30-2 second pulses, 3 times), and the cell debris was removed by centrifugation for 30minutes at 17,000 rpm. The cleared lysate was passed through pre-equilibrated (with lysis buffer) Ni-Nta resin. Following a quick wash with lysis buffer, the resin was washed with wash buffer (50mM phosphate pH8, 300mM NaCl, 20mM imidazole) until little protein eluted by Coommassie. When little protein washed off, protein was eluted with elution buffer (50mM phosphate pH8, 300mM NaCl, 250mM imidazole), desalted into 25mM phosphate pH8 using DG10 desalting columns, and concentrated. Typical yield for 1L of culture was 10 mg for YaaD and 20mg for YaaE.

6.4.2 Assays

6.4.2.1 Materials: All chemicals were purchased from Sigma. ESI-FTMS was performed by the McLafferty group at Cornell University. NMR spectra were obtained on an INOVA 600MHz spectrometer, UV-Vis spectra were obtained on a Hitachi U2010 spectrophotometer and HPLC was performed on a Hewlett Packard 1100 Series

instrument. Microcons were purchased from Amicon and HPLC column was from Supelco.

6.4.2.2 YaaE glutaminase activity:

34μg YaaD, 80μg YaaE and 10mM glutamine were incubated in 50mM Tris, pH8 at room temperature. After 30 minutes, 10μL of the sample was added to 30μL dansyl chloride solution (10mM dansyl chloride in actone). The pH was adjusted to 9.5 with the addition of 0.6μL 0.3M NaOH. After 30 minutes, 5μL was spotted on Si coated TLC plates, it was allowed to dry, and then developed in chloroform: t-butanol: acetic acid (6:3:1). Controls omitted enzyme, YaaD, and used glutamate in place of glutamine.

6.4.2.3 Covalent modification of YaaD:

A typical reaction contained 200μg YaaD and 10mM ribose-5-phosphate (or ribulose-5-phosphate) in 50mM phosphate, pH8. After 1 hour at 37^{o}C, the sample was frozen for ESI-FTMS analysis.

6.4.2.4 YaaD isomerization of ribose-5-phosphate:

1mg YaaD and 3mM ribose-5-phosphate were combined in 50mM deuterated phosphate, pD 7.8. Isomerization was observed using a 600MHz NMR.

6.4.2.5 Reconstitution of PLP biosynthesis:

UV: 25μg YaaD, 25μg YaaE, 5mM ribulose-5-phosphate, 5mM dihydroxyacetone phosphate and 5mM glutamine were combined in 50mM phosphate, pH8 in 400μL total. Blank contained no dihydroxyacetone phosphate. Wavelength scans were taken every few minutes with a UV-Vis spectrometer.

HPLC: 1mg YaaD and 1mg YaaE were incubated with 1mM ribulose-5-phosphate, 4mM dihydroxyacetone phosphate and 5mM glutamine in 1mL total. After 15 hours at 37^{o}C in the dark, the samples were lyophilized to about 250μL and protein removed with microcon concentrators. Samples were analyzed by HPLC with a LC-18-T column, 15cm x 4.6mm, 3μm with the following solvent system: A, water; B, 100mM KH_2PO_4 pH6.6; C, methanol. 0-6minutes, 100% B; 7minutes, 10% C; 20minutes, 30% C, 30% A; 22minutes, 100% B.

NMR: 3.8mg YaaD, 1.6mg YaaE, 1mM ribulose-5-phosphate, 5mM dihydroxyacetone phosphate and 5mM glutamine were combined in 50mM phosphate, pH8 in 1.5mL total. After 16 hours at 37^{o}C in the dark, 0.5mg Alkaline phosphatase and 1mM $MgSO_4$ were added and allowed to sit for 1.5 hours at 37^{o}C. Following a little lyophilization to reduce the volume, the protein was removed with microcon concentrators and all of the sample was injected into the HPLC (using the same method described above). The pyridoxal peak at 8 minutes was collected, lyophilized, and analyzed on a 600MHz NMR.

6.4.2.6 YaaD isomerization of dihydroxyacetone phosphate:

H/D exchange: 80μg YaaD was incubated with 2.7mM dihydroxyacetone phosphate in 50mM phosphate, pD7.0. Isomerization was observed using a 600MHz NMR.

Dihydroxyacetone phosphate formation: 420μg YaaD was incubated with 2.7mM glyceraldehyde-3-phosphate in 50mM phosphate, pD7.5. Dihydroxyacetone phosphate was observed using a 600MHz NMR.

6.4.2.7 Kinetics of PLP synthase:

In 320μL total, 150μg YaaD and 150μg YaaE were added to 5mM ribose-5-phosphate and 5mM glyceraldehyde-3-phosphate in 30mM phosphate, pH6.6 with various

concentrations of glutamine (100μM – 2.5mM). The reactions were monitored at 390nm at room temperature. Initial rates were plotted vs. substrate concentration to determine V_{max}, K_m and k_{cat} values. Similar analysis was done on each substrate.

E. coli crude cell lysate: 250μL crude cell lysate from YaaD overexpression strain BL21 and 250μL crude cell lysate from YaaE overexpression strain BL21 was mixed with 3mM ribose-5-phosphate, 3mM glyceraldehyde-3-phosphate and 3mM glutamine in 550μL total. Absorbance at 390nm was monitored with time.

B. subtilis crude cell lysate: *B. subtilis* TX1 cells were grown in LB supplemented with 0.1% glucose, 13.4mM KCl, 20μM $MnCl_2$, 1μM $FeSO_4$, 1mM $MgSO_4$ and 1mM CaCl2 at 37^{o}C. After 8 hours, the cells were harvested and stored at -20^{o}C until use. A cell pellet from 300mL culture was resuspended in 25mL buffer (0.1M HEPES, pH7.5; 2mM PMSF; 0.5mg/mL lysozyme) and incubated at 37^{o}C for 10 minutes. The sample was cooled on ice and sonicated 8 times with 30 second intervals with 80/120 mesh glass beads. The cell debris was collected at 10,000xg for 10 minutes. The 25mL was added to 25mL assay buffer, which included 25mM tris, pH7.8, 1mM β-mercaptoethanol, 100mM NaCl, 2mM $MnCl_2$, 20μM GTP and 20μM ATP. To this, 600μg YaaD was added and allowed to sit on ice for 25 minutes. 200μL of this mixture was added to 75μg YaaE, 4.7mM ribose-5-phosphate, 4.7mM dihydroxyaceteone phosphate and 4.7mM glutamine in 360μL total and the absorbance at 390nm was measured with time. After 25minutes, the sample was added to pre-equilibrated Ni-Nta resin. The sample was purified according to the normal protocol for YaaD. Purified YaaD activity was tested with 150μg YaaD, 150μg YaaE, 4.8mM ribose-5-phosphate, 4.8mM dihydroxyacetone phosphate and 4.8mM glutamine in 50mM phosphate, pH6.6, 360μL total.

6.5 References

1. Gupta, R.; Hemscheidt, T.; Sayer, B.; Spenser, I. (2001) *J. Am. Chem. Soc.* **123,** 11353-11359.

2. Zeidler, J.; Gupta, R.; Sayer, B.; Spenser, I. (2003) *J. Org. Chem.* **68,** 3486-3493.

3. Tazuya, K.; Adachi, Y.; Masuda, K.; Yamada, K.; Kumaoka, H. (1995) *Biochim. Biophys. Acta* **1244,** 113-116.

4. Massiere, F.; Badet-Denisot, M.-A. (1998) *Cell. Molec. Life Sci.* **54,** 205-222.

5. Dong, Y.; Sueda, S.; Nikawa, J.; Kondo, H. (2004) *Eur. J. Biochem.* **271,** 745-752.

6. Belitsky, B. (2004) *J. Bacteriol.* **186,** 1191-1196.

7. Dorrestein, P.; Zhai, H.; Taylor, S.; McLafferty, F.; Begley, T. (2004) *J. Am. Chem. Soc.* **126,** 3091-3096.

8. Zhu, J.; Burgner, J.; Harms, E.; Belitsky, B.; Smith, J. (2005) *J. Biol. Chem.* **280,** 27914-27923.

9. O'Donoghue, A.; Amyes, T.; Richard, J. (2005) *Biochemistry* **44,** 2610-2621.

10. Knowles, J.; Hall, A. (1975) *Biochemistry* **14,** 4348-4352.
11. Begley, T. (2006) *Nat. Prod. Rep.* **23,** 15-25.

12. Raschle, T.; Amrhein, N.; Fitzpatrick, T. (2005) *J. Biol. Chem.* **280,** 32291-32300.

13. Mitchell, C.; Vary, J. (1989) *J. Bacteriol.* **171,** 2915-2918.

14. Mitchell, C.; Morris, P.; Vary, J. (1992) *Mol. Microbiol.* **6,** 1579-1581.

Chapter 7

Mechanistic Studies on PLP synthase

7.1 Introduction

The alternate PLP biosynthetic pathway involving YaaD and YaaE is present in pathogens such as *Mycobacterium tuberculosis* and *Plasmodium falciparum*, making it an attractive drug target in these organisms. In order to design and synthesize effective inhibitors against PLP synthase, it is necessary to first understand the mechanism of PLP formation. Mechanistic analysis of PLP synthase will enable us to envision substrate analogs and intermediate analogs which could serve as potential inhibitors.

Unlike the *E. coli* de novo pathway, the alternate PLP biosynthetic pathway involves only two enzymes (YaaD and YaaE), and it appears that the majority of the chemistry is performed by YaaD, the synthase subunit. Chapter 6 characterized the substrates of the PLP synthase reaction as well as three partial reactions catalyzed by YaaD. This chapter will describe the steps immediately following pentose isomerization and adduct formation on YaaD, including the first bond forming reaction and the formation of a stable intermediate.

7.2 Results and Discussion

7.2.1 Ribose-5-phosphate-ammonia bond formation

To probe the early steps of the PLP synthase reaction, we decided to monitor the reaction using mass spectrometry (in collaboration with Yun Xiang and Fred McLafferty). YaaD purifies with a covalent imine adduct **9** of MW 34421 Da with the addition of ribose-5-

phosphate **10** or ribulose-5-phosphate **8** (figure 7.1a). If C-C bond formation between ribose-5-phosphate **10** and dihydroxyacetone phosphate **11** or glyceraldehyde-3-phosphate **12** occurs first to form the carbon backbone of PLP, we would expect to see a higher molecular weight species by mass spectrometry when triose is added. When dihydroxyacetone phosphate **11**, ribulose-5-phosphate **8** and YaaD were mixed, no additional adduct is observed on YaaD; we only observe the ribulose-5-phosphate adduct **9**. We then hypothesized that the ammonia generated from the hydrolysis of glutamine by YaaE may add to the YaaD-ribulose-5-phosphate imine **9** to release the enzyme-bound adduct. When YaaE and glutamine were mixed with YaaD and ribulose-5-phosphate **8**, we observe the release of the adduct from YaaD, forming apo-YaaD with MW 34209 Da. The mass spectrum is shown in figure 7.1b. The reaction depends on glutamine; YaaE alone cannot release the adduct from YaaD. This result suggests that in the absence of the triose, a transimination reaction occurs with ammonia and the YaaD-ribulose-5-phosphate adduct **9**, and this transimination releases the covalent adduct from YaaD to produce a pentulose-imine intermediate **13**, which is shown in figure 7.1c. The first bond formed in the PLP synthase reaction is between ammonia and the C2 of ribose-5-phosphate **10**. This reaction resembles that of imidazole glycerolphosphate synthase (HisF), the enzyme with structural homology to the YaaD model proposed by Bauer.[1] HisF produces the imidazole ring of histidine and is shown in figure 5.6.[2]

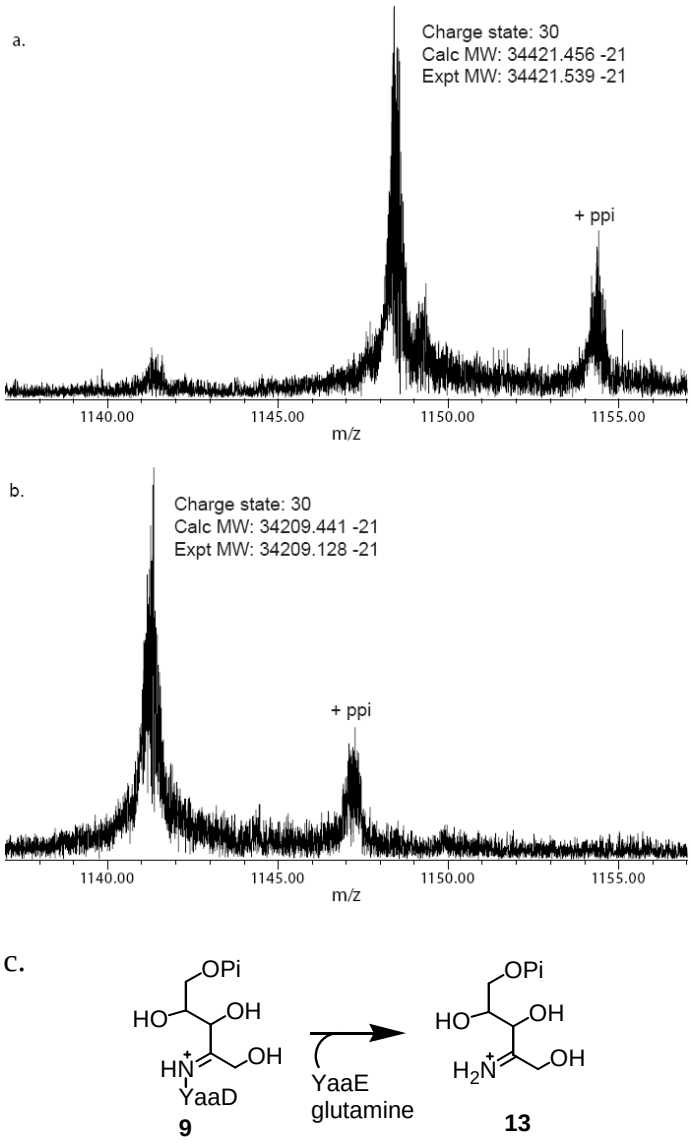

Figure 7.1 ESI-FTMS of the partial PLP synthase reaction a. YaaD incubated with ribose-5-phosphate **10** b. YaaD incubated with ribose-5-phosphate **10**, YaaE and glutamine c. Transimination releases the pentulose covalent adduct from YaaD.

7.2.2 Intermediate formation

To determine whether the pentulose phosphate imine **13** is further processed in the absence of the triose, we monitored the reaction by UV-Vis spectrophotometry. As displayed in figure 7.2a, the PLP synthase reaction in the absence of triose shows an

absorbance at 320nm, which is dependent on the enzyme concentration and time. Addition of dihydroxyacetone phosphate **11** to the intermediate results in an isosbestic point at 340nm (figure 7.2b), and while the intermediate approaches the steady state level, product PLP **1** (measured by its absorbance at 410nm) increases linearly with time (figure 7.2c). This suggests that the absorbance that we observe at 320nm is an intermediate and that it is converted to PLP **1**. The intermediate appears to be tightly

a. b.

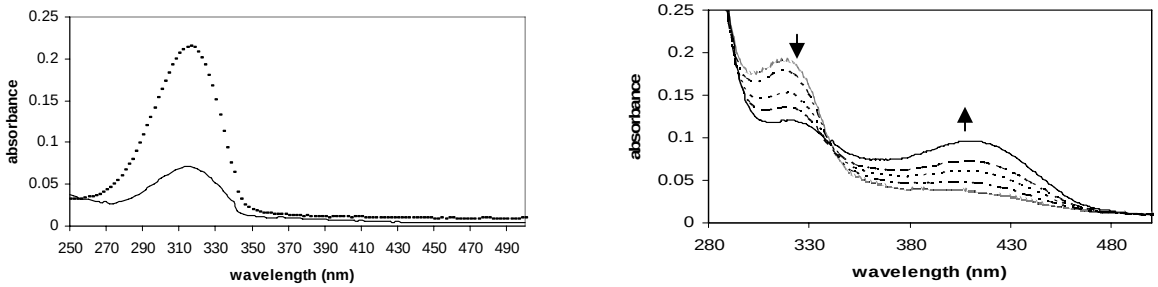

c.

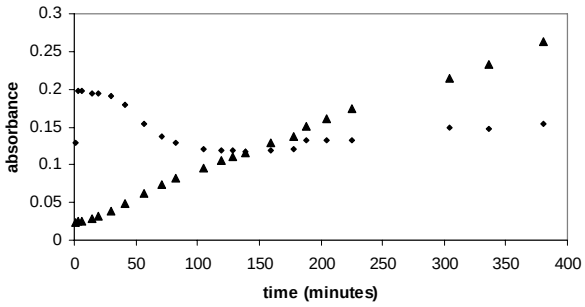

Figure 7.2 YaaD intermediate formation a. Reaction of YaaD, ribose-5-phosphate **10**, YaaE and glutamine after 1 minute (solid line) and 5 minutes (dotted line) b. Wavelength scan of the PLP synthase reaction over time: 30 minutes (dotted line); 41 minutes (dashed line); 56 minutes (dotted line); 71 minutes (dashed line); 105 minutes (flat line) c. Reaction of YaaD, YaaE, ribose-5-phosphate **10**, glutamine and dihydroxyacetone phosphate **11**. Intermediate levels reach steady state (squares; absorbance 320nm), while product PLP **1** increases (triangles; absorbance 390nm).

bound to the enzyme; gel filtration does not separate protein from intermediate absorbance at 320nm and all attempts to remove the intermediate from the active site have failed. *E. coli* ribosephosphate isomerase[3] does not form a similar species when it is incubated with ribose-5-phosphate **10** and glutamine or ammonia, indicating this intermediate is specific for the PLP synthase reaction.

Ribose-5-phosphate **10** and ribulose-5-phosphate **8** are both substrates for the formation of the intermediate, suggesting that isomerization occurs prior to its formation. The formation of the intermediate also depends on YaaD-ribulose-5-phosphate adduct **9** formation because K149A, the mutant that does not form an adduct with YaaD, is still able to isomerize ribose-5-phosphate **10**, yet it is unable to form the intermediate. This suggests that the isomerization of ribose-5-phosphate **10** and the adduct **9** formation on YaaD are necessary for the intermediate formation.

7.2.3 Intermediate characterization: kinetic isotope effect and PLP synthase lag

After several unsuccessful attempts at isolating the intermediate with an absorbance at 320nm, we decided to use alternative methods to characterize it. An absorbance at 320nm suggests extended conjugation in the putative intermediate; compounds such as acrolein and pyridoxine absorb at this wavelength. To better understand the structure of the intermediate, we asked whether we could observe a kinetic deuterium isotope effect on the intermediate formation. Beginning with deuterated ribose, we were able to generate the corresponding deuterium-labeled ribose-5-phosphate (labeled separately at each carbon C1-C5) *in situ* using recombinant *E. coli* ribokinase.[4] We tested each compound for a kinetic isotope effect on intermediate formation at 320nm. To our

surprise, we only observed a kinetic isotope effect for the ribose-5-phosphate labeled at C5, implying the involvement of one of these two protons in the rate determining step towards the intermediate formation. Table 7.1 summarizes these results. The observed kinetic isotope effect (k_H/k_D) of 2.1 is large, suggesting that it is a primary kinetic isotope effect. Testing the isotope effect at C1 serves as a nice control since the deuterium at this position is non-enzymatically exchanged with the solvent, as observed in the NMR in figure 6.3.

Table 7.1 Kinetic deuterium isotope effect on intermediate formation.

	1-^{2}H-ribose-5-phosphate	2-^{2}H-ribose-5-phosphate	3-^{2}H-ribose-5-phosphate	4-^{2}H-ribose-5-phosphate	5-^{2}H-ribose-5-phosphate	5*R*-[5-^{2}H]-ribose-5-phosphate (6.5:1)	5*S*-[5-^{2}H]-ribose-5-phosphate (2.5:1)
k_H/k_D	1.1±0.1	1.2±0.1	1.1±0.1	1.1±0.03	2.1±0.2	1.8±0.3	1.4±0.2
k_H/k_D expected if the C5 pro-*R* diastereomer causes the isotope effect						1.9	1.3
k_H/k_D expected if the C5 pro-*S* diastereomer causes the isotope effect						1.1	1.7

Further investigation, in collaboration with David Hilmey, revealed that it was the C5 pro-*R* enantiomer of ribose-5-phosphate that resulted in the observed isotope effect. Dave Hilmey synthesized 5*R*-[5-^{2}H]-ribose in a 6.5:1 ratio with 5*S*-[5-^{2}H]-ribose and he also synthesized the 5*S*-[5-^{2}H]-ribose in a 2.5:1 ratio with 5*R*-[5-^{2}H]-ribose. These are shown in figure 7.3. If YaaD abstracts the pro-*R* proton of ribose-5-phosphate, we would expect the 6.5:1 mixture of pro-*R*: pro-*S* diastereomers to give a kinetic isotope effect of 1.9 and the 2.5:1 mixture of pro-*S*: pro-*R* would give a kinetic isotope effect of 1.3. The observed isotope effect on the mixture of 6.5:1 pro-*R*: pro-*S* was 1.8 and the observed isotope effect of the 2.5:1 pro-*S*: pro-*R* mixture was 1.4. These values, which are shown

in Table 7.1, are consistent with a kinetic deuterium isotope effect on 5*R*-[5-^{2}H]-ribose-5-phosphate.

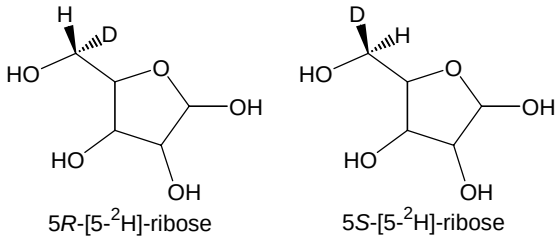

Figure 7.3 The pro-*R* and pro-*S* diastereomers of ribose synthesized by Dave Hilmey.

Interestingly, although there was no change in the rate of PLP formation with 5-^{2}H-ribose-5-phosphate, suggesting that the triose addition is the rate determing step in the conversion to PLP **1**, we did observe something surprising. As indicated in figure 6.5, we always observe a lag in PLP formation. When 5-^{2}H-ribose-5-phosphate was analyzed for PLP formation, the lag was exaggerated, as if there was an isotope effect on the lag. This did not happen with the other deuterated substrates, suggesting it was specific for 5-^{2}H-ribose-5-phosphate. An example of this lag is shown in figure 7.4. The exaggerated lag on the PLP synthase reaction observed with 5-^{2}H-ribose-5-phosphate suggests that it may be caused, at least partially, by the slower intermediate formation due to the kinetic deuterium isotope effect. Moreover, we were able to correlate the rate of intermediate formation with the rate of the lag, again suggesting that the lag in the PLP synthase reaction is partially due to the formation of this intermediate. The initial rate that we observe for PLP formation, therefore, may be the rate of the triose adding to the intermediate, and may not include intermediate formation, as this appears to form the lag.

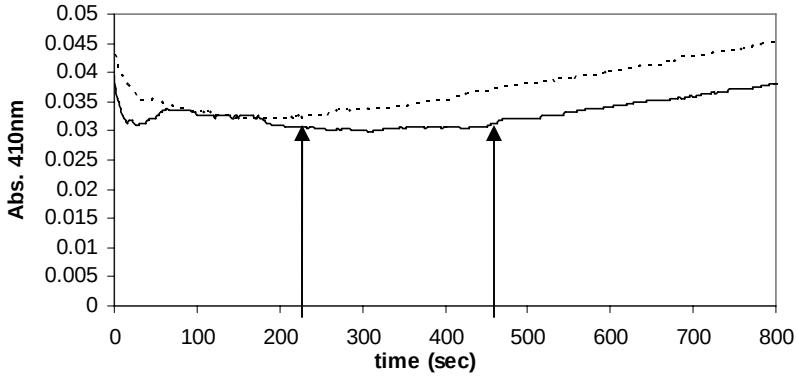

Figure 7.4 Lag in PLP synthase reaction with deuterated ribose-5-phosphate. Dotted line is PLP synthase reaction with H-ribose-5-phosphate; line is PLP synthase reaction with 5-^{2}H-ribose-5-phosphate. 5-^{2}H-ribose-5-phosphate gave about 2x the lag phase.

Our results suggest that a transimination between ammonia and the YaaD-adduct **9** releases the adduct from YaaD to form **13** and that this species is further processed by C5 deprotonation to form an intermediate that absorbs at 320nm. To be consistent with the experimental results, we suggest that the amino-ribulose-5-phosphate **13** tautomerizes to **14**, followed by water elimination to form **15** and C5 deprotonation to form **16**, the proposed intermediate. This is shown in figure 7.5.

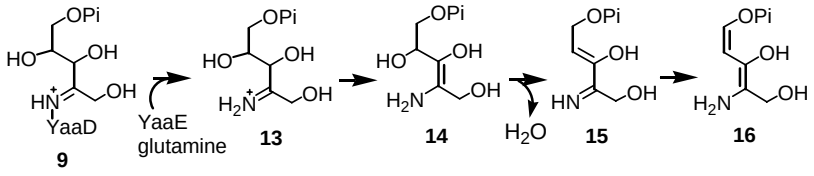

Figure 7.5 Proposed mechanism of intermediate formation at 320nm.

7.2.4 Triose addition to the intermediate

We have characterized the first bond formed in the PLP synthase reaction and also observe a stable intermediate **16** that forms in the absence of the triose. To determine how the triose adds to the intermediate **16**, we looked at which triose, dihydroxyacetone phosphate **11** or glyceraldehyde-3-phosphate **12**, reacts faster with **16**. If

dihydroxyacetone phosphate **11** reacts faster, we would predict C-C bond formation between dihydroxyacetone phosphate **11** and the intermediate, as shown in figure 7.6 reaction A. The carbonyl at C2 of dihydroxyacetone phosphate **11** is set up for C-C bond formation. Alternatively, if glyceraldehyde-3-phosphate **12** reacts faster with the intermediate, we hypothesize that C-N bond formation between the C1 of glyceraldehyde-3-phosphate **12** and the intermediate amine group would occur to yield **21** (figure 7.6 reaction B). The aldehyde at C1 allows for a facile imine reaction between the two species.

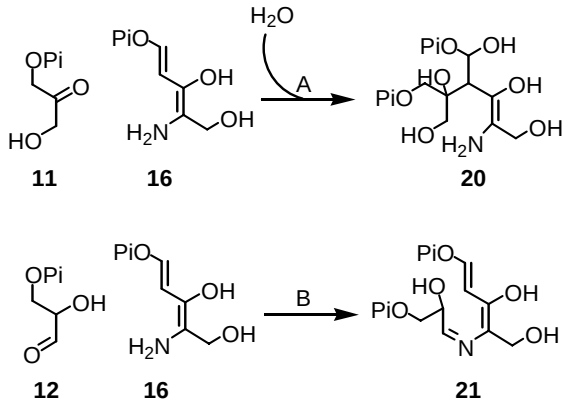

Figure 7.6 Two possible reactions between the triose and the intermediate. A shows C-C bond formation between dihydroxyacetone phosphate **11** and the intermediate and B shows C-N bond formation between glyceraldehyde-3-phosphate **12** and the intermediate.

Both dihydroxyacetone phosphate **11** and glyceraldehyde-3-phosphate **12** cause the intermediate at 320nm to decay with time, however, the reactions appear different by UV-Vis. When we monitor the formation of the intermediate in the presence of dihydroxyacetone phosphate **11**, we observe a similar amplitude for intermediate formation compared to the reaction without triose. This is followed by a slow decay to approach the steady state level of intermediate. This is shown in figure 7.7. Glyceraldehyde-3-phosphate **12** addition to the intermediate yields something very different: the observed initial rate of intermediate formation appears slow compared to

dihydroxyacetone phosphate **11** addition and the reaction approaches the steady state level of intermediate without any apparent decrease, also shown in figure 7.7. The difference in amplitude between the dihydroxyacetone phosphate **11** reaction and the glyceraldehyde-3-phosphate **12** reaction is not due to the rate of formation of the intermediate, which is the same in both cases, it is due to the rate of decay of the intermediate. The rate of intermediate decay is embedded in the rate of intermediate formation; the difference in amplitude implies that glyceraldehyde-3-phosphate **12** reacts with the intermediate faster than dihydroxyacetone phosphate **11**. At every time point, although the intermediate is formed at the same rate, glyceraldehye-3-phosphate **12** reacts faster with the intermediate, giving it a lower amplitude compared to dihydroxyacetone phosphate **11**. Varying the concentration of triose changes the apparent initial rate and the amplitude of the intermediate, verifying that the differences we observe are due to triose addition to the intermediate.

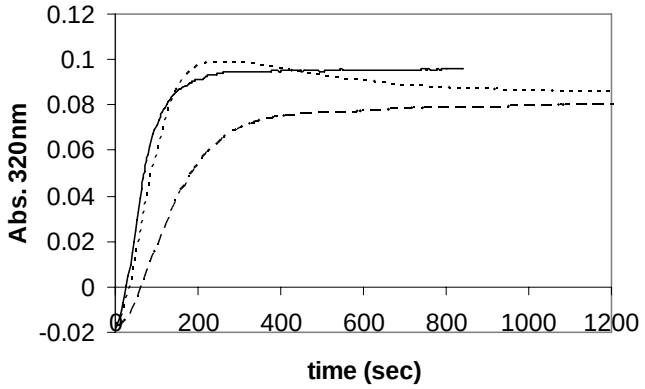

Figure 7.7 Intermediate formation in the presence of dihydroxyacetone phosphate **11** (dotted line); glyceraldehyde-3-phosphate **12** (dashed line); and no triose (filled line).

As described above, glyceraldehyde-3-phosphate **12** is able to add to the intermediate **16** faster than dihydroxyacetone phosphate **11**, and we wanted to know whether this was because dihydroxyacetone phosphate **11** needs to isomerize before it can react with the intermediate. To test this hypothesis, we formed dihydroxyacetone phosphate deuterated

stereospecifically at the C1 position using triose phosphate isomerase in D_2O (the reaction equilibrium lies in favor of dihydroxyacetone phosphate 22:1[5]). Addition of 1-^{2}H-dihydroxyacetone phosphate to the intermediate reaction slowed the addition to the intermediate compared to the fully protonated substrate, as observed in the different amplitudes of intermediate (figure 7.8). Additionally, triose phosphate isomerase speeds up the addition of dihydroxyacetone phosphate **11** to the intermediate when compared to dihydroxyacetone phosphate **11** alone. These results indicate that glyceraldehyde-3-phosphate **12** reacts faster with the intermediate **16** and dihydroxyacetone phosphate **11** needs to isomerize prior to reacting with the intermediate. We suggest that C-N bond formation between the C1 of glyceraldehyde-3-phosphate **12** and the intermediate amine is the second bond to form in the PLP synthase reaction. This is shown in figure 7.9.

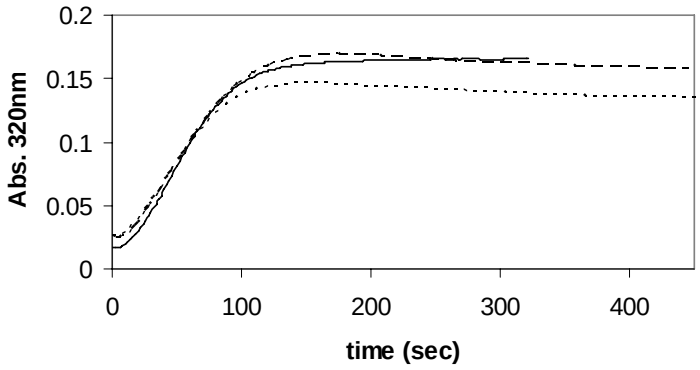

Figure 7.8 Intermediate formation in the presence of dihydroxyacetone phosphate **11** (dotted line); 1-^{2}H-dihydroxyacetone phosphate (dashed line); and no triose (filled line).

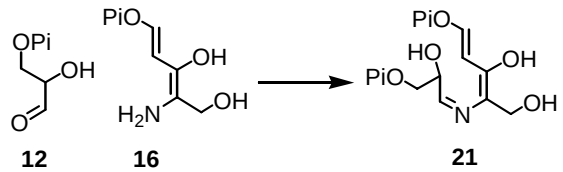

12 **16** **21**

Figure 7.9 C-N bond formation between the C1 of glyceraldehyde-3-phosphate **12** and the intermediate amine is consistent with the experimental observations.

7.2.5 Phosphate release

During the course of the PLP synthase reaction, the phosphate from the triose is retained and the pentose phosphate is removed. To determine if the pentose phosphate is eliminated or hydrolyzed, we used 500MHz ^{31}P-NMR and looked for an isotopic shift when the PLP synthase reaction was run in 39% ^{18}O water. If the phosphate is hydrolyzed, as in figure 7.10a, ^{18}O would be incorporated into phosphate and we would expect 39% of the phosphate signal to be isotopically shifted (note that 0.02ppm can be separated at 145MHz[6]). Alternatively, if the phosphate is eliminated, no ^{18}O would be incorporated into the released phosphate and we should observe one signal corresponding to all ^{16}O-phosphate (figure 7.10b). We did not observe an ^{18}O-P_i isotopic shift when the reaction was run in ^{18}O water, indicated by the singlet at -46.4ppm (figure 7.11), suggesting that the pentose phosphate is eliminated and not hydrolyzed when it is released. Dihydroxyacetone phosphate **11** non-enzymatically eliminates phosphate to methyl glyoxal and a fraction of the phosphate peak is due to this.[7]

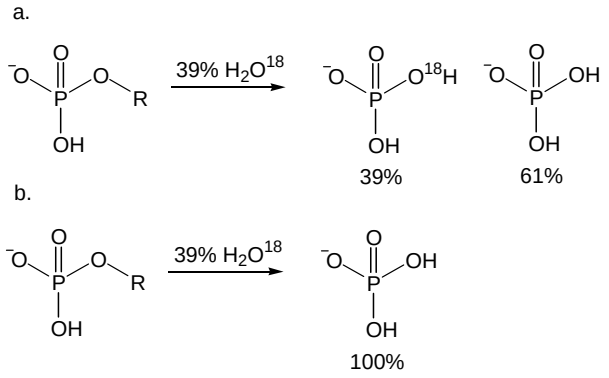

Figure 7.10 ^{31}P-NMR experiment summary a. If phosphate is hydrolyzed, 39% of the phosphate signal will be isotopically shifted by the ^{18}O-Pi b. If phosphate is eliminated, no shift will be observed.

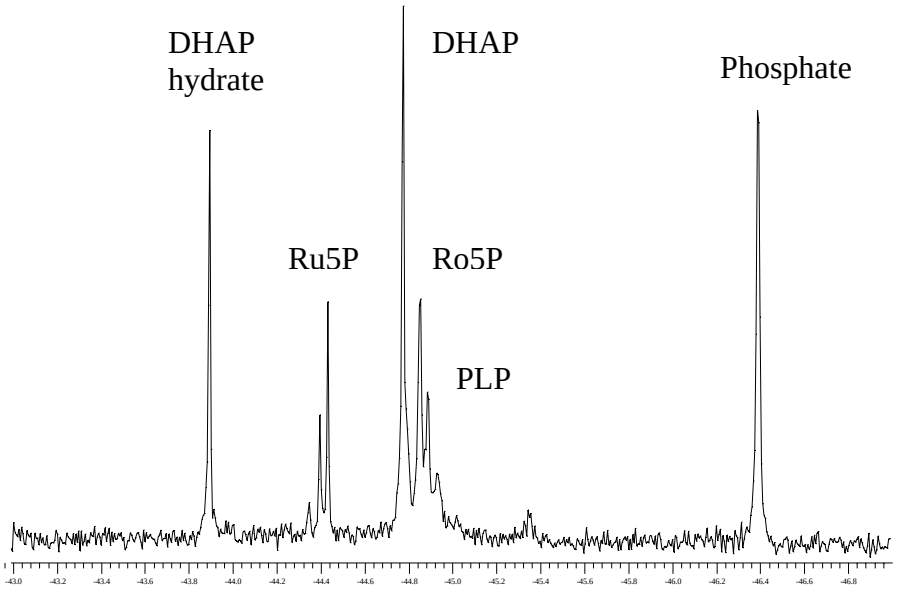

Figure 7.11 ^{31}P-NMR of the PLP synthase reaction. No ^{18}O-P_i isotopic shift is observed, indicated by the singlet at -46.4ppm. DHAP (dihydroxyacetone phosphate), Ru5P (ribulose-5-phosphate), Ro5P (ribose-5-phosphate).

7.2.6 PLP synthase reaction in D_2O

When the PLP synthase reaction was run in deuterated buffer, deuterium incorporation was observed at the C2' (2.25ppm) and C6 (7.45ppm) position of PLP (figure 7.12). Deuterium incorporation at the C2' position results from the isomerization of ribose-5-phosphate **10** and ribulose-5-phosphate **8** and from the non-enzymatic isomerization of ribulose-5-phosphate **8**, which incorporates deuterium at C1 of the pentulose (refer to figure 6.3). Deuterium incorporation at C6 of the PLP ring was observed when both glyceraldehyde-3-phosphate **12** and dihydroxyacetone phosphate **11** were used as substrates. This exchange is most likely due to non-enzymatic isomerization of glyceraldehyde-3-phosphate **12** in solution.

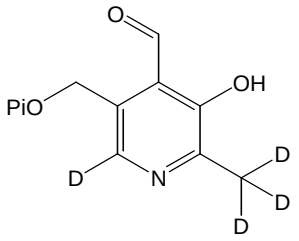

Figure 7.12 Deuterium incorporation into PLP when the PLP synthase reaction was run in deuterated buffer.

7.2.7 2'-hydroxypyridoxol-5'-phosphate is not an intermediate

It was previously suggested based on labeling studies that 2'-hydroxypyridoxol (or its phosphate **17**; figure 7.13) is a precursor for vitamin B6 biosynthesis in *S. cerevisiae* as well as in other eukaryotes.[8,9] *S. cerevisiae* has the YaaD and YaaE family of proteins and we wanted to know whether YaaD and YaaE would accept 2'-hydroxypyridoxol as a substrate. When 2'-hydroxypyridoxol or 2'-hydroxypyridoxol-5'-phosphate **17** (in collaboration with Brian Lawhorn) were incubated with YaaD and YaaE, or with YaaD alone, no PLP **1** or B6 vitamer was observed by HPLC, and the sample did not turn yellow. It is possible that this compound serves as an intermediate in PLP biosynthesis in eukaryotes such as yeast (where the labeling studies were done), but the high degree of sequence similarity between the eukaryotic YaaD and prokaryotic YaaD suggests that this is unlikely. It is also possible that 2'-hydroxypyridoxol can be metabolized to an advanced intermediate (for example, a species such as 2'-hydroxypyridoxol-4',5'-phosphate) that is then accepted by PLP synthase. What is most likely, however, is that 2'-hydroxypyridoxol is the substrate for a PLP salvage pathway in yeast because it was shown to be converted to B6 vitamers in *Kloeckera apiculata*, a vitamin B6 dependent yeast.[9]

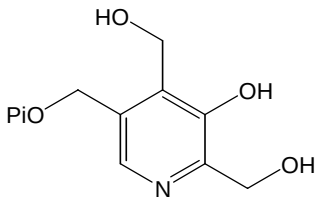

17

Figure 7.13 2'-hydroxypyridoxol-5'-phosphate, which was tested as a substrate for PLP synthase.

7.3 Conclusion

This chapter provides evidence for the early steps in the PLP synthase reaction, including an intermediate that is formed in the absence of the triose substrate. The first bond formed in the PLP synthase reaction is between ammonia and the C2 carbon of ribose-5-phosphate **10**. Ammonia, produced in the active site of YaaE, travels to YaaD and releases the covalent adduct on YaaD to produce **13**, shown in figure 7.14. This species is further processed, as indicated by its absorbance at 320nm, by C5 deprotonation to **16**. Imine formation between the intermediate amine **16** and the C1 of glyceraldehyde-3-phosphate **12** results in **21**. Two successive tautomerization reactions yield **23**. These tautomerization reactions resemble the isomerization of glyceraldehyde-3-phosphate **12** and dihydroxyacetone phosphate **11** and is probably why YaaD can accept both substrates and has triose phosphate isomerase activity. Water addition to **23** followed by phosphate elimination yields **25**. Water elimination, a tautomerization, and another elimination of water yields **28**. Finally, tautomerization gives PLP **1**. This mechanism does not include 2'-hydroxypyridoxol-5'-phosphate **17**, which was shown not to be a substrate for PLP synthase.

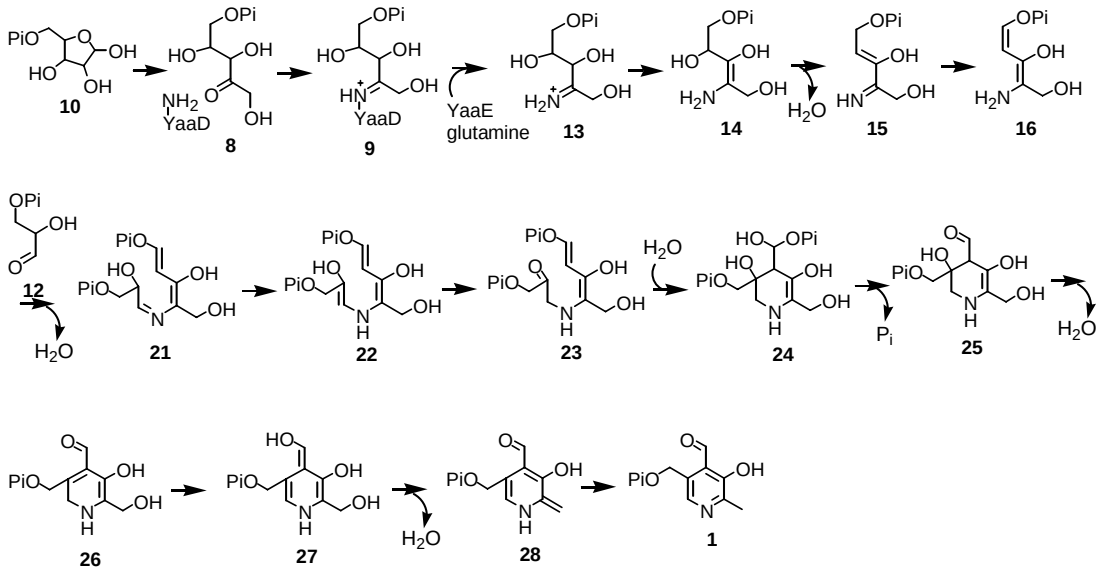

Figure 7.14 Proposed mechanism of PLP synthase.

7.4 Experimental procedures

7.4.1 Materials and methods

7.4.1.1 Materials: All chemicals were purchased from Sigma. Deuterated ribose was from Omicron Biochemicals. ESI-FTMS was performed by the McLafferty group at Cornell University. NMR spectra were obtained on an INOVA 600MHz spectrometer and INOVA 500Mhz spectrometer, UV-Vis spectra were obtained on a Hitachi U2010 spectrophotometer and HPLC was performed on a Hewlett Packard 1100 Series instrument. Microcons were purchased from Amicon, HPLC column was from Supelco and desalting columns from BioRad. Triose phosphate isomerase was from Sigma, ribosephosphate isomerase and ribokinase were gifts from the Mowbray lab at Swedish University of Agricultural Sciences.

7.4.2 Assays

7.4.2.1 Ribose-5-phosphate-ammonia bond formation:

300μg YaaD was mixed with 120μg YaaE and 13mM glutamine in 50mM tris, pH8 in 150μL total volume. A sample with just YaaD and 4mM ribulose-5-phosphate was also incubated for 1 hour at 37^{o}C prior to being frozen at -20^{o}C for ESI-FTMS analysis.

512μg YaaD and 357μg YaaE were mixed with 2.5mM ribose-5-phosphate in 50mM tris, pH8 for 1 hour at room temperature prior to being frozen at -20^{o}C for ESI-FTMS analysis. Half of the sample was also reduced with $NaBH_4$ and desalted prior to ESI-FTMS analysis.

70mg YaaD was mixed with 13mM ribulose-5-phosphate and 13mM dihydroxyacetone phosphate in 50mM tris, pH8 for 1 hour at 37^{o}C. The sample was frozen at -20^{o}C prior to ESI-FTMS analysis.

7.4.2.2 Intermediate formation:

Absorbance at 320nm: In general, 150μg YaaD, 150μg YaaE, 2.8mM ribose-5-phosphate and 2.8mM glutamine were mixed in 50mM tris, pH8 in 350μL total volume. Wavelength scans were taken every few minutes on a UV-Vis spectrophotometer.

Full reaction: In general, 150μg YaaD, 150μg YaaE, 2.8mM ribose-5-phosphate, 2.8mM dihydroxyacetone phosphate and 2.8mM glutamine were mixed in 50mM tris, pH8 in 350μL total volume. Wavelength scans were taken every few minutes on a UV-Vis spectrophotometer.

Isotope effect: In general, 2.5mg YaaD, 2.5mg YaaE, 1.8mM dihydroxyacetone phosphate and 1.8mM glutamine were incubated at room temperature in a total volume of 830μL. After 40 minutes, the samples were desalted into tris. This releases the excess ribose-5-phosphate that purifies out with YaaD. 200μg ribokinase, preincubated with 2 mM ribose (or the corresponding deuterated ribose), 3mM ATP and 0.53mM $MgSO_4$ in 25mM phosphate pH8 was added to 150μg YaaDE (with no adduct) and 2.8mM glutamine in 350μL total. Absorbance at 320nm was monitored with time using a UV-Vis spectrophotometer. Additional experiments were performed in the presence of 2.8mM dihydroxyacetone phosphate.

Lag: To remove the adduct from YaaD, 3mg YaaD, 2mg YaaE, 3.3mM dihydroxyacetone phosphate and 3.3mM glutamine were mixed for 45minutes and then desalted into biospin columns into tris. 340μg ribokinase was preincubated with 4mM ATP, 4mM ribose and 0.3mM $MgSO_4$ for 5minutes at room temperature. To this, 300μg YaaDE, 4mM glutamine and 4mM dihydroxyacetone phosphate were combined in 25mM phosphate, pH8 in 350μL total volume. Absorbance at 410nm was monitored with time.

7.4.2.3 Triose addition to the intermediate:

Intermediate decay with trioses: 150μg YaaD, 105μg YaaE, 2mM glutamine, 2mM ribose-5-phosphate and 5mM dihydroxyacetone phosphate or 5mM glyceraldehyde-3-phosphate were combined in 25mM phosphate, pH8, 350μL total volume. Absorbance at 320nm was monitored with time.

1-^{2}H-DHAP vs. H-DHAP: 4units triose phosphate isomerase was mixed with 1mM dihydroxyacetone phosphate in either H_2O (for H-DHAP) or D_2O (for 1-^{2}H-DHAP) phosphate buffer. After incubating overnight at room temperature, the protein was

removed and the sample lyophilized. 150μg YaaD, 104μg YaaE, 4.8mM ribose-5-phosphate, 4.8mM glutamine were mixed with either 5.7mM 1-^{2}H-DHAP or H-DHAP in 25mM phosphate, pH8 in 350μL total volume. The reaction was monitored at 320nm with time.

Triose phosphate isomerase: 150μg YaaD, 102μg YaaE, 2.8mM ribose-5-phosphate, 2.8mM glutamine and 2.8mM dihydroxyacetone phosphate were mixed with or without 10units of triose phosphate isomerase in 25mM phosphate, pH8 in 350μL total. The reactions were monitored at 320nm with time.

7.4.2.4 Phosphate release:

1.5mg YaaD, 1.5mg YaaE, 5.2mM ribose-5-phosphate, 5.2mM dihydroxyacetone phosphate and 5.2mM glutamine were mixed in 25mM $NaHCO_3$ buffer in 770μL total, with 300μL H_2O^{18} and 50μL D_2O. After 23 hours at room temperature, the sample was analyzed on a 500MHz NMR spectrometer with 2400 scans, as well as a 300MHz spectrometer.

7.4.2.5 PLP synthase reaction in D_2O:

In general, 2mg YaaD, 2mg YaaE, 4.3mM ribose-5-phosphate, 4.3mM dihydroxyacetone phosphate and 4.3mM glutamine were mixed in phosphate buffer in D_2O, pH8.2. The reaction was left at 37^{o}C for 21 hours, and 3mg alkaline phosphatase and 1mM $MgSo_4$ were added for another 1.5 hours. The protein was removed with microcon concentrators and the samples were partially lyophilized to reduce the volume. The sample was analyzed by HPLC with a LC-18-T column, 15cm x 4.6mm, 3μm with the following solvent system: A, water; B, 100mM KH_2PO_4 pH6.6; C, methanol. 0-6minutes, 100% B; 7minutes, 10% C; 20minutes, 30% C, 30% A; 22minutes, 100% B. The peak corresponding to pyridoxal was collected, lyophilized, and analyzed with 600MHz NMR.

7.4.2.6 2'-hydroxypyridoxol-5'-phosphate is not an intermediate:

70μg YaaD and 18μg YaaE were mixed with 0.33mM 2'-hydroxypyridoxol-5'-phosphate (Brian Lawhorn, Notebook B^{10-12}) in 25mM tris, pH8, 60μL total. After 16 hours at 37°C, the protein was removed with a microcon and the sample injected into the HPLC (LC-18-T column, 15cm x 4.6mm, 3μm with the following solvent system: A, water; B, 100mM KH_2PO_4 pH6.6; C, methanol. 0-6minutes, 100% B; 7minutes, 10% C; 20minutes, 30% C, 30% A; 22minutes, 100% B).

7.5 References

1. Bauer, J.; Bennet, E.; Begley, T.; Ealick, S. (2004) *J. Biol. Chem.* **279,** 2704-2711.

2. Chaudhuri, B.; Lange, S.; Myers, R.; Davisson, V.; Smith, J. (2003) *Biochemistry* **42,** 7003-7012.

3. Zhang, R.; Andersson, C.; Savchenko, A.; Skarina, T.; Evdokimova, E.; Beasley, S.; Arrowsmith, C.; Edwards, A.; Joachimiak, A.; Mowbray, S. (2003) *Structure* **11,** 31-42.

4. Andersson, C.; Mowbray, S. (2002) *J. Mol. Biol.* **315,** 409-419.

5. Trentham, D.; McMurray, C.; Pogson, C. (1969) *Biochem. J.* **114,** 19-24.

6. Cohn, M.; Hu, A. (1978) *Proc. Natl. Acad. Sci. U.S.A.* **75,** 200-203.

7. Richard, J. (1984) *J. Am. Chem. Soc.* **106,** 4926-4936.

8. Zeidler, J.; Ullah, N.; Gupta, R.; Pauloski, R.; Sayer, B.; Spenser, I. (2002) *J. Am. Chem. Soc.* **124,** 4542-4543.

9. Scott, T.; Picton, C. (1976) *Biochem. J.* **154,** 35-41.

10. Pocker, A. (1973) *J. Org. Chem.* **38,** 4295-4299.

11. Korytnyk, W.; Srivastava, S.; Angelino, N.; Potti, P.; Paul, B. (1973) *J. Med. Chem.* **16,** 1096-1101.

12. Underwood, G.; Paul, B.; Becker, M. (1976) *J. Heterocycl. Chem.* **13,** 1229-1232.

Chapter 8

Substrate Analogs

8.1 Introduction

In an attempt to understand the mechanism of PLP synthase in more detail, we synthesized substrate analogs that could potentially inhibit, or trap, both early and advanced intermediates in the transformation to PLP. These substrate analogs could also be used in crystallography trials.

This chapter will discuss the synthesis and analysis of 3-deoxyribose-5-phosphate **29** and ribose-5-phosphonate **30** as ribose-5-phosphate **10** analogs, and hydroxyacetone phosphate **31** and 2-deoxyglyceraldehyde-3-phosphate **32** as triose **11** and **12** analogs. The structures of these analogs are shown in figure 8.1.

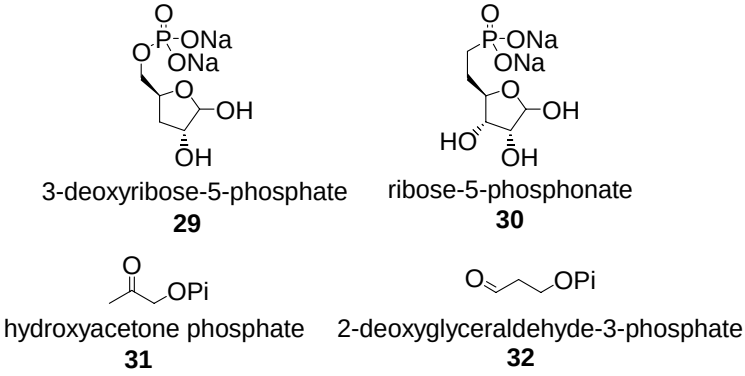

Figure 8.1 Ribose-5-phosphate **10** analogs and triose **11** and **12** analogs synthesized and analyzed for inhibition and mechanistic studies on PLP synthase.

The hydroxyl group on C3 of ribose-5-phosphate **10** stays during the course of the PLP synthase reaction and ends up on C3 of PLP **1**. If the C3 hydroxyl is used during the

course of the reaction, for example, during a tautomerization, we would expect this step to be inhibited with 3-deoxyribose-5-phosphate **29**. We could monitor the inhibition using the techniques described in chapters 6 and 7 to answer the following questions: does YaaD isomerize the inhibitor; does the inhibitor form an adduct with YaaD; does it form the intermediate? Similar questions could be asked for ribose-5-phosphonate **30**, which would not be able to eliminate phosphate.

We used hydroxyacetone phosphate **31** and 2-deoxyglyeraldehyde-3-phosphate **32** as substrate analogs of the triose. Only the phosphate of the triose remains during the course of the PLP synthase reaction and the hydroxyls at C1 and C2 are eliminated as water. We would use hydroxyacetone phosphate **31** and 2-deoxyglyceraldehyde-3-phosphate **32** to monitor the decay of the intermediate absorbance at 320nm to trap intermediates sensitive to these steps. These compounds could also provide additional support for the order of bond formation.

8.2 Results and discussion

*8.2.1 3-Deoxyribose-5-phosphate **29***

In the transformation to PLP, only the hydroxyl group at C3 of ribose-5-phosphate **10** is retained. If we remove this hydroxyl from the starting material, we would expect any step involving this hydroxyl, such as a tautomerization, to be inhibited. Although the proposed mechanism outlined in figure 7.14 does not involve any chemistry at the C3 hydroxyl, we can still use this compound to test for inhibition to ascertain whether the proposed mechanism is correct. For example, if 3-deoxyribose-5-phosphate is isomerized by YaaD, forms the intermediate, and does not make PLP, we know that it binds and does chemistry, however, a step beyond intermediate formation is inhibited by

this compound. This scenario would require modification of the second part of the mechanistic proposal.

3-deoxyribose-5-phosphate was synthesized as outlined in figure 8.2. Briefly, commercially available 1,2-isopropylidene-D-xylose **33** was converted to the protected phosphate **34** using chloro dibenzylphosphite, which was generated *in situ* with dibenzyl phosphite and n-chlorosuccinamide.[1] This compound was converted to the phenylthionocarbonate **35**, which allowed for the deoxygenation of the 3' hydroxyl via a reduction with tin hydride.[2] Deprotection of the isopropyl groups and benzyl groups afforded 3-deoxyribose-5-phosphate **29**.[1,2] NMR confirmed the formation of the products at each step and due to the complexity of the NMR spectrum of the product, ESI-MS confirmed the formation of 3-deoxyribose-5-phosphate with a molecular ion at 213 m/z.

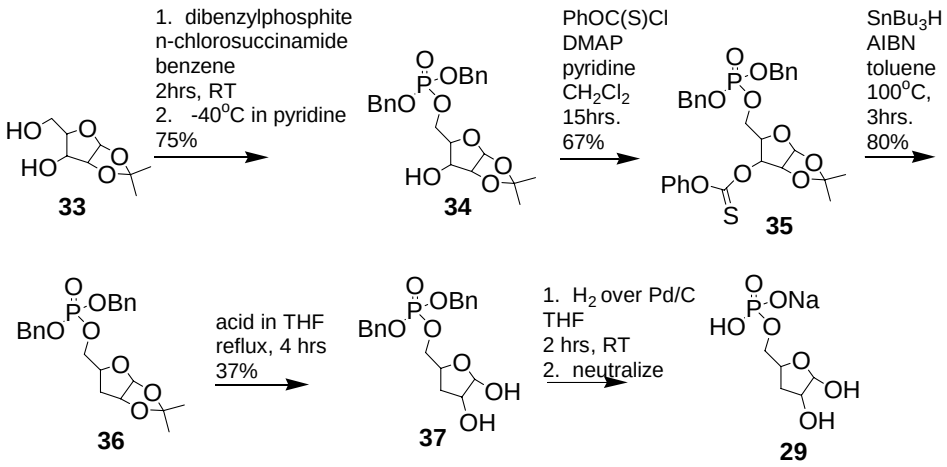

Figure 8.2 Synthesis of 3-deoxyribose-5-phosphate **29**.

To determine whether 3-deoxyribose-5-phosphate **29** is an inhibitor of PLP synthase, YaaD was preincubated with various concentrations of 3-deoxyribose-5-phosphate **29** and the remaining substrates and YaaE were added and analyzed for PLP formation. Under these conditions, no inhibition was observed with 3-deoxyribose-5-phosphate **29** up to 6mM. To test whether 3-deoxyribose-5-phosphate **29** is a substrate for

isomerization by YaaD, we looked for deuterium incorporation into 3-deoxyribose-5-phosphate **29** by ESI-MS. No H-D exchange was observed by ESI-MS, suggesting YaaD is unable to isomerize 3-deoxyribose-5-phosphate **28**, and that the compound is neither an inhibitor nor a substrate for YaaD.

*8.2.2 Ribose-5-phosphonate **30***

In the transformation to PLP, the phosphate of ribose-5-phosphate **10** is removed, and that of the triose is retained. We would expect an analog of ribose-5-phosphate **10** that is unable to have the phosphate removed to be an inhibitor. We chose to synthesize ribose-5-phosphonate **30**, in which the carbon-oxygen bond between ribose and phosphate is replaced by a carbon-carbon bond, making the bond scission impossible. Based on the proposed mechanism outlined in figure 7.14, we would expect ribose-5-phosphonate to inhibit the PLP synthase catalyzed phosphate elimination from **24** to **25**. The reaction would proceed as in figure 8.3, but it would be unable to continue beyond **24***. This inhibitor could also tell us whether phosphate is present in the intermediate **16** or if it is removed prior to intermediate formation.

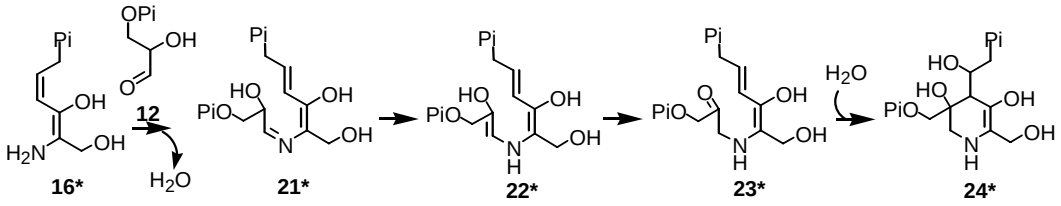

Figure 8.3 Proposed mechanism of inhibition by ribose-5-phosphonate **30**. * are the phosphonate derivatives of the proposed reaction intermediates.

As outlined in figure 8.4, the secondary hydroxyls of ribose **38** were protected in acid using methanol and acetone.[3] After protection, the primary hydroxyl at C5 was oxidized using Mofatt conditions, and a Horner-Emmons condensation using the tetraethylmethylene diphosphonate carbanion afforded the protected phosphonate **41**.[4,5]

Hydrogenation followed by two subsequent deprotections yielded the free phosphonate **30**.[5,6] NMR confirmed the formation of the products at each step and due to the complexity of the NMR spectrum of the product, ESI-MS confirmed the formation of ribose-5-phosphonate **30** with a molecular ion at 227 m/z.

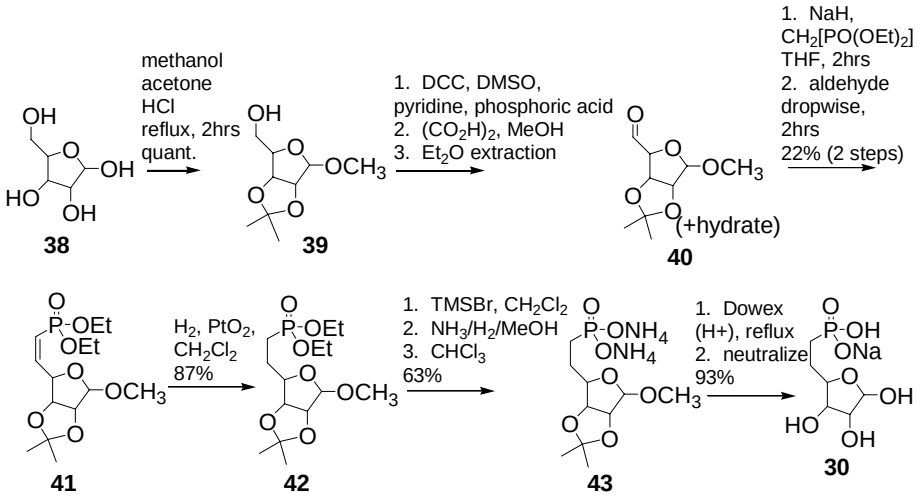

Figure 8.4 Synthesis of ribose-5-phosphonate **30**.

To determine whether ribose-5-phosphonate **30** is an inhibitor of PLP synthase, YaaD was preincubated with various concentrations of ribose-5-phosphonate **30** and the remaining substrates and YaaE were added and analyzed for PLP formation. Under these conditions, no inhibition was observed with ribose-5-phosphonate **30** up to 6mM. To test whether ribose-5-phosphonate **30** is a substrate for isomerization by YaaD, we looked for deuterium incorporation into ribose-5-phosphonate **30** by ESI-MS. No H-D exchange was observed by ESI-MS, suggesting YaaD is unable to isomerize ribose-5-phosphonate **30**, and that the compound is neither an inhibitor nor a substrate for YaaD.

*8.2.3 Hydroxyacetone phosphate **31***

Chapter 7 describes the formation of an intermediate absorbance at 320nm during the course of the PLP synthase reaction in the absence of triose. We propose glyceraldehyde-3-phosphate then adds to this intermediate **16**. To provide further

evidence of this, we synthesized hydroxyacetone phosphate and tested it for addition to the intermediate **16**. Hydroxyacetone phosphate is missing the hydroxyl at C1 and retains the ketone at C2. If the C2 carbonyl of dihydroxyacetone phosphate **11** reacts first with the intermediate, as shown in figure 7.6 reaction A, we would expect to see a decay in the intermediate upon the addition of hydroxyacetone phosphate **31**. This is shown in figure 8.5. Hydroxyacetone phosphate **31** was synthesized in two steps and tested for addition to the intermediate.

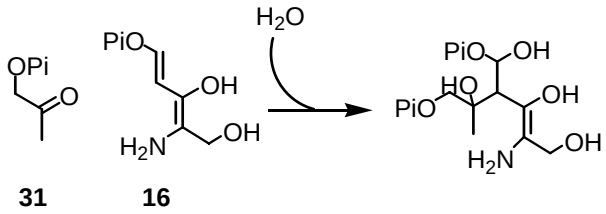

Figure 8.5 Proposed reaction between the intermediate **16** and the putative inhibitor hydroxyacetone phosphate **31** if C-C bond formation between the triose and the intermediate **16** occurs first.

To synthesize hydroxyacetone phosphate **31**, acetol **44** was converted to the protected phosphite **45** with diisopropyldibenzylphosphoramidite (DDP) and tetrazole. Following oxidation to the phosphate with 3-chloroperoxybenzoic acid (mCPBA), hydroxyacetone phosphate **31** was formed upon hydrogenation (figure 8.6).

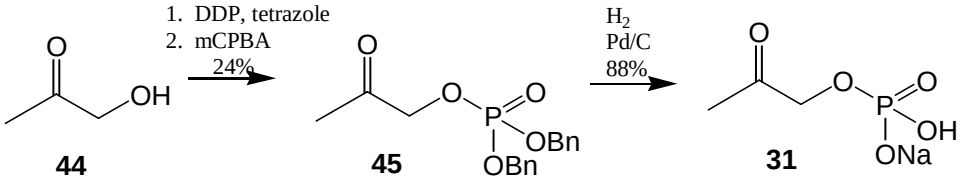

Figure 8.6 Synthesis of hydroxyacetone phosphate **31**.

To test whether hydroxyacetone phosphate **31** could react with the characterized intermediate **16** on YaaD/YaaE, the intermediate was pre-formed on YaaD/YaaE and the

small molecules were removed by desalting. Addition of up to 8.6mM hydroxyacetone phosphate **31** had no affect on the decay of the intermediate, indicating that it does not react with the intermediate. This suggests that either hydroxyacetone phosphate **31** cannot react because it does not have the hydroxyl group at C1 (as we would predict), or that it is not binding PLP synthase. Up to 5.7mM hydroxyacetone phosphate **31** did not interfere with PLP formation when assayed in the presence of 0.2mM dihydroxyacetone phosphate **11**, indicating that it is not an inhibitor of PLP synthase and it is probably not binding at all.

*8.2.4 2-Deoxyglyceraldehyde-3-phosphate **32***

Since hydroxyacetone phosphate **31** retained the C2 carbonyl and did not react with the intermediate, we thought that 2-deoxyglyceraldehyde-3-phosphate **32**, which retains the aldehyde at the C1 position of the triose, would react with the intermediate as glyceraldehyde-3-phosphate **12** does in figure 7.6 reaction B. Because it is missing the C2 hydroxyl, we propose that this putative inhibitor would react with the intermediate **16** and inhibit the tautomerization step proposed from **22** to **23** in figure 7.14. The proposed mechanism of inhibition is shown in figure 8.7.

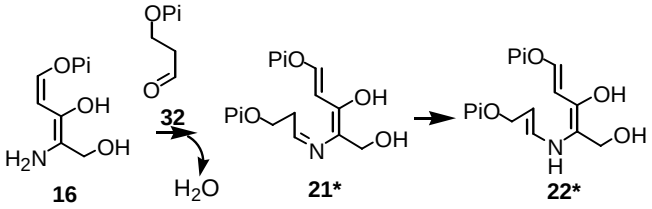

Figure 8.7 Proposed mechanism of inhibition with 2-deoxyglyceraldehyde-3-phosphate **32**. * are the derivatives of the proposed reaction intermediates.

To synthesize 2-deoxyglyceraldehyde-3-phosphate **32**,[7] trans-cinnamaldehyde **46** was converted to the epoxide **47** with trimethylsulfonium iodide (TMSI) in sodium hydride and DMSO (figure 8.8). Diisobutylaluminum hydride (DIBAL-H) converts the epoxide

to the alcohol **48**. A protected phosphite was added with diisopropyldibenzylphosphoramidite (DDP) and tetrazole. Following oxidation to the phosphate **49**, the compound was subject to ozonolysis to afford the aldehyde **50**. Hydrogenation over Pd/C deprotected the phosphates, resulting in 2-deoxyglyceraldehyde-3-phosphate **32**. The final two steps in this synthesis, ozonolysis and hydrogenation, were done in collaboration with David Hilmey.

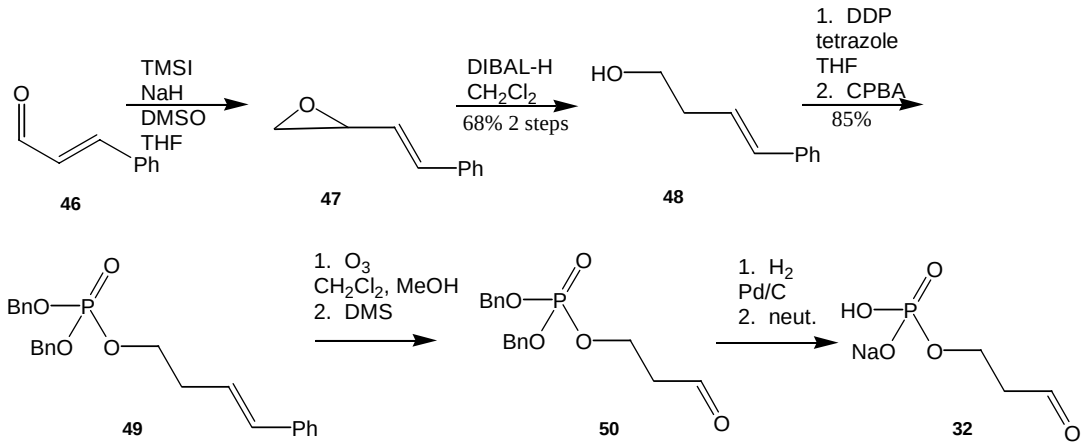

Figure 8.8 Synthesis of 2-deoxyglyceraldehyde-3-phosphate **32**.

When 5.7mM 2-deoxyglyceraldehyde-3-phosphate **32** was added to the pre-formed intermediate, there was no change in the absorbance spectrum; it had no affect on intermediate decay. This suggests that 2-deoxyglyceraldehyde-3-phosphate does not react with the intermediate in PLP synthase.

8.3 Conclusion

Neither of the modified pentoses, 3-deoxyribose-5-phosphate **29** nor ribose-5-phosphonate **30**, were substrates or inhibitors for PLP synthase. Likewise, neither of the triose analogs, hydroxyacetone phosphate **31** nor 2-deoxyglyceraldehyde-3-phosphate **32**, reacted with the proposed intermediate **16** in the PLP synthase reaction. These results suggest that the active site of YaaD is probably very specific.

8.4 Experimental procedures

8.4.1 Materials and methods: All chemicals were purchased from Sigma. ESI-MS was performed at Cornell University's Bioresource Center. NMR spectra were obtained on a Mercury 300MHz spectrometer, UV-Vis spectra were obtained on a Hitachi U2010 spectrophotometer.

8.4.1.1 Synthesis of 3-deoxyribose-5-phosphate **29**

1,2-isopropylidene-D-xylose-5-dibenzylphosphate **34**: 15.6mmol dibenzylphosphite and 15.6mmol n-chlorosuccinamide were mixed in 20mL dry benzene for 2 hours at room temperature. The mixture was dry filtered to remove undissolved n-chlorosuccinamide, and the filtrate was added dropwise to 5.2mmoles of 1,2-isopropylidene-D-xylose **33** in 20mL pyridine at -40^{o}C. After 15 minutes at -40^{o}C, the reaction was stirred at room temperature for 2 hours. The solvent was evaporated, and 200mL ethyl acetate was added. The mixture was extracted with 2x60mL 1M HCl, 2x60mL 1M $NaHCO_3$, and 60mL brine. After the mixture was dried with $MgSO_4$ and filtered, the product was purified by flash chromatography with 98:2 chloroform: methanol. NMR $CDCl_3$ (ppm): 7.35s 10H; 5.0m 4H; 4.25t 2H; 4.05q 1H; 4.25d 1H; 4.55d 1H; 5.9d 1H; 1.31s 3H; 1.48s 3H.

1,2-isopropylidene-3-phenylthonocarbonate-D-xylose-5-dibenzylphosphate **35**: 3.9mmole 1,2-isopropylidene-D-xylose-5-dibenzylphosphate **34** was added to 15mL dichloromethane and 0.85mmoles dimethylaminopyridine. The mixture was placed on ice and after 4.5mmoles of pyridine was added, 2.5mmoles PHOC(S)Cl in 1.36mL dichloromethane was added dropwise. The reaction was kept on ice for 15 minutes and then left at room temperature overnight. The reaction was extracted with 3x10mL water, 2x7mL saturated $CuSO_4$ and 10mL brine. After the mixture was dried with $MgSO_4$ and

filtered, the product was purified by flash chromatography with 99.5:0.5 chloroform: methanol. NMR $CDCl_3$ (ppm): 7.35s 10H; 5.1dd 4H; 4.3t 2H; 4.55td 1H; 5.65d 1H; 4.3t 1H; 6.0d 1H; 1.35s 3H; 1.55s 3H.

1,2-isopropylidene-3-deoxy-D-ribose-5-dibenzylphosphate **36**: 1.13mmoles 1,2-isopropylidene-3-phenylthonocarbonate-D-xylose-5-dibenzylphosphate **35** was added to 6mg AIBN in 10mL toluene. The reaction was kept under argon for 30 minutes at room temperature. 1.3mmoles tributyltin hydride was added and the reaction was refluxed at 100^{o}C for 3 hours. The reaction was cooled, solvent evaporated, and purified by flash chromatography with 3:1 hexane:ethyl acetate. NMR $CDCl_3$ (ppm): 7.35s 10H; 5.05dd 4H; 4.15ddd 1H; 4.0ddd 1H; 4.35m 1H; 2.0dd 1H; 1.7ddd 1H; 4.65t 1H; 5.77d 1H; 1.31s 3H; 1.48s 3H.

3-deoxy-D-ribose-5-dibenzylphosphate **37**: 0.90mmoles 1,2-isopropylidene-3-deoxy-D-ribose-5-dibenzylphosphate **36** was added to 15mL THF and 960μL 2N HCl. The sample was refluxed at 65^{o}C for 3 hours. The reaction was cooled to room temperature and bicarbonate was added to neutralize. The sample was extracted with 10mL ether. Extraction continued with 10mL water and 10mL NaCl. Flash chromatography in 95:5 chloroform:methanol afforded the product. NMR $CDCl_3$ (ppm): α, β-anomers, 7.35m 20H; 5.05m 8H; 3.9ddd 2H; 4.05ddd 2H; 4.4m 1H; 4.5m 1H; 1.95ddd 2H; 2.05ddd 2H; 4.2m 1H; 4.26m 1H; 5.25s 1H; 5.28d 1H.

3-deoxy-D-ribose **29**: 0.10mmoles 3-deoxy-D-ribose-5-dibenzylphosphate **37** was hydrogenated in 20mL THF and 10mg Pd/C. After 4 hours, the reaction was filtered, washed with water, evaporated and lyophilized. MS (m/z): 213.

8.4.1.2 Synthesis of ribose-5-phosphonate **30**

Methyl-2,3-O-isopropylidene-β-D-ribofuranoside **39**: 16mmoles ribose **38** was added to 11mL acetone, 11mL methanol and 0.33mL HCl. The reaction was refluxed for 2 hours and then cooled to room temperature. 30mL water was added and the mixture was extracted with 4x30mL chloroform. The organic layer was dried with $MgSO_4$, filtered and evaporated. NMR $CDCl_3$ (ppm): 3.55m 2H; 4.48d 1H; 4.7d 1H; 4.87s 1H; 3.3s 3H; 1.2s 3H; 1.37s 3H.

Methyl-2,3-O-isopropylidene-5-dehydro-β-D-ribofuranoside **40**: 8mmoles methyl-2,3-O-isopropylidene-β-D-ribofuranoside **39** was added to 14mmoles pyridine, 14mmoles o-phosphoric acid and 45mmoles DCC in 20mL DMSO. After 7 hours at room temperature, the reaction was poured into 0.111moles oxalic acid in 30mL methanol on ice and stirred for 45 minutes. 10mL ether was added and the salts were filtered. The sample was evaporated and water added. The mixture was extracted with 300mL ether, evaporated and left on the high vacuum line overnight.

Methyl-2,3-O-isopropylidene-5-deoxy-5-diethylphosphomethylene-β-D-ribofuranoside **41**: 8mmoles sodium hydride was added to 6mmoles tetraethylmethylene diphosphonate in 5mL dry THF over ice. The reaction was stirred for 2 hours, and then added dropwise to 4mmoles methyl-2,3-O-isopropylidene-5-dehydro-β-D-ribofuranoside **40** in 5mL dry THF. After 3 hours at room temperature, the reaction was extracted with ether and water, the ether layer was dried with $MgSO_4$, filtered and evaporated. The product was purified by flash chromatography with 1:1 hexane:ethyl acetate. NMR $CDCl_3$ (ppm): 1.3t 6H; 4.05m 4H; 5.9ddd 1H; 6.7ddd 1H; 4.75m 1H; 4.65d 1H; 4.6d 1H; 5.0s 1H; 3.35s 3H; 1.3s 3H; 1.45s 3H.

Methyl-2,3-O-isopropylidene-5-deoxy-5-diethylphosphonomethyl-β-D-ribofuranoside **42**: 0.87mmoles methyl-2,3-O-isopropylidene-5-deoxy-5-diethylphosphomethylene-β-D-ribofuranoside **41** was hydrogenated in 30mL absolute ethanol with 20mg PtO_2. After 10.5hours, the reaction was filtered and evaporated. NMR $CDCl_3$ (ppm): 1.2t 6H; 4.0q 4H; 1.75m 2H; 1.75m 2H; 4.0m 1H; 4.41d 1H; 4.5d 1H; 4.85s 1H; 3.23s 3H; 1.23s 3H; 1.37s 3H.

Methyl-2,3-O-isopropylidene-5-deoxy-5-phosphonomethyl-β-D-ribofuranoside **43**: 5.7mmoles TMSBr was added to 0.38mmoles methyl-2,3-O-isopropylidene-5-deoxy-5-diethylphosphonomethyl-β-D-ribofuranoside **42** in 5mL dichloromethane. After 2 hours at room temperature, the solvent was evaporated and 5mL 1:1:1 NH_4OH: H_2O: MeOH was added and stirred for 2 hours. The reaction was extracted with chloroform and the aqueous layer was evaporated prior to lyophilization. NMR $CDCl_3$ (ppm): 1.6m 2H; 1.6m 2H; 4.1t 1H; 4.65d 1H; 4.7d 1H; 4.93s 1H; 3.3s 1H; 1.24s 3H; 1.36s 3H.

5-deoxy-5-phosphonomethyl-β-D-ribofuranoside **30**: 0.24mmoles methyl-2,3-O-isopropylidene-5-deoxy-5-phosphonomethyl-β-D-ribofuranoside **41** was dissolved in 5mL water and the sample was purged with argon. The mixture was refluxed with Dowex 5x4-400 (H^+) for 3 hours under argon. The resin was filtered and washed, and the filtrate was adjusted to pH7 with NaOH. The sample was lyophilized. MS (m/z): 227.

8.4.1.3 Synthesis of hydroxyacetone phosphate **31**

hydroxyacetone dibenzylphosphate **45**: 0.69mmoles acetol **44** was added to 4mL THF, 1.4mmoles tetrazole and 0.9mmoles dibenzyl diisopropylphosphoramidite and the reaction was stirred at room temperature for 30minutes. After 30minutes, the phosphate was oxidized with 2.4mmoles 3-chloroperoxybenzoic acid in 5mL dichloromethane at -60^{o}C, and then allowed to warm to room temperature for 15minutes. The reaction was

neutralized with 5mL 10% $NaHSO_3$ for 10minutes at room temperature, followed by extraction into 20mL ether. The sample was washed with 2x7mL 10% $NaHSO_3$ followed by 2x7mL 5% $NaHCO_3$. Hydroxyacetone dibenzylphosphate was purified by flash chromatography with 99:1 chloroform:methanol. NMR $CDCl_3$ (ppm): 7.35s 10H; 5.1dd 4H; 4.42d 2H; 2.1s 3H.

hydroxyacetone phosphate **31**: 0.17mmoles hydroxyacetone dibenzylphosphate **45** in 12mL absolute ethanol and 10mg 10% Pd/C was hydrogenated for 30minutes. The reaction was filtered through celite, washed, and the ethanol was evaporated. The sample was resuspended in water, neutralized with NaOH, and lyophilized. NMR D_2O (ppm): 4.3d 2H; 2.1s 3H.

8.4.1.4 Synthesis of 2-deoxyglyceraldehyde-3-phosphate **32**

1,2-epoxy-4-phenylbut-3-ene **47**: 3mL dry THF and 3mL dry DMSO were added to 6mmoles NaH. The reaction was cooled in an ice-salt bath. 5.8mmoles TMSI in 4.2mL DMSO was added over 5 minutes. To this, 1.9mmoles trans-cinnamaldehyde **46** was added and stirred for 30minutes at 0^oC, then at room temperature for 1 hour. 12.5mL cold water was added to the sample slowly, followed by extraction with 3x13mL dichloromethane. The organic layer was dried, filtered and concentrated in vacuo. Vacuum distillation afforded the epoxide. NMR $CDCl_3$ (ppm): 7.3m 5H; 6.8d 1H; 5.9dd 1H; 3.5m 1H; 3.05t 1H; 2.75m 1H.

4-phenylbut-3-en-1-ol **48**: 4.2mmoles DIBAL-H in 1M dichloromethane was added over 5 minutes to 2.7mmoles of 1,2-epoxy-4-phenylbut-3-ene **47** in 11.5mL dichloromethane at -78^oC. After 3 hours at room temperature, the reaction was again cooled to -78^oC and 2mL methanol was added dropwise. After 5 minutes, the reaction was brought to room temperature and formed a gel. The gel was washed with 3x20mL ethyl acetate,

concentrated in vacuo and purified by flash chromatography with 80:20 hexane: ethyl acetate. NMR $CDCl_3$ (ppm): 7.3m H; 6.5d 1H; 6.2dt 1H; 3.75t 2H; 2.5q 2H; 2.05s 1H.

4-phenylbut-3-en-1-yl dibenzyl phosphate **49**: 0.37mmoles DDP was added to 0.29mmoles 4-phenylbut-3-en-1-ol **48** and 0.57mmoles tetrazole in 1.6mL THF. After 30 minutes at room temperature, the reaction was taken to -60^{o}C and 0.86mmoles 3-chloroperoxybenzoic acid in 2mL dichloromethane was added. After 15 minutes at room temperature, 2mL 10% $NaHSO_3$ was added for 10 minutes at room temperature. 8mL ether was added and washed with 2x3mL 10% $NaHSO_3$ followed by 2x3mL 5% $NaHCO_3$. The ether layer was dried, filtered and concentrated. The phosphate was purified by flash chromatography with 15:1 dichloromethane: acetone. NMR $CDCl_3$ (ppm): 7.35m 15H; 6.45d 1H; 6.15dt 1H; 5.05m 4H; 4.1m 2H; 2.5m 2H.

3-oxopropyl dibenzyl phosphate **50**: (Dave Hilmey) 5mL dichloromethane and 5mL methanol were added to 0.7mmoles 4-phenylbut-3-en-1-yl dibenzyl phosphate **49**. Ozone was passed through the solution at -78^{o}C until a blue color persisted (about 30 minutes). The reaction was purged with argon and 0.25mL dimethylsulfide was added overnight. The solvent was concentrated and flash chromatography with 4:1 ethyl acetate: light petroleum yielded the aldehyde. NMR $CDCl_3$ (ppm): 9.2s 1H; 7.35s 10H; 5.0m 4H; 4.3m 2H; 2.7m 2H.

2-deoxyglyceraldehyde-3-phosphate **32**: (Dave Hilmey) Hydrogen was passed through a solution of 3-oxopropyl dibenzyl phosphate **50** in THF and 10% Pd/C for 30 minutes. The solution was filtered through celite, concentrated and water was added. The pH was adjusted to 7 with NaOH and ethanol was added. The sample was filtered and the filtrate saved as 2-deoxyglyceraldehyde-3-phosphate. NMR D_2O(ppm) (hydrate): 5.2t 1H; 3.78m 2H; 1.85m 2H.

8.4.2 Assays

*8.4.2.1 3-deoxyribose-5-phosphate **29** inhibition studies*

PLP synthase inhibition: 120μg YaaD was preincubated with various concentrations of 3-deoxyribose-5-phosphate (120μM – 6mM; $2K_m$ – $100K_m$) at room temperature. After 20 minutes, 120μg YaaE, 60μM ribose-5-phosphate, 2mM dihydroxyacetone phosphate and 2mM glutamine were added in 50mM phosphate pH8 to a final volume of 350μL. The absorbance at 390nm was monitored with time.

H-D exchange of 3-deoxyribose-5-phosphate by YaaD: 562.5μg YaaD was incubated with 5mM 3-deoxyribose-5-phosphate in 2.5mM ammonium bicarbonate in D_2O in a total volume of 1mL. The sample was incubated for 15 hours at room temperature, the protein was removed with microcon concentrators, and the sample was lyophilized. The samples were resuspended in water and analyzed by ESI-MS.

*8.4.2.2 ribose-5-phosphonate **30** inhibition studies*

PLP synthase inhibition: 120μg YaaD was preincubated with various concentrations of ribose-5-phosphonate (120μM – 6mM; $2K_m$ – $100K_m$) at room temperature. After 20 minutes, 120μg YaaE, 60μM ribose-5-phosphate, 2mM dihydroxyacetone phosphate and 2mM glutamine were added in 50mM phosphate pH8 to a final volume of 350μL. The absorbance at 390nm was monitored with time.

H-D exchange of ribose-5-phosphonate by YaaD: 562.5μg YaaD was incubated with 2.5mM ribose-5-phosphonate in 2.5mM ammonium bicarbonate in D_2O in a total volume of 1mL. The sample was incubated for 15 hours at room temperature, the protein was removed with microcon concentrators, and the sample was lyophilized. The samples were resuspended in water and analyzed by ESI-MS.

*8.4.2.3 hydroxyacetone phosphate **31** studies*

hydroxyacetone phosphate reaction with intermediate: 2mg YaaD, 1.4mg YaaE, 3.2mM ribose-5-phosphate and 3.2mM glutamine were mixed in 475μL total volume for 30 minutes in 25mM phosphate pH8. After the intermediate formed, the solution was desalted into phosphate. 335μg YaaDE-intermediate was incubated with 4.8mM hydroxyacetone phosphate in 25mM phosphate, pH8. Absorbance spectra were taken over time and the decay at 320nm was monitored over time.

*8.4.2.4 2-deoxyglyceraldehyde-3-phosphate **32** studies*

2-deoxyglyceraldehyde-3-phosphate reaction with intermediate: 2mg YaaD, 2mg YaaE, 3.4mM ribose-5-phosphate and 3.4mM glutamine were mixed in 450μL total volume for 30 minutes in 25mM phosphate pH8. After the intermediate formed, the solution was desalted into phosphate. 200μg YaaDE-intermediate was incubated with 5.7mM 2-deoxyglyceraldehyde-3-phosphate in 25mM phosphate, pH8. Absorbance spectra were taken over time.

8.5 References

1. Strauss, E.; Begley, T. (2002) *J. Biol. Chem.* **277,** 48205-48209.

2. Rizzo, C.; Dougherty, J.; Breslow, R. (1992) *Tet. Lett.* **33,** 4129-4132.

3. Lerner, L. (1977) *Carb. Res.* **53,** 177-185.

4. Le Marechal, P.; Froussious, C.; Level, M.; Azerad, R. (1981) *Carb. Res.* **94,** 1-10.

5. Burgos, E.; Salmon, L. (2004) *Tet. Lett.* **45,** 3465-3469.

6. Unger, F. M. S., D.; Moderndorfer, E.; Hammerschmid, F. (1978) *Carb. Res.* **67,** 349-356.

7. Cotterill, I.; Shelton, M.; Machemer, D.; Henderson, D.; Toone, E. (1998) *J. Chem. Soc., Perkin Trans.* **1,** 1335-1341.

Chapter 9

Conclusion and Outlook

9.1 An Overview

Compared to the *E. coli* system, PLP biosynthesis in *B. subtilis* and other organisms with the YaaD/YaaE family of genes is simplified. What takes six enzymes to do in the *E. coli* system takes only two in the YaaD/YaaE system. Why some organisms evolved the more complex route while others use only two enzymes is not currently known. Although the YaaD/YaaE system is simple and efficient in that the enzymes can perform the task of six enzymes in two, the reaction catalyzed by the YaaD/YaaE system appears to be more complex. We have shown that YaaD has both ribosephosphate isomerase activity as well as triosephosphate isomerase activity, reactions normally catalyzed by two separate and essential enzymes in the cell. YaaD also forms a covalent adduct with the product of ribose-5-phosphate isomerization, ribulose-5-phosphate. YaaD then combines ammonia, which is delivered from the amidotransferase subunit YaaE, as well as the triose to form the product PLP **1**. Unlike the *E. coli* system, no further oxidation is needed to form the active cofactor.

We have reconstituted the biosynthesis of PLP **1** using YaaD and YaaE from *B. subtilis*, outlined and provided evidence for the order of bond formation, and characterized an intermediate formed in the absence of triose. Unfortunately, all attempts at isolating the intermediate with absorbance at 320nm failed. In addition, all attempts at trapping an early or advanced intermediate with substrate analogs also failed. This may be due, at least in part, to the complex structure of the PLP synthase complex. The structure of the YaaD subunit of PLP synthase from *Geobacillus stearothermophilus* at 2.2Å was solved

shortly after the reconstitution.[1] The structure is composed of twelve monomers with a classic $(\beta/\alpha)_8$ barrel fold. Biochemical evidence supports that the subunit exists as a dodecamer and a hexamer in solution. Recently, in collaboration with the Ealick group, we were able to get a crystal structure of the YaaD/YaaE complex from *Thermatoga maratima* at 2.9Å resolution (unpublished). The PLP synthase complex from *T. maratima* has 12 core YaaD monomers with 12 YaaE monomers surrounding them. The structure is shown in figure 9.1. The structure has ribulose-5-phosphate bound in the active site of YaaD. The impressive structure of YaaD and the YaaD/YaaE complex enabled us to rationalize some of our findings. For example, because the complex is so big, it must take coordination and cooperativity to get the complex ready for catalysis. This could explain, at least in part, why the system is very slow, and why it is difficult to denature. The structure also identified key active site residues which were important for catalysis.

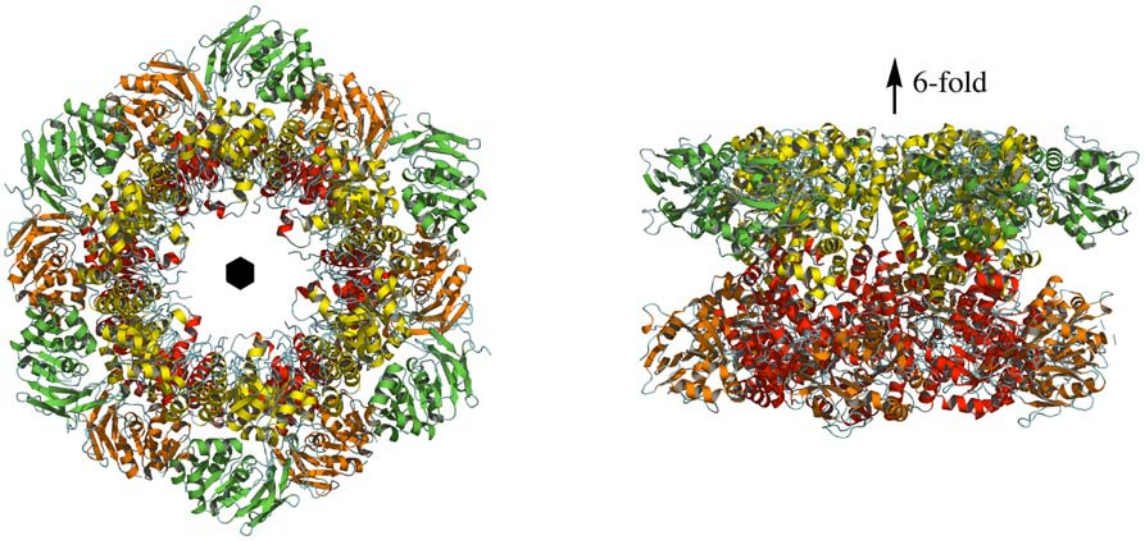

Figure 9.1 Structure of the PLP synthase dodecamer a. View down the molecular sixfold axis b. View perpendicular to the sixfold axis. Yellow and red are the YaaD subunits in the two hexameric layers that join face-to-face to form the dodecamer. Green and orange are the YaaE monomers surrounding the YaaD core.

9.2 Future Directions

As mentioned above, the crystal structure provided us with some insight into the active site residues involved in catalysis. While a few of these residues were mutated, none of them provided any critical information regarding the mechanism (this data was not discussed). The crystal structure did bring up some interesting questions. Our mass spectrometry data suggests the adduct on YaaD is on lysine 149. The structure of the YaaD/YaaE complex, however, has the adduct on lysine 81. In addition, lysine 149 is pointed away from the active site in both the YaaD structure and the structure of the YaaD/YaaE complex. Mutagenesis of either residue abolishes PLP synthase activity. The possibility of both residues involved in PLP formation has not been ruled out and a more detailed analysis of this apparent discrepancy is needed. Another question regarding the PLP synthase structure is the site of triose isomerization. Neither structure has the triose bound, and neither has an obvious binding pocket for the triose. Future studies will focus on determining which residues are important for catalyzing triose isomerization, as this could enable us to trap advanced intermediates with substrate analogs.

The PLP synthase reaction is complex, slow, and most likely has many steps in the mechanism. Because there are quite a few optical signals (ribulose-5-phosphate absorbs at 290nm; intermediate absorbance at 320nm; PLP absorbance at 390nm), and the mechanism appears to involve ordered bond formation, the PLP synthase reaction can be monitored step-wise by absorbance changes. This will enable us to get rates for formation and decay of the optical signals so we can get a kinetic picture of the mechanism. The PLP synthase reaction is far too complicated to understand without putting rates on the signals we observe.

Interestingly, in *S. cerevisiae* and other fungi, vitamin B6 forms the backbone of the cofactor thiamin.[2] *S. cerevisiae* contains three sets of PLP synthase genes, and one set of these genes clusters with thiamin biosynthetic genes. Unpublished results from our lab suggest that the product of the PLP synthase genes in *S. cerevisiae* is PLP, however, the system is unable to isomerize ribose-5-phosphate to ribulose-5-phosphate (Jennie Sanders). Additional evidence suggests that these enzymes require ribosephosphate isomerase for *in vivo* activity, [3] so the 5-carbon substrate in *S. cerevisiae* is most likely ribulose-5-phosphate. The activity of the PLP synthase enzymes from *S. cerevisiae* is robust compared to the activity of the enzymes from *B. subtilis*, and it may provide a better system for studying the mechanism of PLP formation by this family of enzymes. Moreover, it will enable us to probe thiamin biosynthesis in yeast in more detail.

9.3 References

1. Zhu, J.; Burgner, J.; Harms, E.; Belitsky, B.; Smith, J. (2005) *J. Biol. Chem.* **280,** 27914-27923.

2. Zeidler, J.; Ullah, N.; Gupta, R.; Pauloski, R.; Sayer, B.; Spenser, I. (2002) *J. Am. Chem. Soc.* **124,** 4542-4543.

3. Kondo, H.; Nakamura, Y.; Dong, Y.; Nikawa, J.; Sueda, S. (2004) *Biochem. J.* **379,** 65-70.